Technical University of Denmark

Optical Networks Solutions planning - performances - management

Fenger, Christian; Dittmann, Lars; Iversen, Villy Bæk

Publication date:
2002

Document Version
Publisher's PDF, also known as Version of record

Optical Network Solutions

planning - performance - management

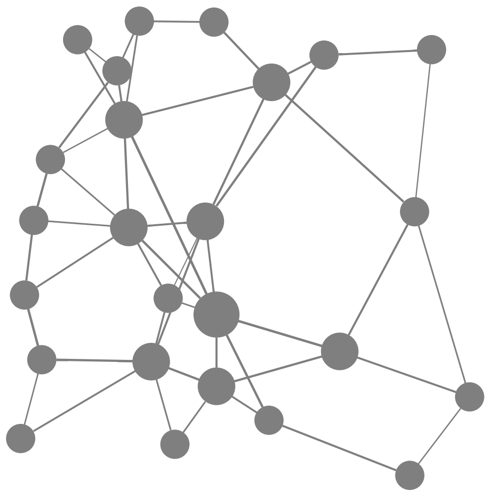

Christian Fenger

PhD thesis

Tele Danmark

Author: Christian Fenger
Title: **Optical Network Solutions** planning - performance - management
Dansk titel: **Optiske netværksløsninger** planlægning - effektivitet - styring
PhD thesis
June 2002

Reseach Center COM
Technical University of Denmark
DK–2800 Kongens Lyngby
Denmark

Front cover: Result of optimization of a 25 node network with biconnectivity requirement. Traffic is uniform, duct prices equal the euclidean distance, fiber prices is 1/20th of duct prices. The node cost parameters are: $C_{core} = 100$, $C_{port} = 1$, and $C_{switching} = 0.01$. The nodes are distributed on a 1000 times 1000 square. The total network cost is 44080, where duct cost is 10718, fiber cost is 18037, and node cost is 15325. See Chapter 8.

Optical Network Solutions
planning - performance - management

Abstract

It has been a decisive goal in the compilation of this thesis to make us capable of realizing the future national and regional telecommunication networks in an efficient and resource optimal way.

By future telecommunication network is assumed an all-optical network where the information in transit are kept optical and not converted into the optical domain.

The focus is on the scientific results achieved throughout the Ph.D. period. Five subjects – all increasing the understanding of optical networks – are studied.

Static wavelength routed optical networks are studied. Management on terms of lightpath allocation and design is considered. By using statistical models (simultaneous analysis of many networks) the correspondence between parameters determining the network topology and the performance of the optical network is found. These dependencies are important knowledge in the process of designing a network. It is also seen (statistically) found that the effect of wavelength converters on the performance of static wavelength routed optical networks is negligible.

Dynamic wavelength routed optical networks are simulated and analyzed. Manangement of dynamic networks is a more complex task than the static case. Several strategies are considered. The alternative study with reel networks as alternative to computer simulations would have been extremely costly or impossible. Different routing methods have been used and studied. The effect of wavelength conversion has been analyzed and contrary to static optical networks the effect of wavelength converters on dynamic optical networks is significant. The effect on

blocking probability of multiple fibers on each link is shown to be significant, and it is concluded that neither limited-range nor full wavelength conversion will find any significant use in all-optical network. Fairness is suggested as a new measure for network performance in line with network blocking probability.

Teletraffic is studied for several purposes. Erlang's fixed point equations have been used verify some results of simulation of dynamic optical networks. An explicit solution for network blocking probability has been derived, and fixed point equations for alternate routing are derived. Secondly is self similar traffic studied and the effect on optical networks considered.

The *Synchronous Optical Hierarchy* is suggested as a new type of network to overcome the technological hurdles of packet switched optical networks and without the capacity granularity problem in wavelength routed optical networks. This new proposal is exactly formulated and experiments are performed to estimate the strengths. In networks, where the typical size of a traffic demand between two nodes is up to two wavelengths, significant capacity savings are possible.

Network planning in the form of optimal design of national and regional telecommunication networks is thoroughly studied and promising computer programs and methods are developed. In the optimization process are both duct, fiber, and switch equipment cost considered. The contribution in network planning are one of the most important contributions with direct usability.

Optiske netværksløsninger
planlægning - effektivitet - styring

Resumé

Det har været et afgørende mål i udarbejdelse af denne afhandling at sætte os i stand til at realisere fremtidens nationale og regionale telekommunikationsnetværk på en effektiv og ressource optimal måde.

Med fremtidens telekommunikationsnetværk formodes der helt optiske netværk, hvor informationen sendes gennem netværket uden undervejs at være konverteret til et elektrisk signal.

Der er i afhandlingen fokuseret på de videnskabelige resultater opnået gennem ph.d.-forløbet. Fem emner, der alle øger forståelsen af optiske netværk, er undersøgt.

Statiske bølgelængderutede optiske netværk er undersøgt. Overvejelser omkring styring af netværket i form af bølgelængdeallokering og design er foretaget. Ved hjælp at statistiske metoder (samtidig analyse af mange netværk) er sammenhængen mellem forskellige parametre, der beskriver netværkstopologien, og det optiske netværks effektivitet blevet klarlagt. Disse sammenhænge er vigtige ved netværk design. Det er ved hjælp af de statiske metoder blevet vist at effekten af bølgelængdekonvertere er negligable i statiske bølgelængderutede optiske netværk.

Dynamiske bølgelængderutede optiske netværk er blevet simuleret og analyseret. Styring af et dynamisk netværk er en mere kompleks opgave end styring af det statiske netværk. Flere strategier er undersøgt. Et tilsvarende studie med et reelle netværk, som alternativ til computersimulering, ville have været ekstremt kostbart eller umuligt. Forskellige rutningsmetoder er blevet undersøgt. Effekten

af bølgelængdekonvertere er blevet undersøgt og i modsætning til statiske netværk så er effekten for dynamiske netværk signifikant. Effekten af flere fibre per link er vist at være betydelig, og det er konkluderet at hverken begrænset eller fuld bølgelængdekonvertering vil finde nogen større anvendelse i helt optiske netværk. Lighed er foreslået som et nyt begreb der skal fungere som vurderingsmål for netværk i stil med blokeringssandsynlighed.

Teletrafik er blevet undesøgt med flere formål. Erlangs fikspunktligninger er blevet brugt til at bekræfte simuleringsresultater af de dynamiske optiske netværk. En eksplicit løsning til netværksblokeringssandsynligheden er blevet udviklet, og fikspunktligninger for alternativ rutning er blevet udviklet. Dels er selv similar traffik blevet undersøgt og denne effekt på optiske netværk blevet vurderet.

Det *Synkrone Optiske Hierarki* er foreslået som en en ny type optisk netværk uden de tekniske problemerne som i pakkekoplede optiske netværk og uden kapacitetsgranularitetsproblemet i bølgelængderutede optiske netværk. Forslaget er eksakt formuleret og eksperimenter er foretaget for at vurdere dets styrker. I netværk med op til to bølgelængder i kapacitetsforbrug mellem knudepar er der betydelige kapacitetsbesparelser at hente.

Netværksplanlægning i form af optimalt design af nationale og regionale telekommunikationsnetværk er blevet grundigt undersøgt og lovende programmer og metoder er blevet udviklet. Til optimeringsprocessen inddrages både kabel-, fiber- og knudeomkostninger. Hvad direkte praktisk anvendelighed angår se bidraget inden for netværksplanlægning som et af de vigtigste bidrag.

Preface and Acknowledgment

This thesis is a partial requirement for obtaining the Ph.D. degree at Research Center COM of Technical University of Denmark. The thesis reflects my work from June 1999 to June 2002 under the supervision of Lars Dittmann (Research Center COM), Bjarke Skjoldstrup (TDC Tele Danmark), and Villy Iversen (Research Center COM).

I would like to my thank supervisors, Lars Dittmann, Bjarke Skjoldstrup, and Villy Iversen, who have given me the best possible working conditions, and who have helped me out, when I needed it.

I have had a very good experience of collaboration with my colleagues, Arne Glenstrup and Thomas Stidsen, with whom I worked closely together during the three years.

Working in the Network Group at Research Center COM has been very attractive due to the professional research environment and the many good people there. In addition the people have the great ability to also include enjoyment and social pleasures.

I am grateful to the people at CUBIN, Department of Electrical & Electronic Engineering, University of Melbourne, Australia, and in particular Rod Tucker. All made my stay there very pleasant.

I thank the people at TDC Tele Danmark for the friendly atmosphere.

Thanks to TDC Tele Danmark and the Danish Agency for Trade and Industri for funding and the Danish Academy of Technical Sciences for the administration.

June 2002 Christian Fenger

List of Abbreviations

AON	All-Optical Network
ARPA	Advanced Research Project Agency
AUR	Adaptive Unconstrained Routing
CPLEX	C-implementation of the simPLEX algorithm
EXPLAIN	EXPLorative networkplAnINg
FDL	Fiber Delay Line
FR	Fixed Routing
GA	Genetic Algorithm
GAMS	General Algebraic Modeling System
Gb	Giga Bit
GB	Giga Byte
ILP	Integer Linear Programming
LSP(Q)	Limited Shared Protection (Quick)
MEMS	Mmicro-Electro-Eechnical Systems
MPLS	MultiProtocol Label Switching
MST	Minimum Spanning Tree
ND	Nominal Design
NSF	National Science Foundation
NSP(Q)	Non Shared Protection (Quick)
OSPR	Optimized Shortest Path Routing
OXC	Optical CROSS Connect
RWA	Routing and Wavelength Assignment
SAL	Simulated ALlocation
SOH	Synchronous Optical Hierarchy
SP(Q)	Shared Protection (Quick)
SSPR	Simple Shortest Path Routing
TSP	Traveling Salesman Probem
WC	Wavelength Converters
WCC	Wavelength Continuity Constraint
WDM	Wavelength Devision Multiplexing
WRON	Wavelength Routed Optical Network

Contents

Chapter 1

Introduction

1.1 Motivation

In the past decades networks have evolved from using fibers with a single wavelength to fibers using a multiple of wavelengths at greater bit rates and over longer distances. The networks have used the optical technology as point-to-point systems. I.e. at each node point the optical signal in the incoming fiber is converted to an electrical signal, processed, and then converted back to an optical signal, and sent out on an outgoing fiber. The vision is that the bulk part of transit traffic in the next generation network will be switched on the optical level, i.e. all-optical networks will appear.

The basis for much of the work in this thesis is the recent development in optical technology and the possibilities it opens up. In particular WDM (wavelength division multiplexing) poses new possibilities, but also constraints when transit traffic is switched optically. Traditionally links connecting the nodes contained fibers carrying only one directional lightpath. With WDM each fiber can carry multiple distinct wavelengths.

Today the optical signal on the fiber is converted to an electrical when it reaches the node, where it is processed and switched electronically and converted back to the optical domain, before it is retransmitted on an output fiber. In al-optical networks the bulk part of the signal is switched optically. This poses two important advantages:

- Smaller delay of signal

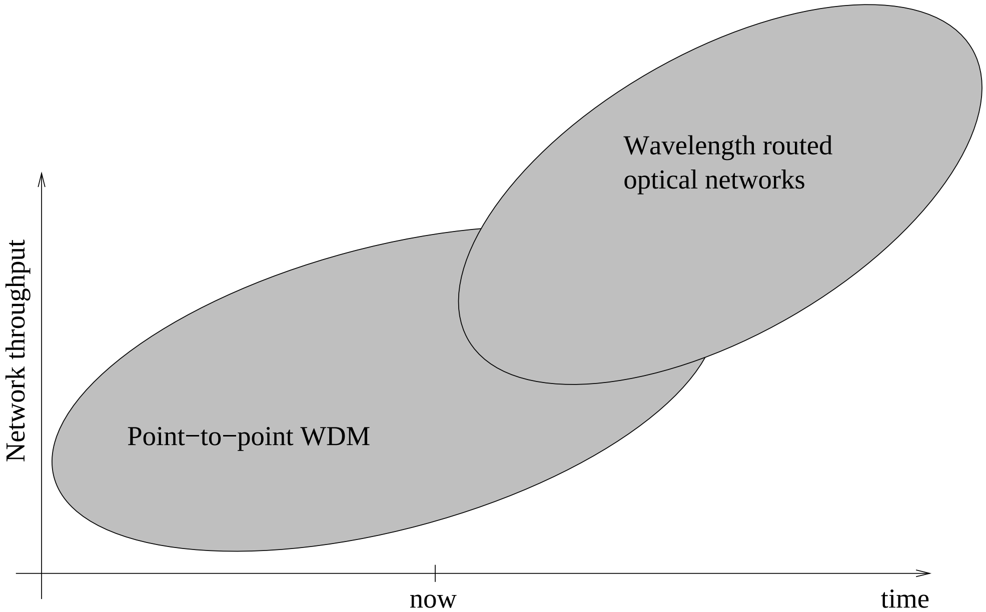

Figure 1.1: Development of optical networks from point-to-point WDM networks to all-optical networks.

- Lower cost

Smaller delay of signal: Optical cross connects are transparent, i.e. the signal travels through the node at the speed of light. In electronic cross connects extra time is spent on conversion and processing. Low delay is key for several applications like the network computer and global computing.

The advantage of electronic switching is the flexibility and fast change of switching configuration. Depending of the technology used for the optical switch the change of switching configuration can be more or less fast, but significantly less than one second. The longer switching time at current technology does not matter in backbone networks where lightpaths would be kept for hours up to years. In case of network failure fast protection becomes important, but with uptime requirement at 99.999%, corresponding to five minutes down time per year, the time used for switching becomes negligible.

Lower cost: Roberts (2000) has studied cost trends in networking. In 1975 Moore, co-founder of Intel in 1968, predicted that computing power per unit cost would double every 18 months. With data up to 1999 the historical doubling has been every 21 months. From the 1960s to 1995 the cost of leased lines required for long distance packet network only halved every 79 months. The combination of this slow decrease in communication cost and the rapid decrease in cost of computing made it economically advantageous to add computing to the network in the form of packet switching, as packet switching requires less bandwidth. From the mid 1990s at the entry of WDM with cost decrease of optical bandwidth of a factor 2 every 12 months, and increased competition the trend of communication cost changed drastically. This lead to the relative increase of switching cost, which is why it is so important to use transparent cross connects, i.e. optical cross connects.

In Figure 1.1 the vision is illustrated. Today point-to-point networks are deployed, but in short term these networks will be supplemented with wavelength routed optical networks with a potentially higher growth rate in bandwidth.

This thesis is focussed on a circuit switched optical transport layer of backbone network. Due to statistical multiplexing of the many traffic sources and the availability of cheap bandwidth then the circuit switched technology will be superior to packet switched technology in backbone networks. However, if the limit of the optical fiber is reached and bandwidth become the scarce resource, then optical packet switching in the transport layer might be preferred in backbone networks.

The issue of packet switched versus circuit switched is often distorted by the discussion of self similar traffic. Self similar is treated in Chapter 5, where one conclusion is that the relative size of bursts are diminished with aggregation in spite of what the term self similar usually implies.

Like WDM then the optical cross connect is a central element in the all-optical network. We shall here define an optical cross connect as a switching device for wavelengths where the only electronic processing is for the control signal and traffic, which is added or dropped to the all-optical network. I.e. transit traffic is kept in the optical domain.

In wavelength routed optical networks without wavelength converters then the wavelength of a lightpath in the network must remain the same at all the links it traverses. This characteristic is named the wavelength continuity constraint. With wavelength converters this constraint does not apply, but increased cost for the

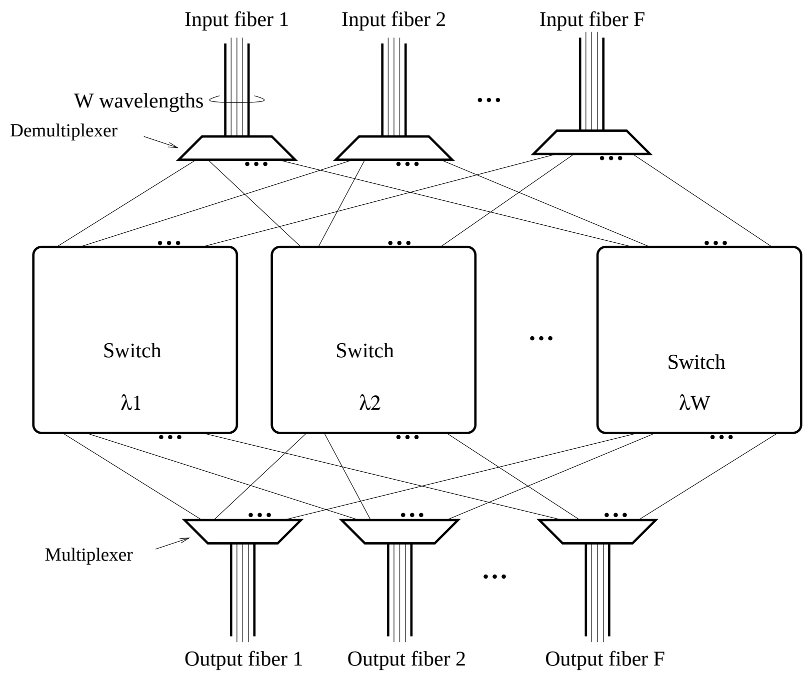

Figure 1.2: The optical cross connect without wavelength conversion capability.

converters and for potentially more complex cross connects should be reckoned in. With the wavelength continuity constraint, the lightpaths cannot change wavelength and the cross connects can consist of *W* smaller cross connects, one for each wavelength, which creates the possibility for a potentially simpler switch, since the complexity of a switch grows faster than linearly with the number of input channels. With the wavelength continuity constraint the optical cross connect can be build as sketched in Figure 1.2. in the top of the figure the input fibers arrive from one or more links. The wavelengths in the fiber are then demultiplexed so that each wavelength can be switched independently. After the switching process the wavelengths are multiplexed to the respective output fibers, which belong to one or more links.

A very promising technology for realizing the optical cross connect is MEMS (micro-electro-mechnical systems) technology. In a MEMS device, tiny mechanical and electrical elements are integrated onto a silicon chip to perform functions such as reflection, attenuation and sensing. Micro mirrors in the MEMS will switch the lightpaths from the input fibers to the correct output fiber. More types of MEMS are used for optical cross connects, one robust fit for small cross cross connect (the 2D MEMS), another has a very scalable structure but more vulnerable (the 3D MEMS). As mentioned above, when the wavelength continuity constraint applies only small optical cross connects are needed. At least 11 companies are working on the production of optical cross connects using MEMS technology, FibreSystemsEurope (June 2002).

In this thesis physical constraints are not considered because of the constant change of the properties of physical components. When it comes to the planning of a specific network then these constraints should be considered.

1.2 Thesis outline

Chapter 2 is a study of static wavelength routed optical networks. With the use of statistical models (simultaneous analysis of many networks) is the correspondence between parameters, determining the network topology, and the performance of the all-optical network been found. These dependencies are important knowledge in the process of designing a network. By use of the statistical method it is found that the effect of wavelength converters on the performance of static wavelength routed optical networks is negligible.

Chapter 3 presents simulations and analyses of dynamic wavelength routed optical networks. The alternative, to study reel networks as alternative to computer simulations, would have been extremely costly or impossible. Different routing methods have been used and studied. The effect of wavelength conversion has been analyzed and contrary to static optical networks the effect of wavelength converters on dynamic optical networks is significant. The effect on blocking probability of multiple fibers on each link is shown to be significant, and it is concluded that neither limited-range nor full wavelength conversion will find any significant use in all-optical network. Fairness is suggested as a new measure as network performance in line with network blocking probability

In Chapter 4 Erlang's fixed point equations have been used verify some results of simulation of dynamic optical networks. An explicit solution for the blocking probability has been derived, and fixed point equations for alternate routing have been derived.

Chapter 5 is a study of self similarity in teletraffic. The possible courses are discussed and it is found that both network behavior and traffic source characteristic give rise to the self similarity. It is also found that self similarity does not give rise to a dramatic increase in blocking probability on heavily aggregated links, which are typical in all-optical networks.

Chapter 6 introduces the Synchronous Optical Hierarchy. It is suggested as a new type of network to overcome the technological hurdles of packet switched optical networks and without the capacity granularity problem in wavelength routed optical networks. The solution has been exactly formulated and experiments have been performed to estimate the strengths. In networks where the typical size of a traffic demand between two nodes is up to two wavelengths, then significant capacity savings are possible.

Chapter 7 describes the work performed with two other participants of the EXPLAIN project (EXPLAIN (1998–)). Complete physical network topology design is studied for the purpose of an optimized minimal cost design. That is, the most optimal placement of duct, fibers, and switching equipment for cities not yet connected, the so called green-field design. Integer linear programming, heuristics, and metaheuristics are used for the purpose of network design.

Chapter 8 describes the work and results of using genetic algorithm for network design. Different protection types are compared, and very promising results are achieved.

Chapter 9 concludes the thesis.

The material in Chapter 2, 3, and 5 is largely based on submitted and accepted papers. The material in Chapter 6 is partly based on a published paper and to large extend on a submitted and in the moment reviewed article. The material in Chapter 7 is partly based on accepted paper. Material in Chapter 4 is not yet published due to a combination of lack of time and that this subject is on the edge of focus of this PhD project, and Chapter 8 has not yet been published, since this is completely new work.

Chapter 2

Static Optical Networks

2.1 Abstract

In this chapter the routing and wavelength assignment problem is studied, including the correlation between topology and wavelength usage. We present a statistical study of wavelength usage in relation to topology characteristics for optical WDM networks with static traffic requirements, where the traffic is routed both with and without wavelength conversion. We identify new general correlations between parameters describing network topologies and wavelength usage. We find that the regularity of a network and the number of spanning trees in a network are accurate measures of the routing efficiency in terms of wavelengths used to accommodate the required traffic. An empirical formula is given for the average number of wavelengths required to accommodate the traffic as a function of the number spanning trees in the network. We observe that in most cases, the wavelength usage with and without wavelength converters are identical. Consequently, the correlations between network topology and traffic assignment efficiency are true for both types of networks.

2.2 Introduction

Parts of this chapter have been published in Fenger et al. (2000a,b). All over the world, many new carriers are investing to deploy completely new networks based on the newest optical fiber technologies. Due to the need for higher bandwidth, the trend moves towards all-optical networks where knowledge of wavelength routed networks becomes increasingly important. Despite this increasingly competitive situation, a general knowledge base on which to build the design and planning of optical networks is still somewhat limited. Up until now, studies of the correlation between network topologies and efficiency in accommodating a certain traffic demand have been based on specific network configurations instead of systematic surveys. See Tan and Pollard (1995); Subramaniam and Barry (1997); Mokhtar and Aziõglu (1998); Baroni et al. (1999). In this new work, we randomly generate a large number of networks of different topologies and study statistically how well the traffic is accommodated in networks with and without wavelength converters as a function of a number of well defined parameters describing the network topology. We can thereby generate a general knowledge base for network designers.

Chlamtac et al. (1989, 1992) proposes wavelength routed optical networks. So called Lightnets are proposed, where optical channels are seen as physical connections, such that the nodes get more neighbors and the diameter in the network is diminished. In Baroni and Bayvel (1997) statistics have been used to study the correlation between topological parameters and network performance. The network performance is measured as function of the physical connectivity, that is, the number of links in the network. In this chapter the number of links are typically fixed and the network is characterized topologically by number of spanning trees and variance of node degree. Uniform traffic is used in both to keep the parameter space restricted. It has previously been shown that wavelength conversion does not lead to a reduction in number of wavelength needed to allocate the traffic demands. This is verified in this chapter in more general terms.

In Section 2.3 we define the problem and describe the routing and wavelength assignment algorithms used for networks with and without wavelength converters. Section 2.4 defines the problems of routing and wavelength assignment mathematically. In Section 2.5 we present the results.

2.3 Problem and algorithm description

The goal of this work is to obtain a general understanding of how different WDM network topologies affect the number of wavelengths required to accommodate a given set of traffic demands. This is achieved by randomly generating a large number of networks (several million) for given numbers of nodes and links. The wavelength usage is evaluated for each network as a function of the average node degree, variance of the node degree, and the number of spanning trees as described in detail in Section 2.5. The degree, d, of a node is the number of links incident on the node, as shown in Figure 2.1. General statistical results are then obtained by averaging over all generated networks for each of these parameters. For each topology we assume one fiber per link, no upper limit on the number of

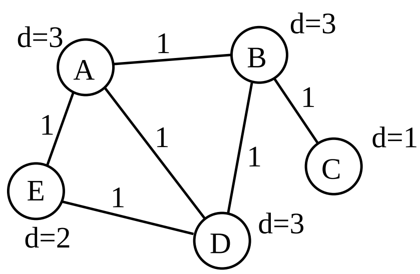

$$T = \begin{bmatrix} 0 & 1 & 1 & 1 & 1 \\ 1 & 0 & 1 & 1 & 1 \\ 1 & 1 & 0 & 1 & 1 \\ 1 & 1 & 1 & 0 & 1 \\ 1 & 1 & 1 & 1 & 0 \end{bmatrix}$$

$$W = \begin{bmatrix} 0 & 1 & \infty & 1 & 1 \\ 1 & 0 & 1 & 1 & \infty \\ \infty & 1 & 0 & \infty & \infty \\ 1 & 1 & \infty & 0 & 1 \\ 1 & \infty & \infty & 1 & 0 \end{bmatrix}$$

Figure 2.1: Example of a network with 5 nodes and 6 links. The weight is one between physical connections. The degree is given for each node. The average node degree is 2.4, and the variance of the node degree is 0.8. The network traffic, T, and link weight, W, matrices are also shown.

wavelengths, uniform traffic, uniform link weight, and bi-directional links. The element of the traffic matrix, $T(i, j)$, gives the traffic between node i and node j in terms of number of wavelengths while the element of the link weight matrix, $W(i, j)$, indicates the distance between node i to node j. Since we in this chapter use hops as the distance measure the element is one if the two nodes are directly connected and infinite otherwise. As an example, consider the network in Figure 2.1.

2.3.1 The Algorithm for networks without wavelength converters

The algorithm for networks without wavelength converters contains basically three steps as described below. Due to the huge number of randomly generated networks (several million), we have carefully chosen well-known and efficient algorithms of low complexity. The routing algorithm is an algorithm by Floyd (1962) that calculates the shortest path of all node pairs with complexity $O(N^3)$, where N is the number of nodes in the network. When all routes are known, the wavelength assignment problem is transformed into a graph coloring problem. It is done by creating a graph for the path collisions such that each node of this graph corresponds to a path and two nodes are adjacent if their corresponding paths share at least one link in the network topology. The obtained path collision graph must then be colored such that no two adjacent nodes have the same color. We chose to solve this problem by using a well-known graph coloring heuristic algorithm called the *largest-first* or the *descending-order-of-degree* algorithm, Welsh and Powell (1967). Since the path collision graph has $N(N-1)/2$ nodes, where N is the number of nodes in the network, then the complexity of the *largest-first* algorithm is $O(N^4)$. This algorithm basically allocates the lowest numbered color to the nodes of larger degree first. To ensure that the results for wavelength usage for networks without wavelength converters do not depend on the graph coloring algorithm efficiency, the *largest-first* algorithm has been compared to the more complex, slower by generally better performing, *Dsatur* graph coloring algorithm, Brelaz (1979). The path collision graphs is also used in Hyytia and Virtamo (1998). In Chlamtac et al. (1992); Ramaswami and Sivarajan (1995); Baroni and Bayvel (1997) a path collision graph is not created, but the paths colored according the length starting with the longest, assuming that the longer paths have more collisions with other paths. That method is faster and requires less memory, but the coloring will be less optimal, which implies a higher wavelength usage. Results are discussed in Section 2.5.

The steps in the algorithm for no wavelength conversion are:

1) A connected network is randomly generated for a given number of nodes and links.
2) The paths between all node pairs are determined using a shortest path algorithm, Floyd (1962).
3) Wavelengths are assigned by transforming the wavelength assignment problem into the graph colouring problem under the restriction that two identical wavelengths cannot share the same link and no wavelength conversion can take place. The graph is coloured using a graph colouring algorithm.

2.3.2 The algorithm for networks with wavelength converters

For networks with wavelength converters the algorithm for determining the number of wavelength needed is simplified. Step three above is replaced with

3) Determine the number of demands on the most congested link

This step is considerably faster and uses a relative negligible amount of memory.

2.4 Mathematical formulation

In this section we define the routing and wavelength assignment problem mathematically both with and without wavelength converters. Note that the routing and wavelength assignment problem with wavelength conversion is simply optimized shortest path routing define by the mathematical formulation below and explained in more detail in Chapter 3 and Section 6.6.2. N is the number of nodes. W is the number of required wavelengths.

2.4.1 Routing and wavelength assignment without conversion

This is the exact definition of the routing and wavelength assignment problem which is NP-hard (Garay and Johnson (1979a)).

indexes:

$$\begin{array}{rcll} s,d,i,j & \in & \{1,\ldots,N\} & \text{network nodes} \\ w & \in & \{1,\ldots,W\} & \text{wavelengths} \end{array}$$

Constants

c_{ij}	connection matrix, integer
Λ_{sd}	demand between node d and s, integer

Variables

W	number of used wavelengths, integer
x_{ij}^{sdw}	flow for node pair s,d on link i,j on wavelength w, integer
λ_{sdw}	flow for node pair s,d on wavelength w, integer

Objective Minimize W

Constraints

$$
\begin{array}{rclll}
\sum_{s,d,w} x_{ij}^{sdw} \leq W & = & W & \forall i,j & \text{wavelength usage} \\
\sum_i x_{ij}^{sdw} - \sum_k x_{jk}^{sdw} & = & \begin{cases} -\lambda_{sdw} & \text{if } s = i \\ \lambda_{sdw} & \text{if } d = j \\ 0 & \text{otherwise} \end{cases} & \forall j,s,d,w & \text{flow conservation} \\
\sum_w \lambda_{sdw} & = & \Lambda_{sd}, & \forall s,d & \text{satisfy all demands} \\
x_{ij}^{sdw} & \leq & c_{ij}, & \forall i,j & \text{only flow on links} \\
\sum_{s,d} x_{ij}^{sdw} & \leq & 1, & \forall w,i,j & \text{WCC}
\end{array}
$$

2.4.2 Routing and wavelength assignment with conversion

When wavelength converters are present, then the wavelength of a flow on a specific link does not matter. Therefore the index w is removed from this formulation.

indexes:

$$s,d,i,j \quad \in \quad \{1,\ldots,N\} \quad \text{network nodes}$$

Constants

c_{ij}	connection matrix, integer
Λ_{sd}	demand between node d and s, integer

Variables

W	number of used wavelengths, integer
x_{ij}^{sd}	flow for node pair s, d on link i, j, integer

Objective Minimize W

Constraints

$$\begin{array}{rcll}
\sum_{s,d} x_{ij}^{sd} \leq W & = & W & \forall i, j \quad \text{wavelength usage} \\
\sum_i x_{ij}^{sd} - \sum_k x_{jk}^{sd} & = & \begin{cases} -\Lambda_{sdw} & \text{if } s = i \\ \Lambda_{sdw} & \text{if } d = j \\ 0 & \text{otherwise} \end{cases} & \forall j, s, d \quad \text{flow conservation} \\
x_{ij}^{sd} & \leq & c_{ij}, & \forall i, j \quad \text{only flow on links}
\end{array}$$

2.5 Results and discussion

Efficient network planning is a complex challenge and knowledge of any general trends in network performance in relation to network topology is desirable as it can reduce planning complexity. Therefore, network planners need reliable parameters to characterize network topologies.

The variance of the node degree is one such parameter as it gives a simple measure of the network regularity (i.e. the variance of the node degree) and complements the information given by the average node degree. In Figure 2.2 we have plotted the average number of wavelengths required to accommodate the traffic demand as a function of the variance of the node degree. As seen, the number of wavelengths used grows with the variance, and the network uses a minimum of wavelengths when it is regular (all nodes are of the same degree). To see how many topologies satisfy the low variance requirement, we have also generated the probability density of the variance of the node degree, as shown in Figure 2.5. As

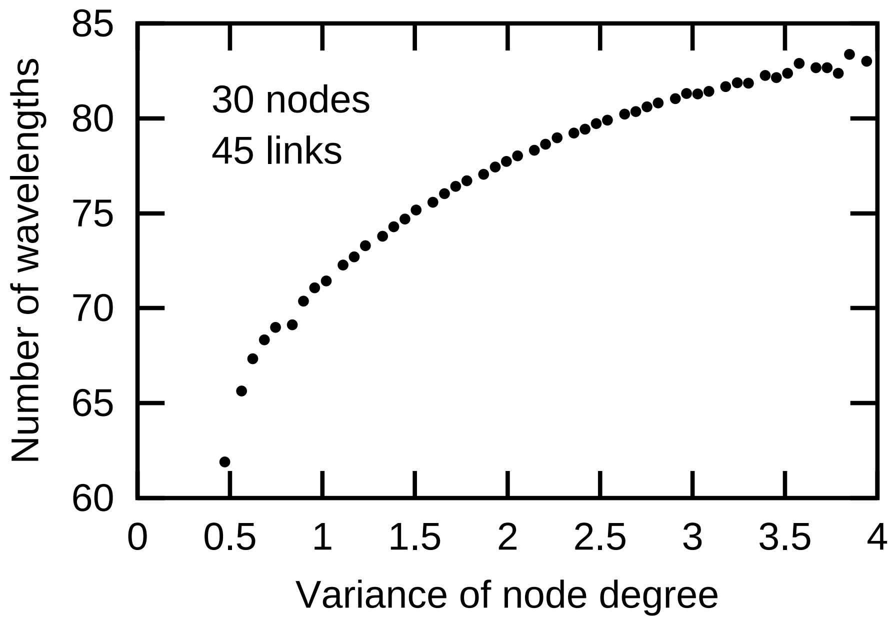

Figure 2.2: Average usage of wavelengths as a function of the variance of the node degree.

seen, very few topologies have very low variance of node degree. This suggests that the number of calculations performed by network optimization algorithms can drastically be reduced.

Another important and more informative parameter for characterizing the topology of an optical network is the number of spanning trees in the network. A tree is a subnetwork of a network, which does not contain any loops, and a spanning tree of a network is a tree containing all nodes of the network. The network shown in Figure 2.1 contains eight spanning trees. The number of spanning trees is a measure of the number of possible routes between nodes in the network. It easily identifies the restriction in the number of routes due to links that disconnect the network when removed (cut-edges). The calculation of the number of spanning trees, S, in a network is easily obtained by calculating the determinant of the product of the matrix A and its transposed matrix A^t where A is an incidence matrix of a directed graph obtained by assigning orientations to the edges of the network

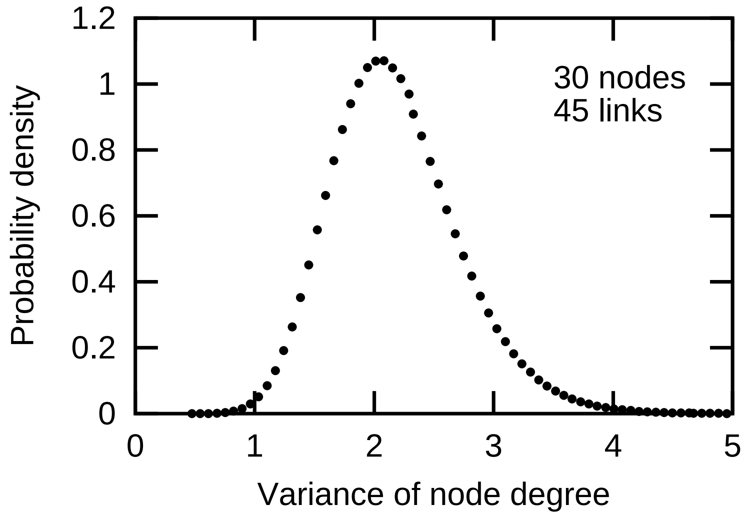

Figure 2.3: Probability density of the variance of the node degree. Notice that the distribution is discrete, due to the limited number of possible variances of node degree. Data from 4 million networks are used for the plots.

topology graph such that no self-loops appears with one row deleted Thulasiraman and Swamy (1992):

$$S = \det(AA^t)$$

In Figure 2.4 we show the average number of wavelengths required as a function of the number of spanning trees in the network. The simulation points form straight lines for two orders of magnitude, on a double-log scale, indicating a power-law. A comparison of the curves shows that the exponent does not depend on the number of links, but only on the number of nodes, and is approximately given by $-3/N$.

The equation below gives the dependency of the average wavelength usage, $\langle\lambda\rangle$, on the number of nodes, N, the number of links, L, and the number of spanning trees, S.

For large networks (more than 10 nodes) with a modest average node degree (3-6) we therefore get an empirical law for the average use of wavelengths as function of the number of spanning trees, S, when the number of nodes, N, and

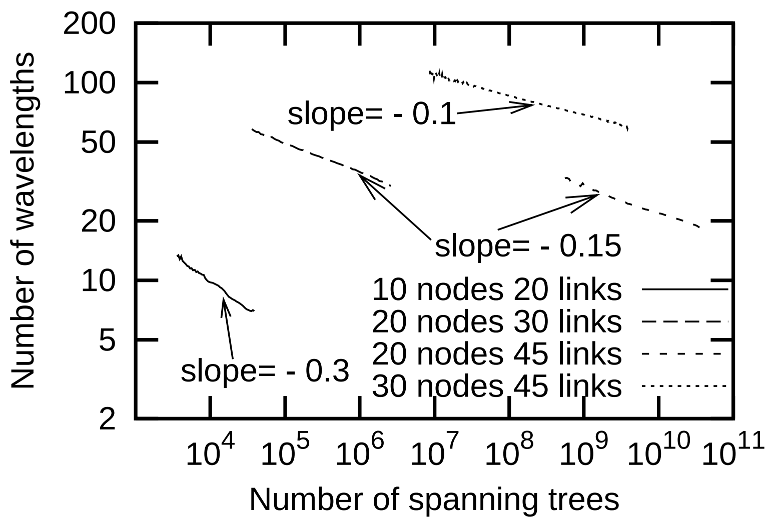

Figure 2.4: Average usage of wavelengths as a function of the number of spanning trees.

the number of links, L, are held constant:

$$\boxed{\langle\lambda\rangle = \alpha(N,L)\cdot S^{-3/N}}$$

Here α is an increasing function of L and a slowly decreasing function of N. For very small networks or very strongly or sparsely connected networks the universal feature expressed by the power-law is disturbed. As the number of nodes rises (while the number of links is held constant) α drops, and as the number of links rises (while the number of nodes is held constant) α rises.

From this general equation the network planner can get an insight into the wavelength usage of the type of topology to which a specific network belongs.

The average node degree is also a relevant parameter for the network planners. In Figure 2.5 we see the relationship between the average node degree and number of wavelengths required to satisfy the traffic demand. To easily compare the results for different network sizes, the number of wavelengths is scaled with the total traffic demand. It is seen that the gain from raising the average node degree from small values has a significant impact on the decrease in wavelength usage, whereas a raise from larger values only has a small effect. This change

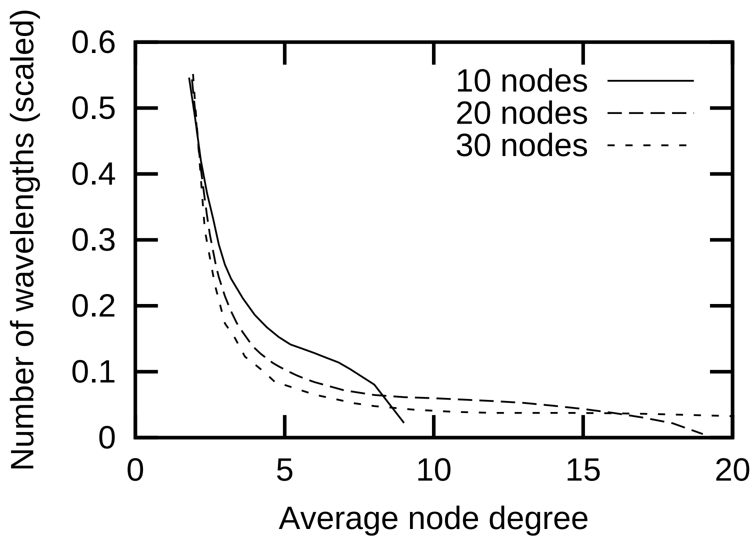

Figure 2.5: Average usage of wavelengths, scaled with the total traffic, as a function of the average node degree.

in gain from raising the average node degree occurs around an average node degree of 4-5 for all networks, indicating that these are near optimum values. In the following section, we investigate wavelength usage for networks with wavelength converters as a function of the same topology parameters, namely the variance of the node degree and the number of spanning trees. Second it is seen that the performance of the algorithm actually rises with the size of the network. Where the performance is measure as the number wavelengths used scaled with the total traffic when the average node degree is held constant. As the total traffic scales with square of the number of nodes and the number of links for a constant average degree scales with the number of nodes, then the number of wavelengths divided by the total traffic should be constant in a network, which does not scale. Here we see that the traffic is more efficiently accommodated for larger networks.

The smallest network displaying a difference between with and without wavelength converters is shown in Figure 2.6. It contains 7 nodes and 6 links. The difference in wavelength usage is 2. When traffic is not uniform minimum network displaying a difference is the 3 node star network, Figure 2.7. In Chapter 6 we find for a special case, the Pan-European network in Figure 6.3, that the difference in wavelength usage for non-uniform traffic is negligible, but the difference remains to be quantified statistically.

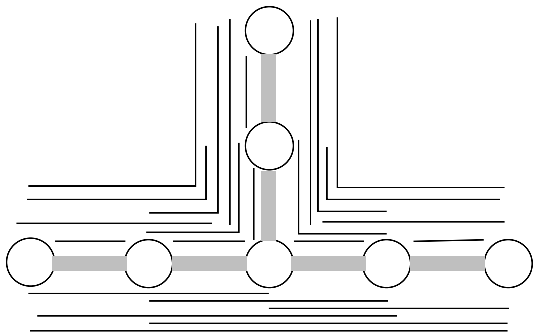

Figure 2.6: Minimum sized network where number of paths on the maximum loaded link differs from the number of wavelengths needed to allocate the traffic. The number of paths on the maximum loaded link is 10 whereas the minimum number of wavelengths needed is 12.

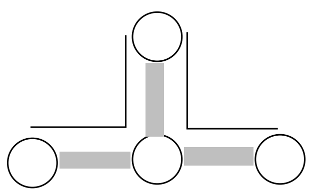

Figure 2.7: Minimum sized network with nonuniform traffic where number of paths on the maximum loaded link differs from the number of wavelengths needed to allocate the traffic. The number of paths on the maximum loaded link is 2 whereas the minimum number of wavelengths needed is 3.

2.6 Comparison with wavelength conversion

The statistical results estimated over millions of networks show that the correlation between topologies and wavelength usage is exactly similar for networks with

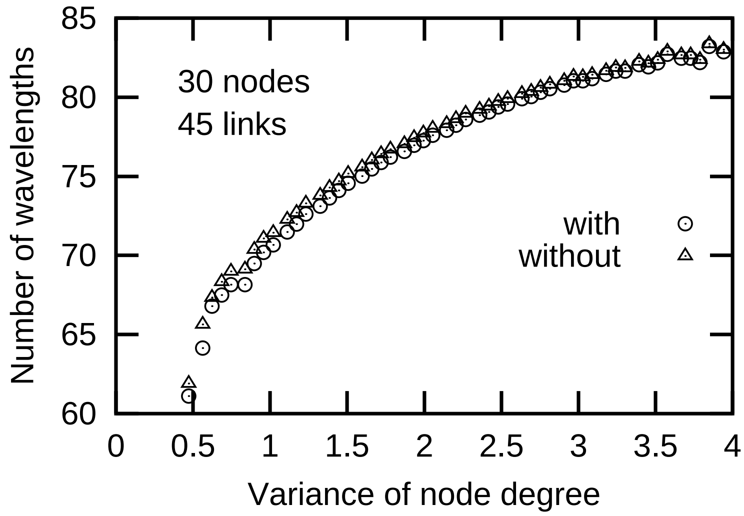

Figure 2.8: Average usage of wavelengths as a function of the variance of the node degree with wavelength converters and without wavelength converters.

and without wavelength converters. However, small differences in wavelength usage were noticed and are discussed in this section. In Figure 2.8 the average usage of wavelength is plotted for networks with and without wavelength converters as a function of the variance of node degree for networks of 30 nodes and 45 links. Although it reduces the blocking probability and reduces management complexity for dynamic traffic assignment it has no (or only a very small) effect on static routing. The curves indicate a very small difference in the number of wavelengths required to assign the traffic. The difference, when it exists, is generally of the order of one or two wavelengths which represents, on average for all networks, an increase in wavelength usage of only 0.5%.

Contrary to what was expected, the difference in wavelength usage increases for networks with small variances (regular networks) as shown in Figure 2.9. We believe that this is mainly due to the increase in the inefficiency of the *largest-first* graph coloring algorithm as the networks become more regular. To verify this assertion, we have in a provisional study compared the *largest-first* algorithm to the more complex graph coloring algorithm, *Dsatur* Brelaz (1979), in which the *Dsatur* algorithm proved better than the *largest-first* by sometimes using fewer

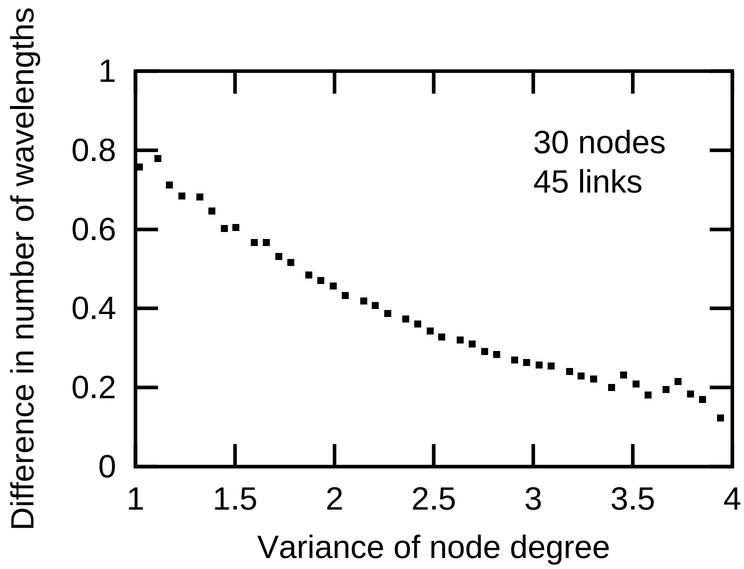

Figure 2.9: Difference in average usage of wavelengths between traffic with and without wavelength converters as a function of the variance of the node degree.

wavelengths in the few cases where the network with wavelength converters had a lower wavelength usage. This matter is, however, still under investigation. The conclusion in Hyytia and Virtamo (1998) was however that the coloring of paths in static wavelength routed optical networks is an easy coloring problem, i.e. more advanced coloring problems does not improve wavelength usage. See also Parkinson and Warren (1995) for a comparison between different heuristic methods of graph coloring.

In Figure 2.10, the wavelength usage for networks with and without wavelength converters is plotted versus the number of spanning trees of the network topologies. Results for networks without wavelength converters are shown for the *largest-first* graph coloring algorithm. It is clearly seen that the analytical formula of Section 2.5 is still valid for networks with wavelength converters.

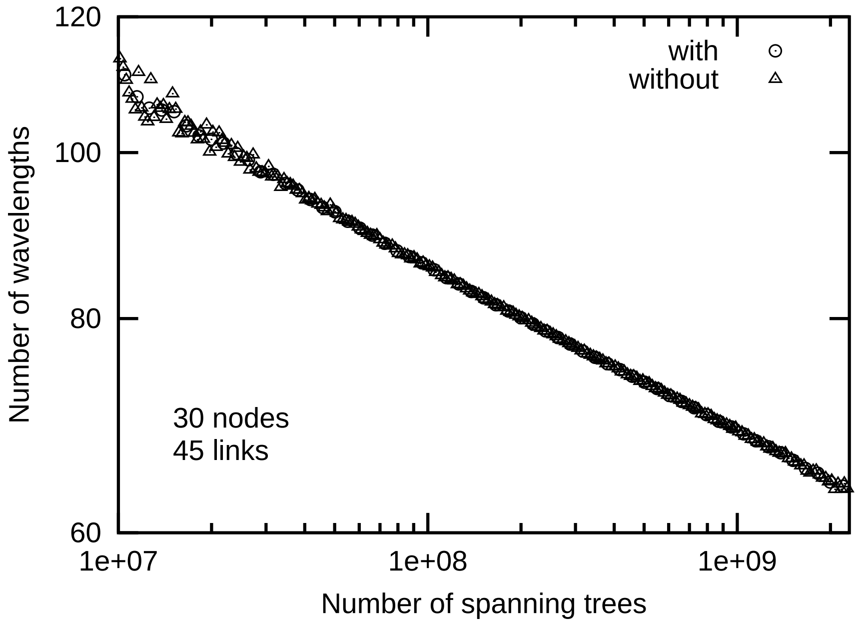

Figure 2.10: Average usage of wavelengths as a function of the number of spanning trees with wavelength converters and without wavelength converters.

2.7 Conclusion

This chapter contains a thorough investigation of the influence of network topology on wavelength usage. This investigation was done through an exhaustive statistical study of randomly generated topologies for networks with and without wavelength converters. We define general parameters that accurately describe network topology properties and clearly identify the correlation between the topology properties and the wavelength usage in networks. The correlations are exactly identical for networks with and without wavelength converters. I.e. previous results showing that wavelength converters have a negligible effect on wavelength usage for intelligently colored lightpaths is static wavelength routed optical networks are verified. It is shown that for a given number of nodes there are only very few topologies that perform efficiently in terms of wavelength usage and we indicate the criteria that identifies them. These criteria can be used to simplify the optimization process during network planning.

We have shown that, in general, networks that have an average node degree of 4-5 and a low node degree variance are among the best possible in terms of wavelength usage and from a cost points of view. Furthermore, we have clearly identified the number of spanning trees as a very accurate measure of the quality of a network in terms of traffic accommodation efficiency, such that a large number of spanning trees induces a low wavelength usage. A simple equation for the average number of wavelengths required for a given topology as a function of the number of the nodes, links, and spanning trees it contains has been empirically derived.

This study was performed for networks with uniform traffic requirements. In Chapter 6 we find for a special case, the Pan-European network in Figure 6.3, that the difference in wavelength usage for non-uniform traffic is negligible, but the difference remains to be quantified statistically. The routing method used in this chapter is simple shortest path routing, which requires a higher wavelength usage than optimized shortest path routing. Due to time limitations the results for this chapter is from using simple shortest path routing although the routing and wavelength assignment has been modified to have the option of using optimized shortest path routing. For more elaborate discussions of these routing methods see Chapter 3 and 6. From an example in Chapter 6 optimized shortest path routing does not seem to change the difference in wavelength usage between with and without wavelength converters in the case of static wavelength routed optical networks. This does, however, still need to be clarified and quantified statistically. The feature of having confidence intervals for the data points displaying averages has been implemented, but due to lack of time the experiments have not been remade. In conclusion, we present a statistical analysis of the general network behavior in terms of wavelength usage over a very large number of network topologies and obtain general trends as well as a formula that can drastically narrow down the number of solutions that need to be considered when designing a network.

Chapter 3

Dynamic Optical Networks

3.1 Abstract

Dynamic wavelength routed all-optical networks are studied in this chapter and performance evaluations are performed. We present results of computer simulations of network topologies where traffic demands, given in the granularity of wavelengths, are set up and released dynamically. The simulations are made with a simulator developed from scratch for maximum flexibility. It can simulate wavelength routed traffic for any network topology, traffic distribution, and multiple fibers between nodes. Different wavelength assignment and routing methods are applied. This flexibility is new and many combinations of these features have not been reported previously.

In this chapter we show results of simulations where we study the blocking probability for a given network, fiber placement, and traffic distribution. We study the blocking probability for different routing methods with and without wavelength converters, and we study the trade off between having many wavelength on a fiber and having many fibers on a link.

For scientific reasons it is essential to have simulation results to verify approximate analytical models. In the case of deployment of wavelength routed networks with appearance and disappearance of traffic demands it is important to run simulations before deployment for correct dimensioning and topology. The simulation tool can be the experimental platform for testing new ideas for validity. Corresponding studies on real networks would at present be impossible or

very costly.

A novel definition of fairness in a network is introduced. It is a measure of how equal different source-destination pairs are treated with respect to blocking probability. High fairness is key for performance guaranties. Networks and routing and wavelength assignment strategies should not only be compared on overall blocking probability but also on fairness. It is found that both the inclusion of wavelength converters and the use adaptive unconstrained routing increases fairness in the network.

Independently of network topology, routing method, and the inclusion of wavelength converters, we find that the overall blocking probability in the network displays power-law behavior as function of the offered load, when the blocking probability is small.

3.2 Introduction

Some parts of this chapter has been published in Fenger and Tucker (2002). Several types of optical networks have been proposed, such as optical link networks, broadcast-and-select networks, wavelength routed networks, and photonic packet-switched networks Veeraraghavan et al. (2001). A promising solution for high capacity networks is the wavelength routed network, since it accommodates high traffic loads and seems technologically feasible. In wavelength routed networks connections are set up as lightpaths, which are routed through the networks without any electrical to optical conversion.

We study here all-optical wavelength routed WDM networks with optical switches in the nodes, where the lightpaths are routed dynamically. The lightpaths are switched individually from one fiber to another.

Today, emerging commercial optical cross connects are based on micro-electro-mechanical systems, which operate in the order of milliseconds. Much faster cross connects could be available with technology based on semiconductor optical amplifiers.

The protocol needed to manage an all-optical wavelength routed network is suggested to make use of MPLS in the control plane of optical cross connects (multi protocol lambda switching), which will allow for lightpaths to be set up and released on demand Awduche and Rekhter (2001).

In recent years there has been much focus on the factors determining performance of wavelength routed networks. These factors include the topology of the networks, the routing and wavelength assignment methods, the effect of wavelength conversion, and the effect of having multiple fibers on each link.

For maximum flexibility we have developed a simulator written in C++ to simulate traffic in wavelength routed optical networks. The point is to be able to test routing and wavelength assignment strategies for different traffic distribution. Further the simulator should be used before deployment of optical networks for correct dimensioning. Testing different network architectures with forecasted traffic and assumed routing and wavelength assignment strategies before deployment is key for correct dimensioning and architecture of the network.

In this chapter these questions will be studied by simulating traffic dynamically on wavelength routed networks. Several papers have presented simulations of dynamically wavelength routed networks Ramaswami and Sivarajan (1995); Chlamtac et al. (1992); Birman (1996), but with fixed or alternate routing and only treatment of the case with a single fiber on each link. In Karasan and Ayanoglu (1998) a fixed alternate routing algorithm is studied where the choice of path depends on the network state, Least Loaded Routing Karasan and Ayanoglu (1998). Eight wavelengths on each fiber is considered, where each fiber is bidirectional and connections are full duplex. Networks with multiple fibers on each link are studied, but the number of fibers on each links are heterogeneously distributed. In Mokhtar and Aziõglu (1998) an adaptive unconstrained routing algorithm is studied for up to 8 wavelengths on each fiber. The case of two fibers on each link is studied, but for fixed routing.

We consider many wavelengths (up to 256) on each fiber and many fibers (up to 256) on each link in each direction. Part of our study of networks with multiple fibers on each link can be viewed as a study of limited wavelength conversion Ramaswami and Sivarajan (1998), which has only been simulated on smaller networks and with fixed routing Yates et al. (1996); Tripathi and Sivarajan (2000), but is here performed for adaptive unconstrained routing and realistic sized networks, 30 nodes and 47 links.

We characterize a network by a number of nodes and links. Every node acts as a source and destination for traffic, which is dynamically set up and released in the granularity of lightpaths. The links connect the nodes by optical fibers. One or more fibers in each direction can associated with a link. Each lightpath is transmitted from its source to its destination through a number of nodes and links on its path, and is switched by optical cross connects in the nodes. The non blocking cross connects are all either with or without wavelength converters. In the case of no wavelength conversion then the wavelength continuity constraint applies. Lightpaths with the same wavelength must therefore use fiber-disjoint routes.

Because of common practice we have in these simulations chosen the traffic to be pure chance - type 1. That is, Poisson arrivals, i.e. exponentially distributed inter arrival times of traffic demands with identical parameter for all node pairs, and exponentially distributed life time of the traffic demand with the parameter depending on the source and destination of the traffic demand. The true distribution describing the traffic in an all-optical network will depend on the services running on the network and the level of aggregation.

When a traffic demand arises, then a path through the network from origin to destination is assigned if idle capacity is available. If it is not possible to find a path then the lightpath is blocked and lost. No buffering is used.

We use the following terms for describing the traffic in the simulations. The *offered traffic* is the average number of demanded concurrent lightpaths, the *carried traffic* is the average number of concurrent lightpaths in the network, *blocked traffic* is the offered traffic subtracted the carried traffic, and the *blocking probability* is the blocked traffic divided by the offered traffic.

Below we sketch the simulator in pseudo code. In addition to the stated steps the effect of a transient has been removed.

Table 3.1: Pseudo code for the Simulator

(1) Define network, routing parameters and total number of demands.

(2) Increment the time by an amount, which is determined from the inter arrival time distribution.

(3) Terminate lightpaths for which life time is reached.

(4) Assign source and destination to new lightpath.

(5) Assign a life time to the lightpath determined by the life time distribution for this source and destination.

(6) Route and assign wavelength to lightpath according to chosen methods.

(7) If total number of demands has been offered then end otherwise go to (2)

We have used the two networks, Arpa2 and NSF, seen in Figures 3.1 and 3.2.

The Arpa2 network with 21 nodes and 26 links is smaller and more spare and the NSF with 30 nodes and 47 links is larger and more connected. The traffic is chosen to be uniformly distributed, that is, on average the offered traffic loads between all node pairs are equal.

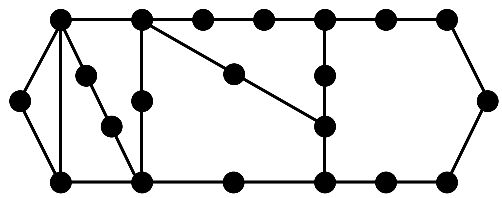

Figure 3.1: Arpa2 network, 21 nodes, 26 links.

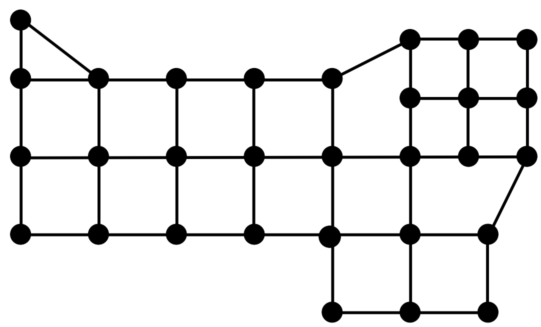

Figure 3.2: NSF network, 30 nodes, 47 links.

3.3 Routing and wavelength assignment

When a demand for a lightpath between two nodes arises, then the lightpath has to be routed in the network and a wavelength has to be assigned to the lightpath. We use two different routing and wavelength assignment methods, *fixed routing with first-fit wavelength assignment* and *adaptive unconstrained routing*.

In fixed routing with first-fit wavelength assignment a traffic demand is allocated on a predetermined path between the source and destination nodes, if capacity is available, after which the wavelength is chosen. Fixed routing is a fast method because the routes are predetermined and fixed throughout the simulation. It is simple, since the routes do not depend on the network state. The routes are chosen using a shortest path algorithm, and also called fixed shortest path routing Schwartz and Stern (1980). In the literature of dynamic routing it is not specified how the shortest path are chosen except for the routing algorithm: the Dijkstra algorithm, Dijkstra (1959), the Floyd algorithm Floyd (1962), and the Bellman-Ford algorithm Bellman (1958); Ford (1956).

As in Fenger and Glenstrup (2002a) we distinguish between simple shortest path routing (SSPR) and optimized shortest path routing (OSPR). Both routing methods refer to complete routing between all node pairs in the networks between which a traffic demand exists. We define simple shortest path routing as routing using shortest paths without consideration of congestion of the links. Optimized shortest path routing is defined as routing making use of only shortest paths, but where the paths are chosen such that the link with the highest traffic load carries as little traffic as possible. The metric used here is number of hops. For simplicity only one path for each demand is considered. Finding the routes for which the link with the highest traffic load carries as little traffic as possible can be a time costly affair and there is a trade off with time. Further the routes from OSPR do not necessarily yield the lowest blocking as they minimized the wavelength usage in static all-optical networks as seen in Chapter 2.

The method for finding the optimized shortest path routing used here is similar to the one used in Baroni and Bayvel (1997). It is a near optimal method, i.e. we can not guarantee that the most congested link carries as little traffic as possible, but almost. When routing the traffic demands, we employ shortest path routing, using the number of hops as the distance measure. Since usually more than one shortest path exists between each node pair a certain degree of freedom is available and is used to balance, as evenly as possible, the paths among all the links. This contributes to the reduction of number of lightpaths to be rerouted in case of a link failure and to minimize the network wavelength requirement. The path allocation is performed as follows: For each node pair an alternative shortest path substitutes the one previously assigned when the number of channels used on the most loaded link with the alternative path is lower. The process is repeated until no further improvement can be made. Although allowing longer paths than the shortest path between a node pair could lower the the number of channels used on the most loaded link, we do not allow this, since the overall capacity usage would be increased. For simplicity we route all demands between two nodes on the same path. The routing depends on the traffic demands; when the demands change, rerouting must be performed.

The *first-fit* wavelength assignment method is used, because it is efficient and simple in the way that it does not require information about the network state. Different wavelength assignment methods were compared in Karasan and Ayanoglu (1998); Mokhtar and Aziõglu (1998); Harai et al. (1997). In the first-fit method the wavelengths are preordered, and a lightpath is assigned a wavelength by choosing the first available free wavelength. In the case of multiple fibers per link, the fibers too are ordered. When a traffic demand arises then the first ordered fiber leaving the source node with an available lightpath, which can accommodate the traffic demand, is chosen. Then the first ordered wavelength, which can accommodate the traffic demand, is chosen. On each link the lowest available fiber is chosen. We made simulations where we instead of choosing the lowest ordered fiber, chose the fibers randomly, but no statistical significant change in the blocking probability could be observed.

The second routing and wavelength assignment method is adaptive unconstrained routing Mokhtar and Aziõglu (1998). The paths and wavelengths used are found as the traffic demands arise, whereby these paths depend on the network state. When a traffic request arises the shortest available path is found for each wavelength using a shortest path algorithm. If two paths are equally short then the least loaded path will be chosen. If two paths are equally loaded then the path which can accommodate the lowest wavelength is chosen.

We will see that adaptive unconstrained routing is superior to fixed routing in capability of allocating traffic, but it is also, due to its adaptability, well suited in cases of link and node failures where restoration needs to be included.

3.4 Results

3.4.1 Simulation

As seen from Table 3.1 traffic is set up and taken down. This will result is a fluctuating amount of carried traffic in the network. In Figure 3.3 the carried amount of traffic in the first 10 time units. Since no traffic is allocated at time zero, then the graphs start in $(0,0)$. To avoid any influence of this effect in the measurements of blocking etc., then the typical time simulated to avoid any transient effects is

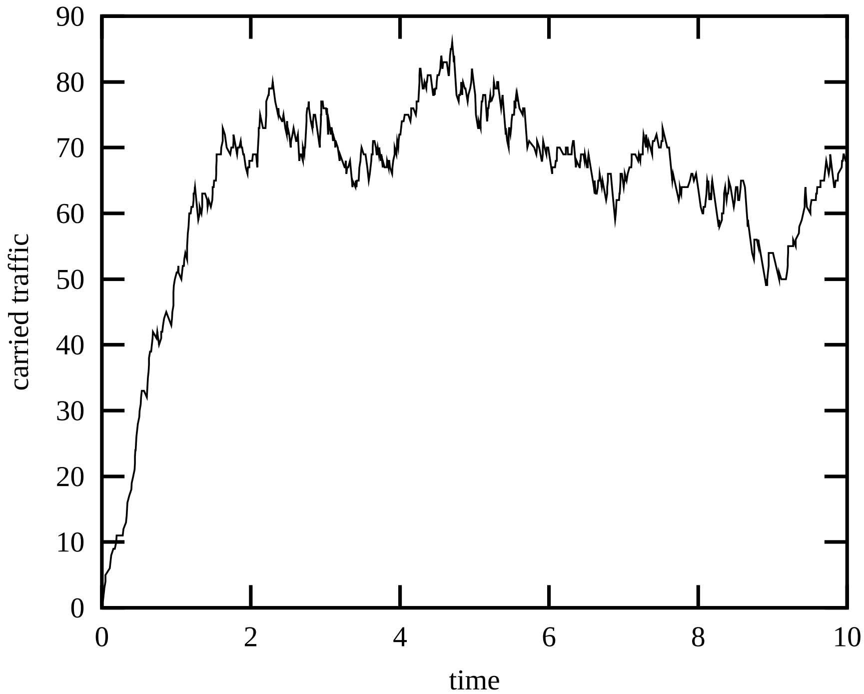

Figure 3.3: Simulation. 8 wavelengths, single fiber, offered traffic: 70 erlang. NSFnet.

time 100 times the simulation time in Figure 3.3. In Figure 3.4 is displayed the carried traffic for the first 100 time units. With a load 70 erlang, then 100 time units correspond to about 7000 traffic demand appearances.

3.4.2 Routing methods and wavelength conversion

In Figure 3.5 we evaluate different routing methods. Plots have been made for fixed routing without wavelength converters, fixed routing with wavelength converters, adaptive unconstrained routing without wavelength converters, and adaptive unconstrained routing with wavelength converters denoted by FR, FR/WC, AUR, and AUR/WC, respectively, in the key field of the figure. Each data point is

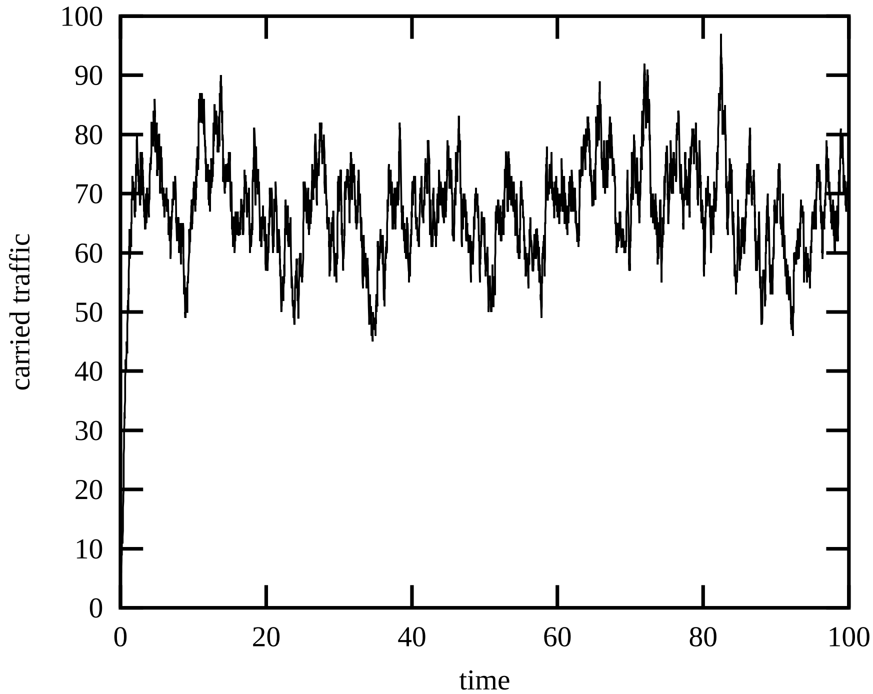

Figure 3.4: Simulation. 8 wavelengths, single fiber, offered traffic: 70 erlang. NSFnet.

the output of up to 10^8 traffic demands arises.

The bars shown illustrate the *95 percent confidence interval*, which is calculated by use of the method of batch means, which take into account that the probability of demands being blocked is correlated in time. That the blocking are indeed correlated is seen by the fact that the variance if the estimated mean blocking probability obtained through the method of batch means is higher than the variance obtained by assuming that the blocking occurs truly randomly. To calculate the confidence interval the observations of weather or not a traffic demands has been blocked is treated as a random variable which gives a series of zeroes and ones. Zero representing no blocking and one representing a block. The average blocking probability, P_B, is the average of this series. If the observations

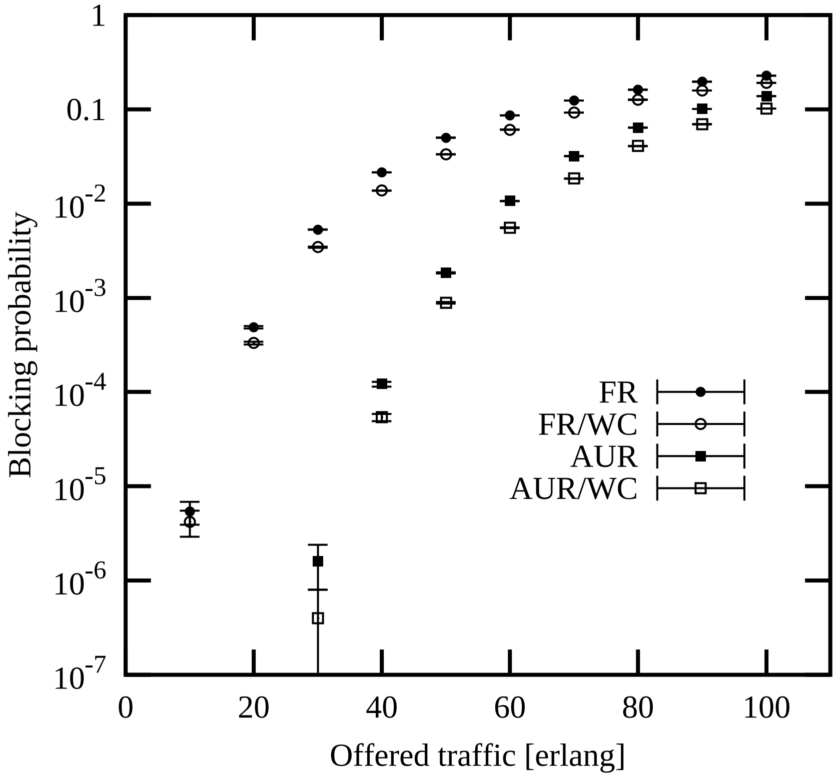

Figure 3.5: Comparison of different routing methods, fixed (FR) and adaptive unconstrained routing (AUR), with and without wavelength converters (WC). 8 wavelengths, single fiber. NSFnet.

are uncorrelated then the standard deviation of the average blocking probability can be found using the Central Limit Theorem. It states that the average blocking probability follows the normal distribution with mean μ and standard deviation $\sigma/\sqrt{n}$, where μ is the mean of the random variable, σ is the standard deviation of the random variable, and n is the number of demands. Then the 95 percent confidence interval is $[P_B - 2\sigma/\sqrt{n}; P_B + 2\sigma/\sqrt{n}]$. However, since the random variable is correlated, we use the method of batch means to determine the 95 percent con-

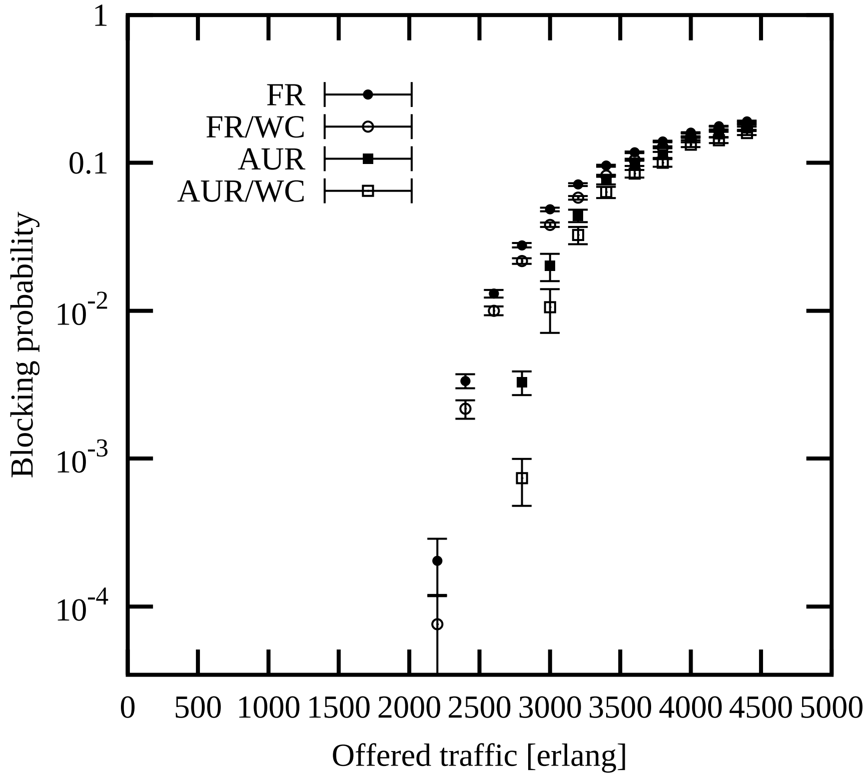

Figure 3.6: Comparison of different routing methods, fixed (FR) and adaptive unconstrained routing (AUR), with and without wavelength converters (WC). 256 wavelengths, single fiber. NSFnet.

fidence interval (Perros (1999)).

It is in Figure 3.5 seen that as the offered traffic is raised, all the curves converge to a common blocking probability, since they all have to approach unity for high traffic loads, because the larger the load the smaller is the fraction of allocated demands, due to high congestion. It is seen that using wavelength converters reduces the blocking, but using adaptive unconstrained routing instead of fixed routing has a much larger effect. Naturally, using adaptive unconstrained routing with wavelength conversion has the lowest blocking probability.

3.4.3 Multiple fibers

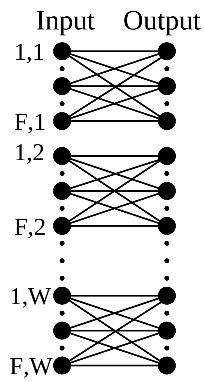

Figure 3.7: Illustration of how multiple fibers correspond to limited wavelength conversion. F fibers and W wavelength on each fiber are shown. The number f,w to the left corresponds to the fiber and wavelength number.

With multiple fibers limited-range wavelength conversion is achieved in the nodes. Figure 3.7 illustrates how multiple fibers correspond to limited-range wavelength conversion. We assume an optical cross connect with any number of input and output links each with F fibers, and W wavelengths on each fiber. Then one lightpath, which has to be switched from an input link to a specific output link, has the choice of up to F available fibers. This situation corresponds to have one fiber on each link, and $F \cdot W$ wavelengths on each fiber, where the wavelengths can be converted freely in groups of F. In this case we define the degree of wavelength conversion to be F. A degree of 1 would correspond to no wavelength conversion and a degree of $F \cdot W$ would correspond to full wavelength conversion.

In Figure 3.6 simulation results for the NSF network with 256 wavelengths have been plotted. Each data point for the low blocking probability is the output of 10^6 traffic demands. It is seen that the blocking probability drops off faster as the offered traffic is reduced than it was the case for the simulations shown in Figure 3.5. This is due to the smoothing effect of aggregating traffic. At 2500 erlang the blocking probability with fixed routing is less than 1% and with adaptive unconstrained routing less than 0.01%. That is, on average the network accommodates 2500 concurrent lightpaths at low blocking probability. Again it is seen that wavelength converters decrease the blocking probability for both fixed routing and adaptive unconstrained routing, and the blocking for alternate unconstrained routing is less than the blocking for fixed routing.

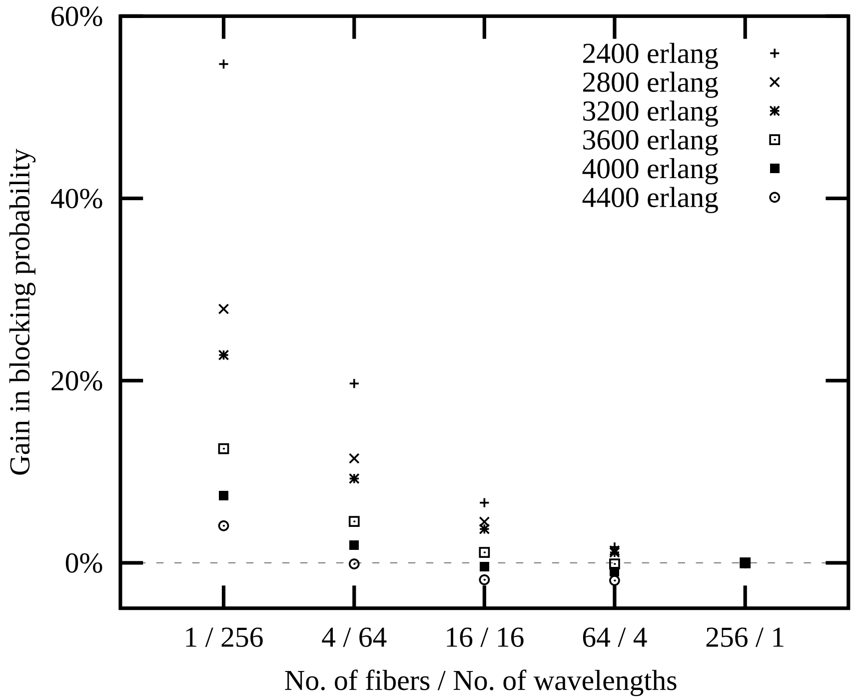

Figure 3.8: Gain in blocking probability using wavelength converters as function different ratios between fibers and wavelengths in the case of fixed routing. Up to 256 fibers / wavelengths. Logarithmic plot. NSFnet.

To increase the transmission capacity while holding the bit rate on each wavelength constant either the number of wavelengths on each fiber can be increased

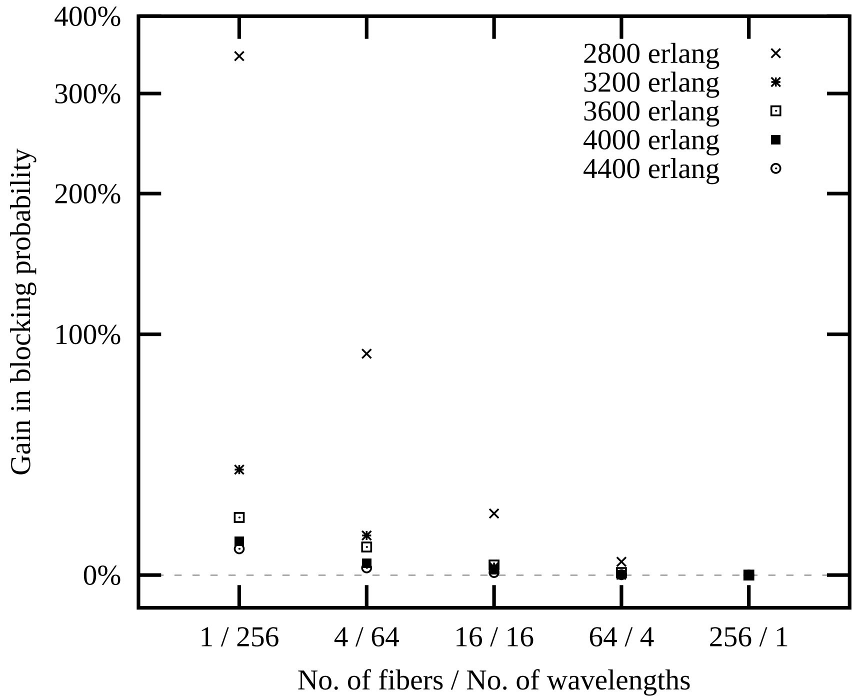

Figure 3.9: Gain in blocking probability using wavelength converters as function different ratios between fibers and wavelengths in the case of fixed routing. Up to 256 fibers / wavelengths. Logarithmic plot. NSFnet.

or the number of fibers on each link can be increased. We will in this section study the trade off between having many fibers and many wavelengths. Given that the capacity on each wavelength is kept constant then the capacity on a link is given by multiplying the number of fibers with the number of wavelengths per fiber. It can be seen that when the links contain one or more fibers with only one wavelength per fiber, then wavelength conversion will not have any effect on blocking probability. Having two or more fibers on each link with two or more wavelength on each fiber corresponds to limited-range wavelength conversion Ramaswami and Sivarajan (1998). Therefore lowering the number of wavelengths on each fiber but raising the number of fibers on each link while keeping the total capacity on each link constant would normally lower the blocking probability by raising the wavelength conversion ability.

We have performed simulations with different combinations of wavelengths and fibers ranging from 1 to 256 fibers corresponding to 256 to 1 wavelengths. The routing methods used were fixed routing (Figure 3.8) and for adaptive unconstrained routing in (Figure 3.9), where the percentage gain in blocking probability by using the specified number of fibers and wavelengths as compared to using full wavelength conversion has been plotted. For each number of fibers we have made the plot for different values of offered traffic. In case of fixed routing then multiplying the number of fibers by four divides the gain of using wavelength conversion with more than two for almost every traffic load and combination of number of fibers / number of wavelengths. In case of adaptive unconstrained routing the effect of multiple fibers is even larger.

For a few combinations of traffic loads and number of fibers / number of wavelengths in Figure 3.9 the gain is less than one, which means that adding conversion capability actually raises the blocking probability. This phenomenon has also been reported in Karasan and Ayanoglu (1998); Kovačević and Acampora (1996). That a network with wavelength conversion capability can have higher blocking than one without at the same level of offered traffic is caused by the formers higher ability to route longer paths, which take up more capacity than shorter paths. Thereby the fairness in equal blocking probability between long and short connection is increased. We have only observed this phenomenon in the case of congestion.

The gain of wavelength converters is high for relative low networks load but approaches 0% as the load increases since the blocking probability, independently on routing principle, always approaches one for rising offered network load.

Conclusion

We have shown how multiple fibers correspond to limited-range wavelength conversion. By simulation we find that multiple fibers reduce the blocking significantly and quickly to the level of full wavelength conversion both for fixed routing and unconstrained adaptive routing. Neither static nor dynamic wavelength routed networks will gain from wavelength conversion. Therefore neither limited-range nor full wavelength conversion will find any significant use in all-optical networks.

3.4.4 Fairness

The overall blocking probability of a network is an incomplete measure of the networks ability to carry traffic. The overall blocking probability does only by the average take into account that some node pair can have a very high blocking probability. We have therefore defined the *fairness* as a measure of the equality in the network.

To the authors knowlegde fairness has not before been applied to dynamic networks. To determine fairness in terms of available capacity betweem each node pair several definitions have been proposed, max-min fairness (Hahne and Gallager (1986); Katevenis (1987)), proportional rate fairness (Kelly et al. (1998)), and relative fairness (Cinkler and Laborczi (2002)).

To define fairness consider the following. By simulation an estimated blocking probability can be assigned to each source-destination pair for traffic between that source-destination pair. For these blocking probabilities we calculated the standard deviation – a measure of the width of the distribution of the individual source-destination pairs. Since the standard deviation of the individual source-destination blocking probabilities is roughly proportional to the overall blocking probability we defined the fairness as the overall blocking probability divided by the standard deviation of the individual blocking probabilities of each source-destination pair, such that the fairness only reflects the inequality and is independent of the overall blocking probability:

$$\text{Fairness} \equiv \frac{\text{Overall blocking probability}}{\text{Std.Dev. of source-destination pair blocking}} \tag{3.1}$$

This definition of fairness is very general, but it has the draw back of being difficult to determine, since determining the standard deviation of the individual source-destination pairs requires many blockings, due to the Law of Large Numbers. In Table 3.2 we evaluate the ability of simulations to determine the fairness. We have performed five simulations with identical parameters except that the length of the simulations differ. Each run had 10000 preliminary demand arises to avoid transient effects. Thereafter the length for each simulation varied from 10^4 to 10^8 demands. The 95% confidence interval is given for the overall blocking probability P_B, and it is seen that the blockings all are consistent. As mentioned above the standard deviation requires long simulations, and it is seen in the table that the number of demands must be higher than 10^6 assuming that the fairness for the longest simulation is very close to correct. Since the overall blocking probability here is 2% we had for 10^6 demand arises 20000 blocks, that is about 50 blocks per source-destination pair in average. For all our later measurements the simulations will have at least 50 blocks per source-destination pair independently of the network.

Table 3.2: Evaluation of fairness measurements. Fixed routing (OSPR). Offered traffic is 30 erlang. Arpa2 network, 21 nodes, 26 links, 8 wavelengths, single fiber. The $\pm$ on the blocking probability determines the 95% confidence interval.

load	Demands	P_B	Std.Dev.	Fairness
30	10^4	$0.021 \pm 4 \cdot 10^{-3}$	0.035405	0.599
30	10^5	$0.0197 \pm 1.2 \cdot 10^{-3}$	0.019771	0.9979
30	10^6	$0.0202 \pm 4 \cdot 10^{-4}$	0.018947	1.0673
30	10^7	$0.02046 \pm 1.2 \cdot 10^{-4}$	0.018850	1.0856
30	10^8	$0.02050 \pm 4 \cdot 10^{-5}$	0.018880	1.0859
100	10^8	$0.32388 \pm 1.2 \cdot 10^{-4}$	0.80288	1.4001
20	10^8	$0.002338 \pm 1.1 \cdot 10^{-5}$	0.0020715	1.1286

In Table 3.3 we have given the blocking probabilities and the standard deviation of the blocking for each node pair from an simulation of the Arpa2 network with 8 wavelengths per fiber and one fiber per link in each direction at an offered traffic of 100 erlang.

It is seen that the gain in blocking probability underestimates the positive effects of wavelength converters and more advanced routing. We find that using wavelength converters or using adaptive unconstrained routing instead of fixed routing increases the fairness in blocking.

This traffic load results in a very high blocking, but lowering the traffic load would result in too few blocked calls whereby the standard deviation would be determined less precisely, since a statistical insufficient amount of data would cause a higher standard deviation. From the table we find that using adaptive unconstrained routing instead of fixed routing increases the fairness with 12% without wavelength converters and 32% with wavelength converters. Using wavelength converters increases the fairness about 24% in case of fixed routing and 46% in case of adaptive unconstrained routing. We conclude that at least for high blocking probabilities wavelength converters and adaptive unconstrained routing increases the fairness in addition to lowering the blocking.

Table 3.3: Fairness study. Offered traffic is 100 erlang. Arpa2 network, 21 nodes, 26 links, 8 wavelengths, single fiber.

	FR	FR/WC	AUR	AUR/WC
P_B	0.327	0.289	0.307	0.289
Std.Dev.	0.232	0.165	0.194	0.125
Fairness	1.41	1.75	1.58	2.31

In conclusion, including the fairness as a performance measure for networks in line with network blocking probability makes the evaluation of routing methods, wavelength conversion, etc. more correct.

3.4.5 Power-law behavior

In Figure 3.10 we have plotted the blocking probability verses the offered traffic for the Arpa2 network with 8 wavelengths per fiber and one fiber per link in each direction in a double logarithmic plot. We will from this plot extract an interesting behavior.

For a blocking probability higher than 0.1 the growth of the blocking probability as function of the offered traffic is approximately linear Lee and Li (1993). The linear growth stops as the blocking probability approaches unity to which it will converge as the offered traffic is raised.

For a blocking probability below 10^{-3} the blocking probability falls off as a power law as the offered traffic is lowered. This is seen from the fact that the curves form straight lines in the double logarithmic plot illustrated by the two straight lines drawn in Figure 3.10. Therefore the blocking probability has the analytical form:

$$P_B(T) = aT^b \quad \text{for} \quad P_B \ll 1$$

where a and b are positive constants, and where T denotes the offered traffic. Networks usually operate in the domain of a blocking probability below 10^{-3}, so this behavior is practical valuable and it should allow analytical models, which can predict a power law behavior.

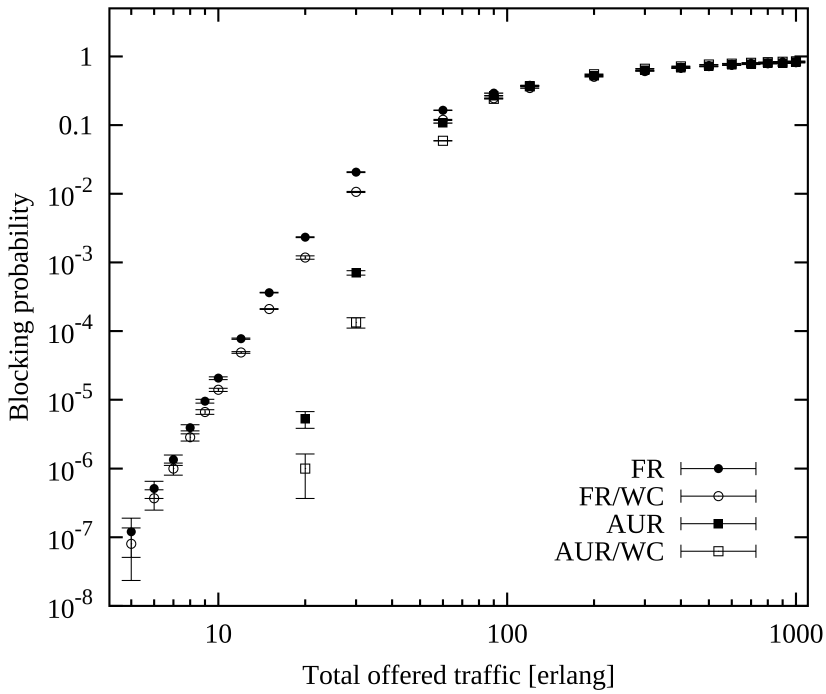

Figure 3.10: Demonstration of power law behavior of the performance curves in a double logarithmic plot. Arpa2, 21 nodes, 26 links, 8 wavelengths, single fiber.

It is from the figure observed that the exponent *b* of the power laws is different for the two routing methods, FR and AUR, however it seems independent of the availability of wavelength conversion.

To find if and how the power-law is present in other networks, we have plotted blocking as function of the offered traffic for the NSF network in a double logarithmic plot. We find again that below 10^{-3} the blocking probability falls off as a power law as the offered traffic is lowered. Actually the exponents of the power-laws are the same for the same routing methods in the two networks. As mentioned earlier the blocking for the NSF network with 256 wavelengths on each fiber fall off faster as the offered traffic is reduced, whereby the exponents of the power-laws will be higher. Further studies should be made to determine how

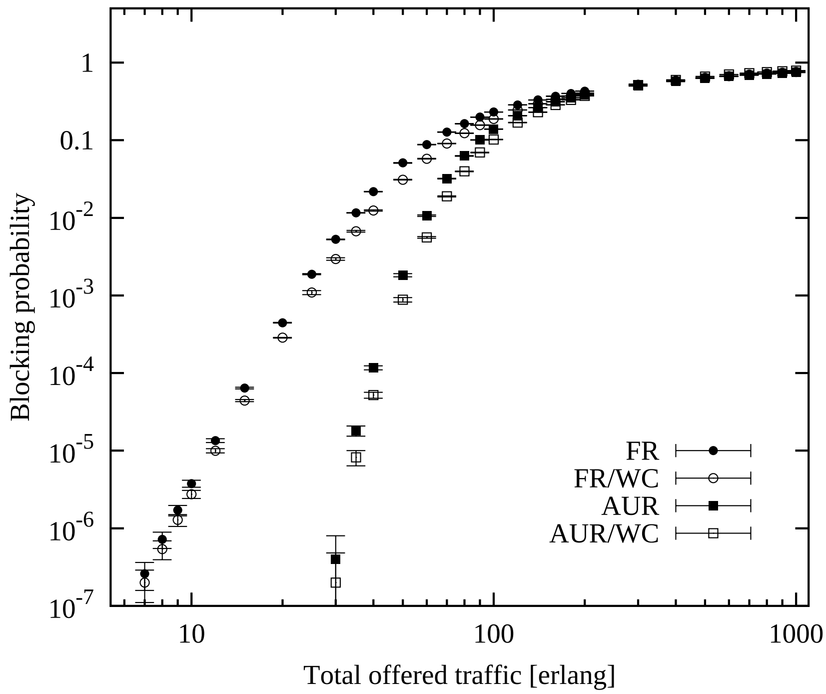

Figure 3.11: Demonstration of power law behavior of the performance curves in a double logarithmic plot. NSF, 30 nodes, 47 links, 8 wavelengths, single fiber.

the constants *a* and *b* depend on parameters like capacity, networks, etc.

If the exponent, *b*, is known for a specific setup the blocking probability curves is known from only one data point, otherwise two data points will give the curve for a blocking probability below 10^{-3}.

We define the gain of using one method of routing over another use for comparing the two methods. It can be defined as either a gain in blocking probability, G_{P_B}, when the offered offered traffic kept equal for the two methods or a gain in traffic, G_T, when the blocking probability is kept equal for the two methods.

The gain in blocking probability is defined as

$$G_{P_B}(T) = \frac{P_{B,1}(T)}{P_{B,2}(T)}$$

where $P_{B,i}(T)$ is the blocking probability as function of the offered traffic, T, for method i.

Similarly the gain in traffic is defined as

$$G_T(P_B) = \frac{T_1(P_B)}{T_2(P_B)}$$

where $T_i(P_B)$ is the offered traffic as function of the blocking probability, P_B, for method i.

When the gain for two curves for the blocking probability, $P_{B,1}(T)$ and $P_{B,2}(T)$, is measured for low blocking, where the power-law behavior is present, then a simple conversion formula between the gain in blocking probability, G_{P_B}, and the gain in traffic, G_T, can be found.
Assume:

$$P_{B,1}(T) = a_1\, T^{b_1} \quad \text{and} \quad P_{B,2}(T) = a_2\, T^{b_2}$$

then it can be derived that

$$G_{P_B}(T) = G_T(P_{B,1}(T))^{b_2}$$

given that $P_{B,1}(T) \neq P_{B,2}(T)$.

This conversion formula between gain in blocking and gain in traffic, since in simulations and experimental measurement the gain in blocking is easier obtainable, but the gain in traffic is of practical importance, since it gives increase in traffic (number of customers) the network can accommodate.

3.5 Conclusion

In this chapter we presented simulations of all-optical wavelength routed networks with routing and wavelength assignment methods for practical usage. Topology, fiber placement, and traffic distribution can be chosen freely. Simulations have been performed using the NSF network and the Arpa2 network with uniform traffic distribution. The number of fibers varied.

We determine the blocking probabilities for two routing methods, fixed routing and adaptive unconstrained routing, with and without wavelength conversion capability. For both methods the inclusion of wavelength converters decreases the blocking probability. However, choosing adaptive unconstrained routing instead of fixed routing has a larger effect on the blocking probability.

It has been described how a multiple number of fibers corresponds to limited range wavelength conversion. For both routing methods we find that increasing the number of fibers while reducing the number of wavelengths on each fiber proportionally, exponentially reduces the gain in blocking probability using wavelength converters, so that raising the number of fibers by a factor four decreases the gain in blocking probability using wavelength converters by a factor two. It can therefore be concluded that neither limited-range nor full wavelength conversion will find any significant use in all-optical networks.

We have defined a measure for fairness in the network. The fairness is influenced by network topology, routing methods and the inclusion of wavelength converters. We find that more flexible routing methods and the inclusion of wavelength converters raise the fairness in the network besides lowering the overall blocking probability in the network. The fairness should together with the blocking characterize the ability of the network to carry traffic, and the fairness measure is key for the operators quality of service garanties. Including the fairness as a performance measure for networks in line with network blocking probability makes the evaluation of routing methods, wavelength conversion, etc. more correct.

We show that the overall blocking probability in the network grows as a power-law with the offered load in the network for small blocking probabilities both in case of fixed routing and in case of adaptive unconstrained routing. The exponent is dependent of routing method but independent of network size and topology. This quality makes it possible for the operator to predict the blocking at lower or higher offered load as long as this load is in the region of power-law behavior. In Chapter 4 we will a.o. discover why this is so and explain the size of the exponent.

Chapter 4

Analytical Analysis of Stochastic Traffic

4.1 Abstract

In this chapter the Erlang fixed point equations are derived, and the numerical results are compared the results from the simulation in the previous chapter for verification purposes. Further an explicit expression in stead of the Erlang fixed point equations are derived. This expression is applicable for most practical purposes. An implicit and an explicit solution for blocking with alternate fixed routing has been derived and discussed.

4.2 Introduction

In this chapter an analytical solution for any traffic distribution and characteristic only under the assumption of independence of link blocking probabilities and fixed routing is derived. In particular Poisson arrivals with exponentially distributed holding times is used to compare and verify the solutions in Chapter 3. The motivation has been partly a search for understanding of the numerical solution and partly a wish of verification of the numerical solution. Getting verification from other software packages would be difficult because of differences in routing methods and doubt about the quality of these solutions. As a spin off of the search for understanding and verification a new better analytical solution has been found. All links are directed.

Due to the large capacity of wavelengths, only single-rate traffic is considered. That is, no single traffic demand is larger than the capacity of one wavelength.

4.3 Definitions and fundamentals

For the derivations we need some definitions:

E	Overall blocking probability
E_{sd}	Blocking probability for the source-destination pair s,d
E_{sd^p}	Blocking probability for the source-destination pair s,d using path p
E_l	Overall blocking probability for all source-destination pairs on link l
n_l	Maximum capacity in erlang on link l
A	Total offered traffic to the network
A_l	Offered traffic experience by link l
l_{sd}	Set of links in path between source-destination pair s,d
$(sd)_l$	Set of source-destination pairs for which the path use link l
$(sd^p)_l$	Set of source-destination pairs and path number for which the path use link l
sd	Set of all source destination pairs
P_{sd}	Number of paths for source-destination pair s,d
l_{sd^p}	Set of links using path p between source-destination pair s,d

The total load for a network is per definition the sum of loads between all node pairs:

$$A \equiv \sum_{sd} A_{sd} \tag{4.1}$$

The overall blocking probability is the weighted average for the blocking probability of each node pair:

$$E \equiv \frac{\sum_{sd} A_{sd} E_{sd}}{A} \tag{4.2}$$

Notice that the symbol used in previous chapters for the blocking probability P_B is, strictly speaking, the estimated overall blocking probability.

With the assumption of independent link blocking probabilities then the blocking probabilities for the source-destinations are given by:

$$E_{sd} = 1 - \prod_{l_{sd}} (1 - E_l) \tag{4.3}$$

This approximation is in Kelly (1986) justified for large link capacities together with large offered link loads, which is typical for large networks.

The expression for the link load are the load between all source-destinations using the link except what is blocked on other links.

$$A_l = \frac{1}{1-E_l} \sum_{(sd)_l} A_{sd}\,(1-E_{sd}) \tag{4.4}$$

4.4 Implicit solution

Inserting expression (4.3) in expression (4.4) :

$$A_l = \frac{1}{1-E_l} \sum_{(sd)_l} A_{sd} \left(\prod_{l_{sd}} (1-E_l) \right) \tag{4.5}$$

For any traffic type E_l is given by the link load A_l and the number of channels on the link n_l. In case of finite variance of the holding and waiting times distributions then according to Erlang (1917) the blocking probability for a link is:

$$E_l = \frac{\frac{{A_l}^{n_l}}{n_l!}}{\sum_{i=0}^{n_l} \frac{A_l^i}{i!}} \tag{4.6}$$

Finite variance of the holding and waiting times distributions are not always present. I case of infinite variance the Central Limit Theorem does not apply, Grinstead and Snell, and aggregation of traffic yields similar traces just on a larger scale. Self similar traffic is discussed in the next chapter.

Expression (4.5) is a set of coupled fix point equations for A_l. From the solution to these, i.e. the A_l's which satisfy (4.5) we can get the blocking probabilities for the individual source-destination pairs by expression (4.3) and the overall blocking probability in the network by expression (4.2).

The solution sketched above is know as the Erlang fixed-point approximation developed in Katz (1967).

In Kelly (1986) it was shown that the Erlang fixed-point approximation is asymptotically correct, i.e. when the capacity of link and the offered traffic are increased together, then asymtoticaly the blocking probabilities are given as if the links blocks independently.

In Hart and Martínez (2002) it is proved that these fixed-point equations converge by sequential iteration, however they can be quite intractable to evaluate computationally. Therefore an explicit solution is derived in the next section.

4.5 Explicit solution

In Section 4.4 we found the overall blocking probability given by a set of coupled fix point equations.

In this section we avoid any coupled fix point equations by approximating the load of the links by assuming small link blocking probabilities. To first order in the blocking probability on links we get from expression (4.5):

$$A_l = \sum_{(sd)_l} A_{sd} + O(E_l) \tag{4.7}$$

Inserting expression (4.3) in expression (4.2):

$$E = A^{-1} \sum_{sd} A_{sd} \left(1 - \prod_{l_{sd}} (1 - E_l) \right) \tag{4.8}$$

This equation together with expression (4.7) directly yields the overall blocking probability, when E_l is a function of just A_l and n_l, which is the case in the regime of the Erlang blocking formula.

For faster computation the approximation from The Erlang blocking formula can be approximated, Störmer (1963):

$$E_l = \begin{cases} {A_l}^{n_l} e^{-A_l} k(n_l) & \text{if } A_l \leq n_l \\ \frac{A/n_l - 1}{A/n_l} + \frac{1}{A/n_l (A/n_l - 1)} n_l^{-1} - \frac{2}{(A/n_l - 1)^3} n_l^{-2} + O(n_l^{-3}) & \text{if } A_l > n_l \end{cases} \tag{4.9}$$

where

$$k(n) \equiv \frac{e^n}{\sqrt{2\pi}\, n^n} \left[n^{-1/2} - \frac{1}{12} n^{-3/2} + \frac{1}{288} n^{-5/2} + O(n^{-7/2}) \right] \tag{4.10}$$

In case that the Erlang blocking formula is used and $A_l \leq n_l$, which is the case when then approximation of small blocking probabilities are good, then we can use expression (4.9):

$$E = A^{-1} \sum_{sd} A_{sd} \left(1 - \prod_{l_{sd}} (1 - k(n_l) A_l^{n_l} e^{-A_l}) \right) \tag{4.11}$$

Inserting expression (4.7):

$$E = A^{-1}\sum_{sd} A_{sd}\left(1-\prod_{l_{sd}}\left(1-k(n_l)\left(\sum_{(sd)_l} A_{sd}\right)^{n_l} e^{-\sum_{(sd)_l} A_{sd}}\right)\right) \tag{4.12}$$

This expression can be fully determined, when the routing in the network is done.

For uniformly distributed traffic, then $A_{sd} = \frac{A}{N(N-1)} \forall s,d$ where N is the number of nodes in the network. This together with equal capacity on all links, i.e. $n_l = n$, and small blocking probability, then from expression (4.12) :

$$E \propto O(A^n) \tag{4.13}$$

4.6 Alternate fixed routing

In fixed alternate routing two or more paths are assigned to each source-destination pair.

For each path p the blocking probability is given by expression (4.3):

$$E_{sd^p} = 1-\prod_{l_{sd^p}}(1-E_l) \tag{4.14}$$

Assuming that the paths allocated to each node pair are link disjoint and independence of link blocking probabilities, then

$$E_{sd} = \prod_{p=1}^{P_{sd}} E_{sd^p} \tag{4.15}$$

Combining the two we get:

$$E_{sd} = \prod_{p=1}^{P_{sd}}\left(1-\prod_{l_{sd^p}}(1-E_l)\right) \tag{4.16}$$

According to equation (4.4) then the link load is given by:

$$A_l = \frac{1}{1-E_l}\sum_{(sd^p)_l} A_{sd^p}(1-E_{sd^p}) \tag{4.17}$$

with

$$A_{sd} \equiv \sum_{p=1}^{P_{sd}} A_{sd^p} \tag{4.18}$$

We see that for each source-destination pair only the sum of the loads for each path is fixed. The ratios can be chosen freely. The blocking probability will of course depend on the choice.

4.6.1 Implicit solution

An implicit solution can now be achieved by inserting expression (4.14) into expression (4.17). We get a set of coupled fix point equations:

$$A_l = \frac{1}{1 - E_l} \sum_{(sd^p)_l} A_{sp^p} \prod_{l_{sd^p}} (1 - E_l) \tag{4.19}$$

4.6.2 Explicit solution by approximation of link load

From expression (4.17) we approximate the link load:

$$A_l = \sum_{(sd^p)_l} A_{sd^p} + O(E_l) \tag{4.20}$$

with A_{sd^p} given from expression (4.18).

Using expressions (4.2), (4.16), and (4.20) we get an explicit expression for the overall blocking probability:

$$E = A^{-1} \sum_{sd} A_{sd} \prod_{p=1}^{P_{sd}} \left(1 - \prod_{l_{sd^p}} (1 - E_l) \right) \tag{4.21}$$

Using expression (4.9) for $A_l \leq n_l$ we get:

$$E = A^{-1} \sum_{sd} A_{sd} \prod_{p=1}^{P_{sd}} \left(1 - \prod_{l_{sd^p}} \left(1 - k(n_l) \left(\sum_{(sd^p)_l} A_{sd^p} \right)^{n_l} e^{-\sum_{(sd^p)_l} A_{sd^p}} \right) \right) \tag{4.22}$$

4.6.3 Minimization of blocking

Expression (4.20) is a very important since it illustrates that the offered load for a source destination pair can be distributed freely on the available paths for the source-destination pair. The question related is, how should the load be distributed such that the overall blocking probability is minimal.

When the offered load for each source-destination pair is given then the overall blocking is determined by $\sum_{sd}(P_{sd}-1)$ different variables. For a logically fully connected network with 30 nodes with P_{sd} $\forall s,d$ this yields 1740 variables which is a non trivial sized solution space.

If the overall blocking has one global minimum and no other local minima then finding the global minimum is easy for example by use of the method of Steepest Descend,00 Maruster et al. (2001). However due to several nonlinearities many local minima are possible, and any easy method for finding the global minimum does not exist and metaheuristics would be more applicable.

4.7 Numerical comparisons

For Poisson arrivals with mean inter arrival time μ, identical for all source-destination pair, and exponentially distributed holding times with mean λ_{sd} for source destination pair s,d, we have that $A_{sd} = \lambda_{sd}/\mu$.

Using the program developed for Chapter 3 we compare results from simulation with the results from the analytical work, i.e the implicit expression and the explicit expression for the overall blocking probability obtained by approximation of the link load, with and without Taylor development of the expression for source-destination blocking probability.

We have used the two networks, Arpa2 and NSF, seen in Figures 3.1 and 3.2. The Arpa2 network with 21 nodes and 26 links is smaller and more spare and the NSF with 30 nodes and 47 links is larger and more connected.

In the Figures 4.1 and 4.2 the comparisons for the two networks are shown. They show the blocking probability as function of the offered network load. A double logarithmic plot is chosen to include wide ranges of loads and blocking probabilities. In both cases the agreement between simulation and Erlang fixed-point approximation are almost exact for all values of offered traffic. However, the analytical result were slightly larger. Since the only assumption were the independence of link blocking probabilities then the deviation should be explained

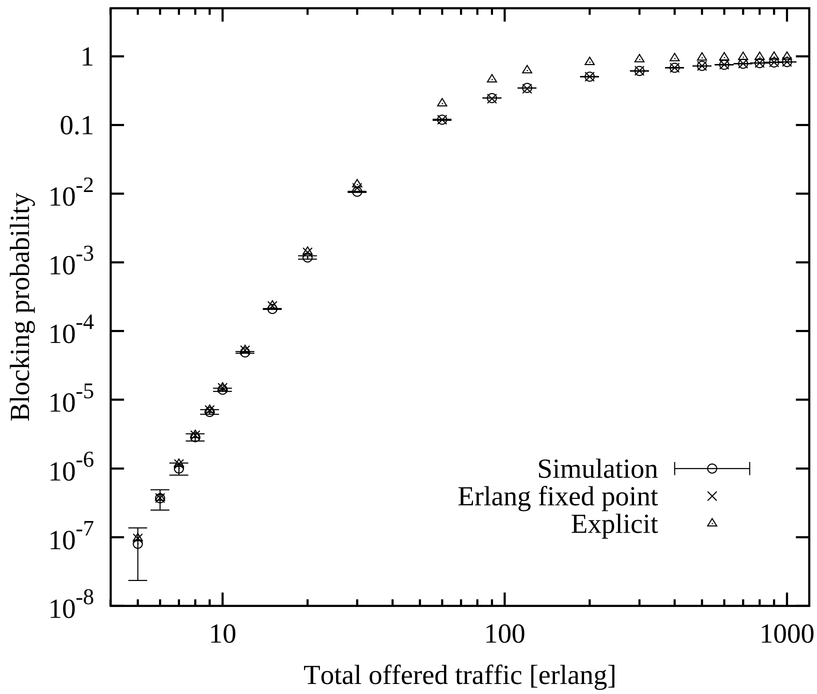

Figure 4.1: Comparison of simulation result with approximative analytical result. Error bars indicate the 95% confidence interval. Double logarithmic plot. Arpa2, 21 nodes, 26 links, 8 wavelengths, single fiber, wavelength converters. Expression (4.8) is used for the explicit solution.

from this assumption. When one look more closely at the solution of the analytical result it can be seen that the blocking probabilities for the long paths are too large and therefore contribute to the larger overall blocking probability. When congestion on one link on a path then other links on the same paths are typically congested as well, whereby blocking on two links simultaneously are more probable with link blocking dependence. To have the same average link blocking then the link blocking probability in case of less congestion must be lower. All together link dependence lowers the average path blocking. Therefore the analytical results displays slightly larger blocking probability.

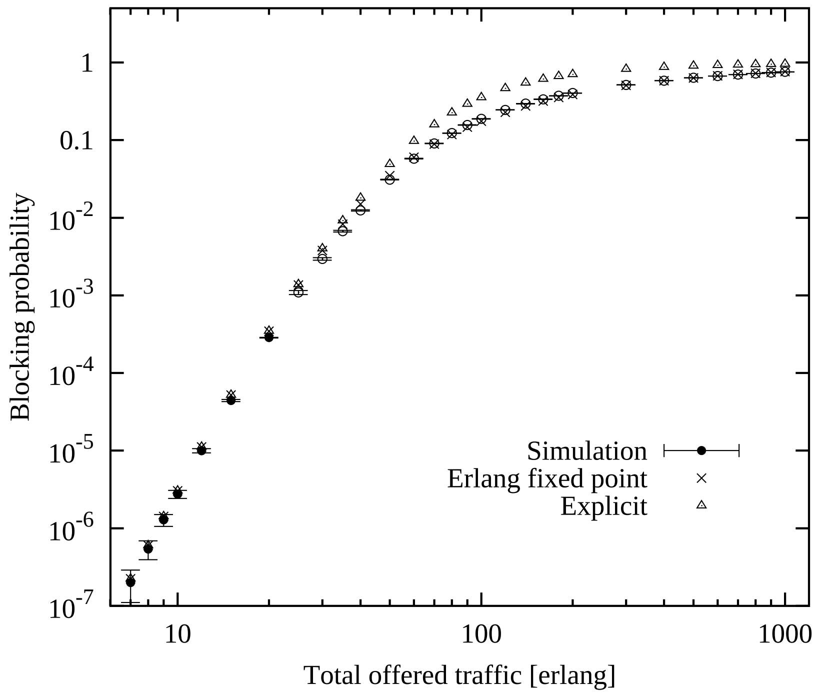

Figure 4.2: Comparison of simulation result with approximative analytical result. Error bars indicate the 95% confidence interval. Double logarithmic plot. NSFnet, 30 nodes, 47 links, 8 wavelengths, single fiber, wavelength converters. Expression (4.8) is used for the explicit solution.

The result for the explicit solution given by expression (4.8) for the overall blocking probability under the link load assumption is also shown in the Figures 4.1 and 4.2. It is seen that for blocking probabilities usually in the interest of telecom operators, i.e. below 10^{-2}, the agreement between simulation and the explicit solution is very good. For higher link loads the explicit solution deviates from simulation. but stays below one and gives an upper bound for the simulation result. With the link load approximation the link load (expression (4.7)) has been overestimated whereby it is clear that the overall blocking probability is also overestimated.

From expression (4.13) it is seen that for small network loads the blocking probability falls off as a powerlaw with the exponent n, i.e. the capacity of a link. This results is confirmed in the Figures 4.1 and 4.2, where the curves for both simulation and analytical results form a straight line in the double logarithmic plot.

4.8 Conclusion

In this chapter Erlang's fixed point equations have been derived, as well as a faster explicit solution for the blocking probability. The explicit solution is an upper bound for the Erlang's fixed point equations solution. The two solutions are almost identical for network blocking probabilities at and below 1% network blocking. In the case that the implicit result is not obtainable as in case of lack of convergence of the coupled fix point equations then the explicit results will be necessary. For small blocking probabilities it could require hours of simulation time to obtain comparable results. For large networks it would in practice be impossible to obtain results from simulation, and only approximative analytical results would be viable.

Implicit and explicit expression were also derived for alternate fixed routing. Unfortunately there where no time for testing the approximative analytical results for alternate routing. Because of the very good agreement for fixed routing between simulation and the analytical result from both the Erlang fixed-point approximation and the explicit solution then the analytical results for alternate fixed routing are promising.

From expression (4.19) it is seen that the distribution of the offered load to each path for each node pair is important for the overall network blocking probability.

From the equations it is seen that the distribution of the offered load influences the blocking probability and the distribution should

The determination of the individual path loads requires that a set coupled non-linear equations are solved. This is a complex task but the solution will potentially lead to a lower blocking probability tham the simpler model like the overflow model. A combination of the two methods would seem as the obvious extension.

From comparison with the simulation program developed for Chapter 3 we find very good correspondence between simulation results and the implicit result for all values of network load.

Chapter 5

The Self Similarity of Data Traffic

5.1 Abstract

We verify by simulation that the self similarity of data traffic can be caused by the traffic distribution of the sources. It is further shown that the burstiness caused by the self similarity becomes negligible for highly aggregated traffic. This is shown for for uncapacitated link. The introduction of a capacity limit on links does not increase or decrease the self similarity by neither reliable (TCP-like) traffic or by unreliable (UDP-like) traffic. Simulations of unreliable and reliable protocols in the framework of the ON/OFF model were performed. For sufficiently capacitated flow traffic on a unreliable protocols will suffer from packet loss, where traffic on a reliable protocol will be retransmitted. It is shown that for both of these protocols no extra self similarity is introduced.

A study of round trip times of Internet traffic destined to different locations in the world has been performed. This study shows that IP traffic is self similar and that the degree of self similarity is changing both in time and space indicating a more complex dynamics as the origin to the self similarity than the source traffic distribution.

Previous studies of data traffic are reviewed and it is found that these studies are focused on traffic, which only have few simultaneously active source-destination pairs, indicating that the relative effect of self similarity is stronger

with few than with many simultaneously active source-destination pairs. Further the decrease of burst sizes as the time scale rises depends on the parameters in the ON/OFF model.

The source level characteristics do give rise to self similar traffic, which is seen by simulation of the ON/OFF model. The model is described and expanded to a fractional ON/OFF model, which gives better resemblance to real data traffic.

From simulations of the fractional ON/OFF model it is seen that the relative size of bursts decreases as the number of simultaneously active source-destination pairs rises, which is in god correspondence with measurements of real data traffic.

5.2 Introduction

Self similarity is believed to have a significant impact on network performance, and understanding the causes, effects, and prevalence of this traffic characteristic in data networks is therefore of key importance for the network planer.

There has in recent years been several reports that data traffic differs fundamentally from traditional telephony traffic, Leland et al. (1994); Willinger et al. (1997); Paxson and Floyd (1995); Roughan and Veitch (1999). The fundamental difference is that data traffic is significantly more bursty in the sense that the relative variations in traffic load decreases much slower with the level of aggregation in time and space. This has the consequence of increased delays and packet loss.

In this paper we first turn to the definition of self similarity, where after a review of previous studies is presented. Thereafter a new study of international Internet traffic is presented, which shows the prevalence of self similarity in data traffic. Possible origins of self similarity are discussed. Some of these origins are at the source level. The effects from the source level characteristics on the traffic of are simulated via the ON/OFF model, which is also used for a study of the differences between reliable and unreliable traffic with respect to self similarity.

5.3 Self similarity

This section both introduces self similarity and introduces a heavy tailed distribution. Heavy tailed distributions plays a fundamental role in self similarity, since the variance for heavy tailed distribution can be infinite, the Central Limit Theorem does not apply. The term self similar was coined by Mandelbrot who is the father of the famous Mandelbrot set, where the same structure can be found on infinitely many length scales. Self similarity is found all over in nature: in river systems, lungs, and in the branching of trees. That is, a zoom of the original figure looks similar to the original figure.

An intuitive definition of self similarity is that a system is self similar if no special scale exist. That is the system looks similar on different scales. A formal definition of self similarity for a stochastic process is: The distribution, P_T, of changes, x, at a time scale, T, may be obtained from that of a shorter time scale, $\tau < T$, by an appropriate rescaling of the variable:

$$\boxed{P_T(x) = \left(\frac{\tau}{T}\right)^{-H} P_\tau\left(\frac{T}{\tau}x\right)} \tag{5.1}$$

where H is the self similar exponent or Hurst exponent, which usually lies within the interval $[0.5;1]$ whereby x has a long range dependence. See Cox (1984) for a more in depth discussion of self similarity and long-range dependence.

5.4 Traffic measurements

5.4.1 Previous reports

There have been several measurements of data traffic, which display self similar behavior Leland et al. (1994); Willinger et al. (1997); Paxson and Floyd (1995); Roughan and Veitch (1999). All these measurements have been made on small networks with few simultaneously active source-destination pairs. The measurements give convincing evidence that some kind of self similarity exists for data traffic. To illustrate this an early pictorial proof for self similarity in a data network is plotted in figure 5.1. The figure presents data collected from 27 hours of Ethernet traffic at BellcoreLeland et al. (1994). The figure presents five plots for five different time scales. Each figure has time out of the x-axis and packets per time unit up of the y-axis. The time unit for the figures span over five orders of magnitude, from 0.01 second up to 100 seconds. It is seen that for the smallest time unit the traffic is very bursty, and that the bursts are partially preserved after aggregation over longer time all the way to 10 seconds per time unit. In figure 5.1(a) the data are collected over 27 hours whereby the time of the day will play a large role and this figure should therefore be carefully interpreted. In the case of telephony traffic the decrease of bursts with the time scale would have been much faster, and it would have become completely uniform for the largest scale except for time periodic changes.

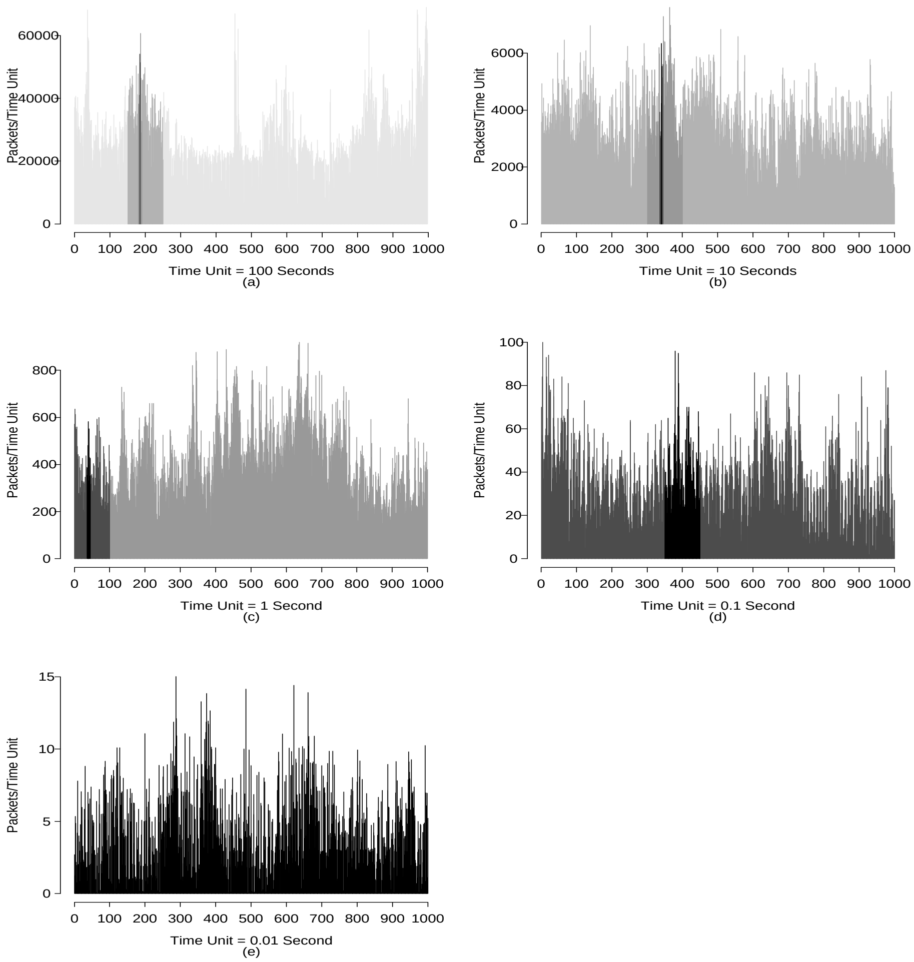

Figure 5.1: Data collected from Ethernet traffic over 27 hours. From Leland et al. (1994).

The burstiness of data traffic is not just a feature of Ethernet network, but is also seen for traces of external traffic coming into an Ethernet network Willinger et al. (1997). Burstiness has also been seen on a 155 Mbit/s ATM link J.L. Jerkins (1997), where 20% of the traffic on this link was measured, since one connection used 80% of the link capacity, and again it seems that only a few simultaneously active source-destination pairs have been involved.

Another way to see that the traffic is self similar is to plot the differences in arrival times for packets in a network. In figure 5.3(a) an unnormed probability density function (PDF) for data traffic, also taken from Bellcore's Ethernet, has been plotted. It turns out that this PDF is power-law distributed, which is a fundamental ingredient in self similar systems. The exponent of the power-law is by a best fit found to be -2.3, that is, if no border effects were present both the variance and the mean of the time span between two arrival times would be infinite.

5.4.2 New traffic study for global data traffic

In this section a global study of the self similarity of IP traffic is presented, which to our knowledge is the first of its kind. With this study it is answered how the traffic on the highest level with all aspects of traffic, protocols, buffers, routes etc. performs.

The round trip times for different destinations were recorded over time periods spanning from 10 hours to 14 days. The study was performed using the ping command, which uses the Internet Control Message Protocol (ICMP), which runs over the Internet Protocol (IP). The ping command returned the round trip time every second.

In figure 5.2 several rescaled range plots have been made to estimate the Hurst exponent. The rescaled range method is an approximative method for determining the Hurst exponent, cf. Feder (1988). From the figure it can be seen that all the plots can be enveloped by two lines with exponents 0.6 and 1, indicating that the Hurst exponent lies in that interval, that is, the traffic displays self similarity.

The first destination was located 20 km away from the source nearby Copenhagen, where the others were placed in Chile and Australia. One of the destinations in Australia was used at two different times. From the figure it seems difficult to give any dependence between distance to the destination and the Hurst exponent. Even the same destination gives different Hurst exponents for different times, which is seen from comparing the two plots for www.unimelb.edu.au.

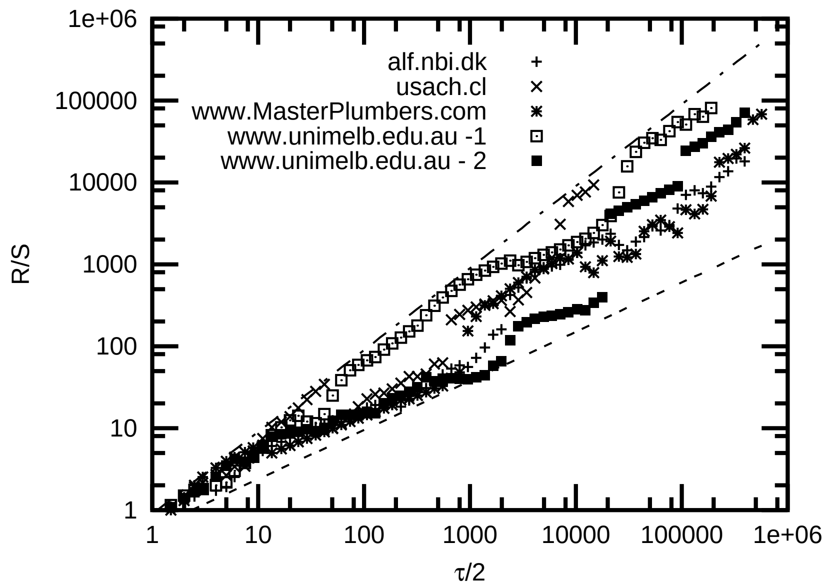

Figure 5.2: Rescaled range plots for round trip times over the Internet Protocol from www.dtu.dk to destinations given in the key field. The data are collected over time periods from 10 hours to 14 days. The strait lines on each side of the plots indicate that the Hurst exponent lies in the interval between 0.6 and 1 for all the plots.

5.5 Origins of self similar behavior

Just like the source level characteristics for telephony determines the statistical properties of this traffic, then a number of source level characteristics, which could underlie the bursty behavior in data traffic, can be mentioned:

- Power-law distributions for file sizes in UNIX file systems, see figure 5.3(b) and Park et al. (1998), and on WWW-serves Arlitt and Williamson (1997); Crovella and Bestavros (1997) with exponent around 1 for the power-law have been found.

- A power-law distribution for measured CPU time of a process Leland and

Ott (1986).

- Indications of heavy tailed probability distribution for human-computer interaction times Meier-Hellstern et al. (1991).

- The distribution for the sizes of files for variable-bit-rate (VBR) video service has been showed to be heavy tailed Beran et al. (1995).

An explanation of self similarity, which does not originate at the source level, would be to assume some kind of dependence between the sources leading to a group effect, which would induce self similarity. In case of human control of computer-network interaction, then activity will depend on events in real life. From the smallest events where one person tells a friend about an interesting web site to large events like the release of a new version of a downloadable software product. The sizes of such events are often given by heavy tailed distributions Bak et al. (1988). According to the study of round trip times of Internet traffic some effects on the higher level seem to be present since the Hurst exponent changes in time and space. In Willinger et al. (1997) it has however been reported that the activity of the sources in a LAN network are independent, and this will also be the hypothesis in the traffic simulation via the ON/OFF model.

5.6 Modeling

One way to discover the consequences of some of the underlying reasons is through the ON/OFF model, which directly models the source level characteristics.

5.6.1 The ON/OFF model

The ON/OFF model, which originally was proposed by Mandelbrot Mandelbrot (1969), can be adopted to simulate the load on a data link in a network. As sketched in figure 5.4 the load on a data link is the aggregated traffic transmitted from a number of sources to some destinations. The sources can be either on or off corresponding to transmitting data at a rate 1 and 0 data units per basic time unit, respectively. In this ON/OFF model the length, Δt, of the ON and OFF periods are identical and independently distributed where the distribution of this transmission time is heavy tailed, that is, it has infinite variance, but a finite mean.

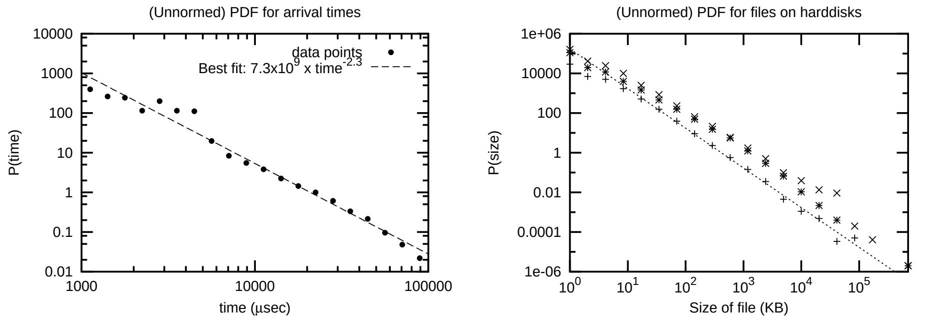

(a) Arrival times

(b) File sizes

Figure 5.3: (a) Data from Bellcore Leland et al. (1994), which contained the arrival times for packets on the Ethernet. (b) Data for file sizes on three different UNIX-machines, one with Digital Unix and two with Linux, indicated by the different kind of crosses. The line has a slope equal to -2.

The distribution used is the Pareto distribution:

$$P(\Delta t) = \begin{cases} \alpha k^{\alpha} \Delta t^{-(\alpha+1)} & \Delta t > k \\ 0 & \Delta t \leq k \end{cases}$$

with $1 < \alpha \leq 2$. If there are M sources, where each source, $W^m(t)$, at time t is 1 if on and 0 if off, then then traffic load on the link is given by

$$\text{traffic load} \; : \; \sum_{m=1}^{M} W^{(m)}(t) \tag{5.2}$$

An example of what determines the ON periods and what determines the OFF periods could be that if files transmitted are heavy tailed distributed then this corresponds to that the ON periods are heavy tailed and if a heavy tailed distributed process is executed before transmission then this would correspond to heavy tailed OFF periods.

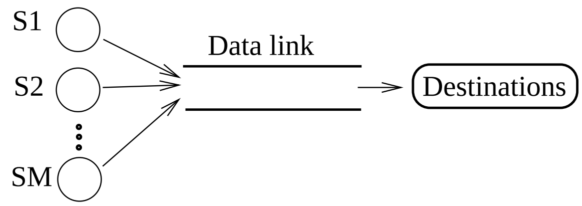

Figure 5.4: Generic network for data transmission. Data is transmitted from some sources, S1 up to SM, to some unspecified destinations through a data link.

5.6.2 Analytical result for the ON/OFF model

For the given ON/OFF model above a fundamental result has been derived in Taqqu et al. (1997). Suppose that μ are the mean of the distributions for the ON and OFF periods which are Pareto distributed with exponent, $\alpha > 1$. For large M and T the aggregate cumulative traffic behaves like

$$\int_0^T \left(\sum_{m=1}^{M} W^{(m)}(u) \right) du \approx \frac{1}{2} T M + T^H M^{1/2} L(T) B_H(1) \tag{5.3}$$

Where $H \approx (3 - \min\{\alpha, 2\})/2 \in [\frac{1}{2}, 1[$, and $L(T)$ is a slowly varying function, and B_H is fractional Brownian motion, and $B_H(1)$ is power-law distributed with exponent H. In case that $H = \frac{1}{2}$ we have normal Brownian motion for which $B_H(1)$ would be Gaussian distributed. We see that one part of the expression is deterministic and the other part gives rise to self similar behavior. The theorem is, however, only strictly valid for infinitely large values of M and T, so simulations of the ON/OFF model with more appropriate values for M and T are needed.

In case of a negligible stochastic part and identical distributions for the ON and OFF periods then the traffic load cumulated over a time span, T, becomes $\frac{1}{2} T M$.

The main consequence of the theorem is that the stochastic part, that is, the part that gives rise to self similarity, becomes negligible in case of many sources. In case that $H < 1$ then the stochastic part also becomes relatively smaller when the time scale rises.

A result similar to equation 5.3 would be obtained if just either the ON or OFF period was heavy tailed distributed. But here we work with the same distribution for both the ON and OFF periods to avoid unnecessary complications.

5.7 Simulation of the ON/OFF model

The ON/OFF model has been simulated with a program written in C. The ON and OFF periods for every source are strictly alternating, which in Willinger et al. (1997) is reported not to have a crucial effect on the behavior, and the periods are i.i.d. with the same Pareto distribution. The input to the program is the number of sources, the form of the Pareto distribution, the time length of the run and the time scale. The output is the aggregated traffic load on the link.

An extension has been made to the usual integer ON/OFF model. In the traditional model the value of the sources, $W^{(m)}(t)$, is either 0 or 1. This corresponds to that the source transmits nothing and fully, respectively. This gives bad resemblance to real traffic for especially small file sizes, since the stochastic variable chosen from the Pareto distribution then only can take on integer values, which would correspond to that modems would be either transmitting fully for a given time or not at all. This is here avoided by allowing the load of the sources to be between zero and one in the last time interval, whereby we get the fractional ON/OFF model.

Introducing fractional values in the ON/OFF model gives better resemblance to real data traffic, which can be seen in figure 5.5, where real data traffic, fractional simulated traffic, and integer simulated traffic are displayed. In both cases of the simulated traffic the number of sources is $M = 7$ and the exponent $\alpha = 1.1$, but with the cut-off constant $k = 0.1$ and $k = 1$ respectively. The cut-off determines the smallest allowed file size to be transmitted.

5.7.1 Uncapacitated traffic

From simulation of the fractional ON/OFF model plots similar to figure 5.1 have been made in figure 5.6. The lower right plot of figure 5.6 is the traffic load seen shortest time scale, where no accumulation in time has been made. In the lower left plot the traffic has been accumulated over 10 basic time units, where one basic time unit could be interpreted as 0.01 second, the lowest scale in figure 5.1. When accumulating the traffic over 10 basic time units then the load per time unit becomes approximately ten times as high. The darker area of the plots

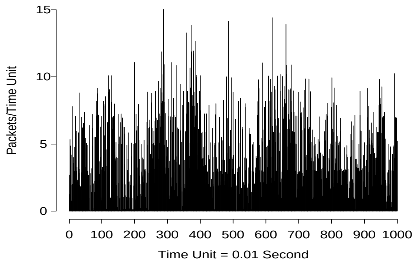

(a) Real Ethernet traffic

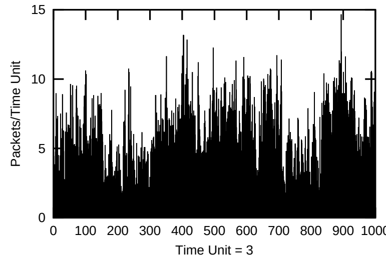

(b) Fractional ON/OFF

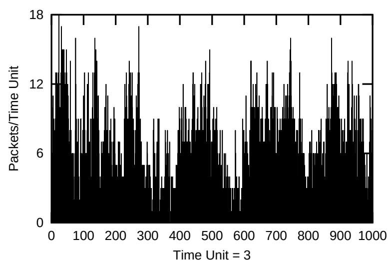

(c) Integer ON/OFF

Figure 5.5: (a) 10 seconds of Ethernet traffic at Bellcore Leland et al. (1994). (b) Simulation of the fractional ON/OFF model. $\alpha = 1.1$, $M = 7$, $k = 0.1$. (c) Simulation of the integer ON/OFF model. $\alpha = 1.1$, $M = 7$, $k = 1$.

corresponds to the plot for the less accumulated traffic. If one compares figure 5.1 and figure 5.6 for the four lowest time scale, where the period of the days does not influence the real traffic data, one can seen striking similarities in the way the bursts decrease. And similar to the real traffic data the simulated traffic data does also exhibit self similarity, which can be seen from figure 5.7, which is rescaled range plots for different values for the exponent used in the Pareto distribution for the ON and OFF periods. From data points from the rescaled range analysis a best fit is made to determine the Hurst exponent. For $\alpha = 1.2$ then $H = 0.85$ and for $\alpha = 1.5$ then $H = 0.72$, which stems with the approximative analytical result,

$H \approx (3-\alpha)/2$ for $\alpha \in [1,2]$ which gives $H \approx 0.9$ and $H \approx 0.75$ respectively.

The number of sources plays a significant role for the relative influence of self similarity. In figure 5.8 plots for three different number of sources have been plotted. It is seen that the burstiness decreases very fast with M. This is in god agreement with the approximative analytical result, equation 5.3. One should not look too strictly on the number of sources as absolute values. The values for M in this model is not necessarily comparable to M in real networks, because the ON and OFF periods are here chosen to have the same mean length, whereas for real networks the sources might be more inactive than active. We conclude that the more heavily loaded with source destination pairs a link is, the more insignificant is the signs of self similarity. This is in god agreement with the fact that no self similarity has been reported for larger networks.

5.7.2 Capacitated traffic - Unreliable versus reliable traffic

The model can also simulate the traffic when there is a capacity limit on the link with either unreliable or unreliable traffic, which in the IP world is realized by the UDP and TCP protocol. The two protocols differ in the way that TCP retransmits in case of packet loss, where UDP does not. Further TCP has some extra features like slow-start, which is not modelled here. In the regime of the ON/OFF model it can be tested if retransmission or no retransmission influences the self similarity of traffic.

To get packet loss a maximum link capacity is introduced. In the case of simulation of unreliable traffic, packets were simply lost if the load of the link was higher than the maximum capacity, whereas for the simulation of reliable traffic the packets were put on a hold. In figure 5.9 plots of the traffic load are shown for two very different time scales for both reliable and unreliable traffic, where the same parameters as for the simulation behind figure 5.6, that is, $\alpha = 1.2$, $M = 20$, $k = 0.1$, were used. The capacity of the link is 5 packets per basic time unit. By a careful comparison of the two large scale plots it can be seen that the average throughput is slightly higher for the reliable traffic. In figure 5.10 the rescaled range plots are seen, and the Hurst exponent for the unreliable traffic is 0.87 and the Hurst exponent for the reliable traffic is 0.89 compared to 0.85 for the uncapacitated traffic. This difference is too small to conclude that retransmission or no retransmission has any effect on the degree of self similarity. However, it can be concluded that retransmission or no retransmission is not crucial for the

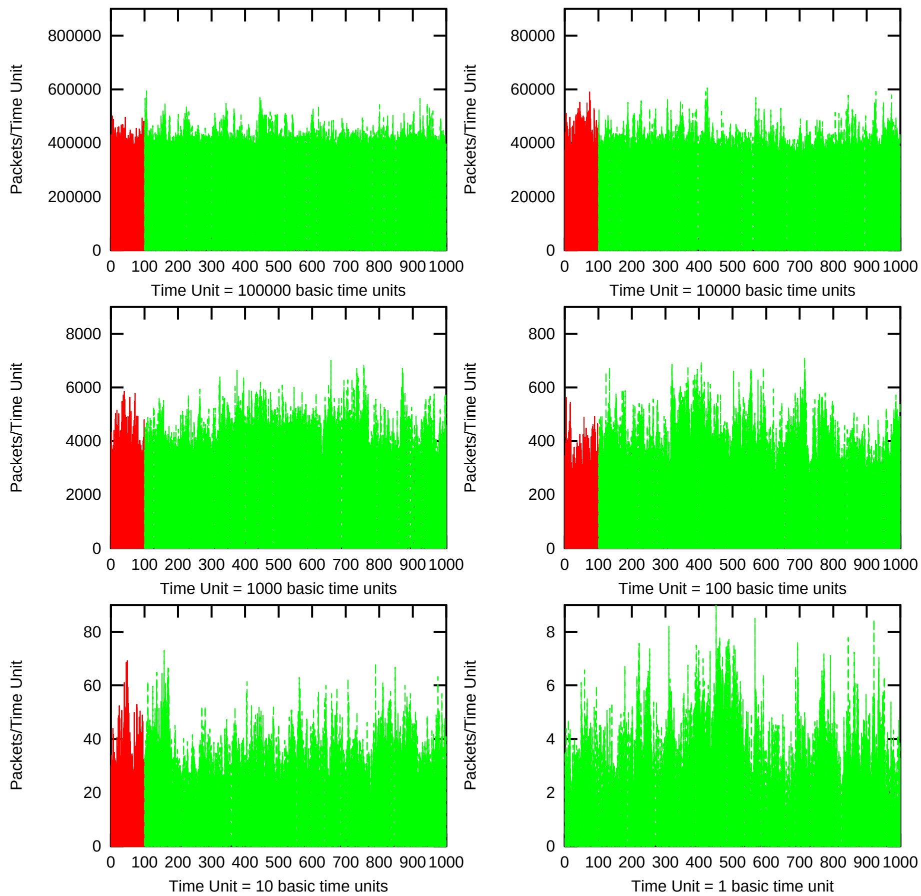

Figure 5.6: Simulation of ON/OFF model. ON and OFF periods i.i.d. $\alpha = 1.2$, $M = 20$, $k = 0.1$.

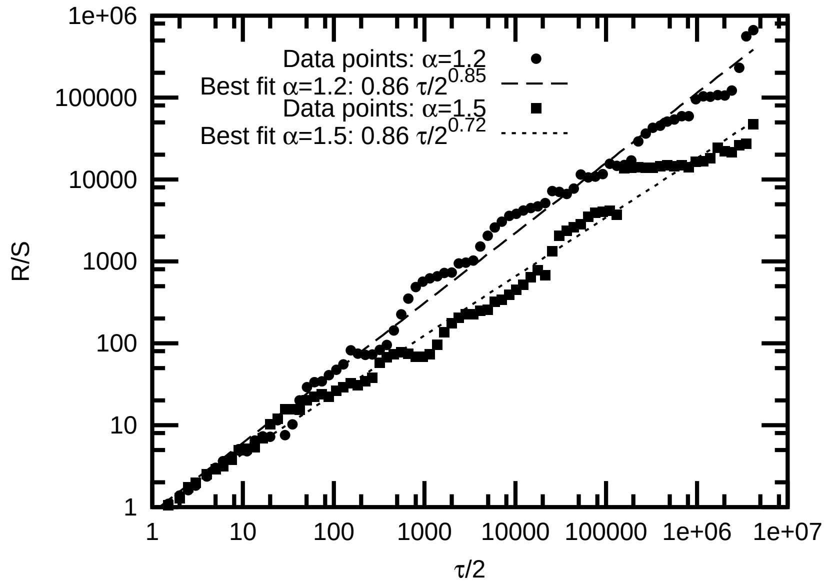

Figure 5.7: Rescaled range plots. Simulation of ON/OFF model. ON and OFF periods i.i.d. $\alpha = 1.2$, $M = 20$, $k = 0.1$ and with $\alpha = 1.5$, $M = 20$, $k = 0.1$. By best fit with a strait line the Hurst exponent becomes $H = 0.85$ for $\alpha = 1.2$ and $H = 0.72$ for $\alpha = 1.5$.

degree of self similarity.

In figure 5.9(a) simulated UDP traffic has been plotted for six time scales with the parameters $\alpha = 1.2$, $M = 20$, $k = 0.1$, and with link capacity set to 5 packets per basic time unit. This is the same parameters as used for figure 5.6 except that no link capacity was used there. When comparing these two figure it is seen that the only difference for the smallest time unit is that in the UDP simulation packets causing the load to be higher than the maximum capacity have been lost. This smoothes the traffic, and when comparing the two figures for the largest time scale it is also seen that UDP traffic smoother. Also it is seen that the UDP traffic has a lower mean, which is a natural consequence from the packet loss.

In the TCP simulation a number of active sources is chosen to go into a pause mode when the load of the link reaches a given level, the maximum capacity, such

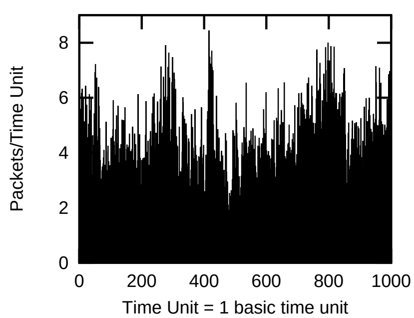

(a) $M = 20$

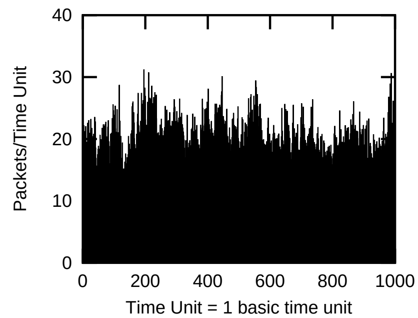

(b) $M = 100$

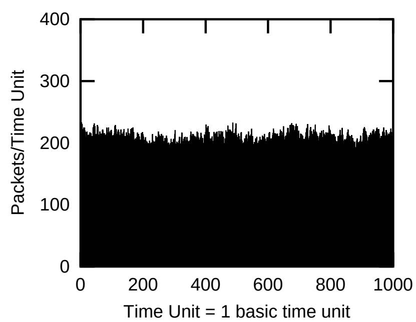

(c) $M = 1000$

Figure 5.8: Plots with different number of sources, M. For all three plots: $\alpha = 1.2$, $k = 0.1$.

that the load stayed at or below the maximum capacity. When active sources in this way pauses the respective ON periods are extended equally. In figure 5.9(b) a simulation of TCP traffic has been plotted for six time scales with the parameters $\alpha = 1.2$, $M = 20$, $k = 0.1$, and with link capacity set to 5 packets per basic time unit. One could think that big bursts in this would be prolonged, whereby bursts at large time scales would be large. This is not the case as seen by comparing the figure with figure 5.6. It is seen that figure 5.6 is more bursty on all time scales. This can be explained by that bursts might be prolonged with TCP but the maximum link capacity makes it impossible for the burst to grow in packets per time unit. It is also seen that then mean traffic load for TCP is larger than for UDP but largest when there is no maximum link capacity.

The sources have in the simulation been priority differentiated. That is the sources all had different priority such that the sources with the lowest priority had their packets lost. Some other possibilities could have been to make a simulation of packet switched or circuit switched traffic. Choosing the group active sources to loose their packets to get the link load below the maximum capacity randomly for every time step would correspond to a packet switched network, whereas choosing the youngest active sources to loose their packets would correspond to a circuit switched network.

5.8 Heavy tailed distributions

A heavy tailed distribution is a distribution with infinite varianse. Compared to the Gaussian distribution which has finite varianse, extreme events are more probable for heavy tailed distributions. Another important property of heavy tailed distribution that the sum of such distributions does not converge to a Gaussian as stated by the Central Limit Theorem, since the requirement of finite varianse is not fulfiled. Actually the sum of identical heavy tailed distritions gives the same distribution, which is why the definition, equation 5.1, of self similarity is fulfilled for systems where the changes are heavy tailed distributed.

The distributions, which fall off as a power-law,

$$P(x) \propto x^{-(\alpha+1)} \text{ for } x \to \infty \tag{5.4}$$

is heavy tailed for $1 < \alpha < 2$.

An example of such a distribution is the Pareto distribution:

$$P(x) = \begin{cases} 0 & \text{for } x < k \\ \alpha k^{\alpha} x^{-(\alpha+1)} & \text{for } x \geq k \end{cases} \tag{5.5}$$

where $\alpha, k > 0$. Its distribution function has the form

$$F(x) = 1 - (k/x)^{\alpha} \tag{5.6}$$

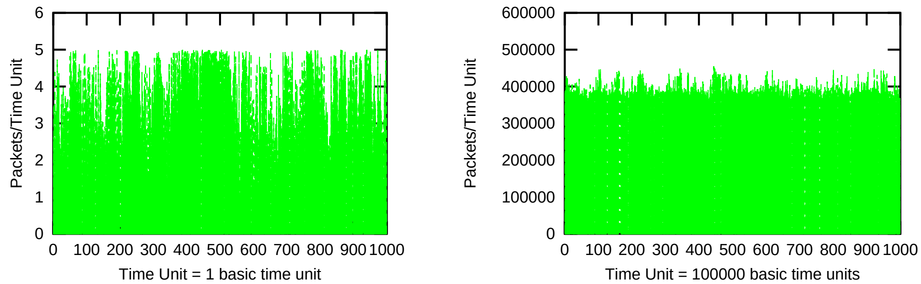

(a) Unreliable traffic

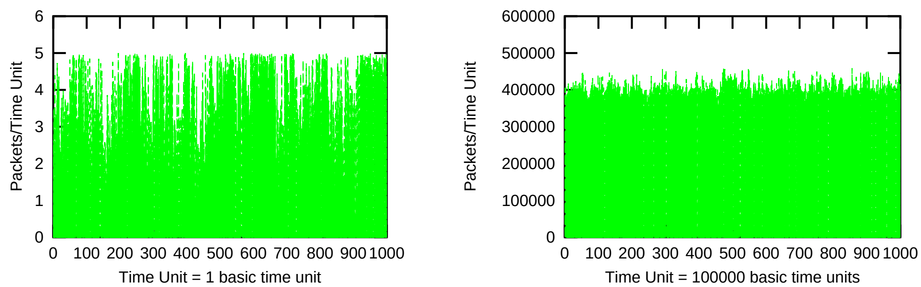

(b) Reliable traffic

Figure 5.9: (a) Simulation of ON/OFF model for unreliable traffic. ON and OFF periods i.i.d. $\alpha = 1.2$, $M = 20$, $k = 0.1$. Link capacity: 5 packets per basic time unit. (b) Simulation of ON/OFF model for reliable traffic. ON and OFF periods i.i.d. $\alpha = 1.2$, $M = 20$, $k = 0.1$. Link capacity: 5 packets per basic time unit.

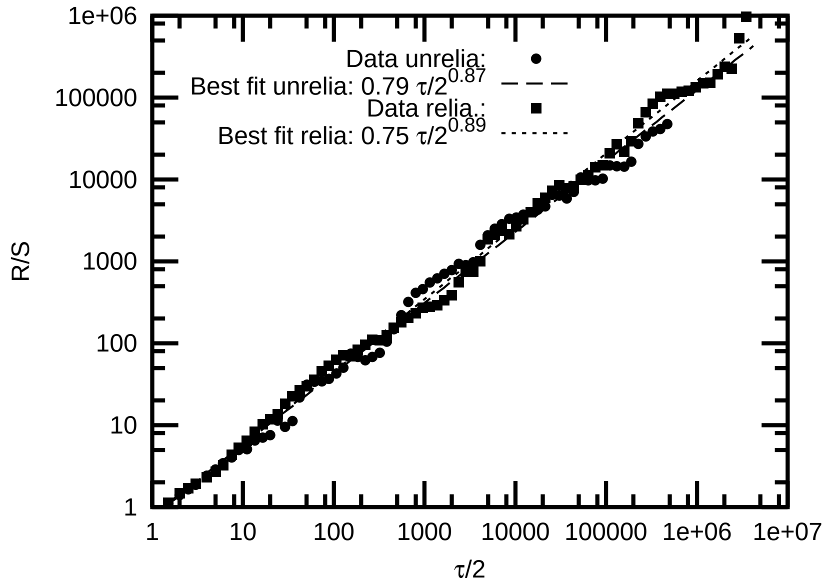

Figure 5.10: Rescaled range plots. Simulation of ON/OFF model for unreliable and reliable traffic. ON and OFF periods i.i.d. $\alpha = 1.2$, $M = 20$, $k = 0.1$. Link capacity: 5 packets per basic time unit. By best fit with a strait line the Hurst exponent becomes $H = 0.87$ and 0.89 respectively.

If $\alpha \leq 2$ the distribution has infinite variance, and if $\alpha \leq 1$ then the distribution has also infinite mean. The mean is:

$$\mu = \int_k^\infty x \alpha k^\alpha x^{-(\alpha+1)} dx = \begin{cases} \infty & \text{for } \alpha \leq 1 \\ \frac{\alpha}{\alpha-1} k & \text{for } \alpha > 1 \end{cases} \tag{5.7}$$

The variance is:

$$\sigma^2 = \int_k^\infty (\mu - x)^2 \alpha k^\alpha x^{-(\alpha+1)} dx = \begin{cases} \infty & \text{for } \alpha \leq 2 \\ \left(\frac{\alpha}{\alpha-2} - \frac{\alpha^2}{(\alpha-1)^2} \right) k^2 & \text{for } \alpha > 2 \end{cases} \tag{5.8}$$

An example of a self similar system is given in Bak et al. (1997), where it is stated that the price changes, Δp, occur with a probability $P(\Delta p) \sim (\Delta p)^{-\alpha-1}$

with $\alpha \simeq 1.4$ for the Standard and Poor 500 index on time scales from a minute to a day. The distribution converges to a approximate Gaussian at a time scale around a month. The reason for this convergence to Gaussian can be due to the lack of independence and/or that the distribution for the smaller time scales is only almost heavy tailed.

5.9 Methods for determining the Hurst exponent

5.9.1 Probability of return

H can be found by plotting the probability of return to zero:

$$P_T(0) = \left(\frac{\tau}{T}\right)^H P_\tau(0) \tag{5.9}$$

as a double log plot with T out of the x-axis and $P_T(0)$ up the y-axis.

In the case of data traffic then P_T is the distribution for the cumulated aggregated traffic over a period of length T.

5.9.2 Rescaled range, R/S, analysis

The following is taken from Feder (1988). Let $X = \{X(i), i \geq 1\}$ be a stationary sequence, e.g. the traffic load, or round trip time for a packet. The average traffic load over a period of τ basic time units is

$$\langle X \rangle_\tau \equiv \frac{1}{\tau - 1} \sum_{t=1}^{\tau} X(t) \tag{5.10}$$

Let $Z(t)$ be the accumulated departure of the traffic load

$$Z(t,\tau) \equiv \sum_{u=1}^{t} (X(u) - \langle X \rangle_\tau) \tag{5.11}$$

The maximum difference i $Z(t,\tau)$ is $R(\tau)$

$$R(\tau) \equiv \max_{1 \leq t \leq \tau}\{Z(t,\tau)\} - \min_{1 \leq t \leq \tau}\{Z(t,\tau)\} \tag{5.12}$$

The standard deviation:

$$S(T) = \left(\frac{1}{\tau} \sum_{t=1}^{\tau} (X(t) - \langle X \rangle_\tau)^2 \right)^{1/2} \tag{5.13}$$

Hurst found that the following empirical equation holds quite well:

$$R/S = (\tau/2)^H \tag{5.14}$$

5.10 Conclusion

It was found that data traffic is bursty, both for local area network and for networks covering more continents, which involves many aspects in layered networking. The degree of self similarity changes with respect to place and time indicating that on this level the origin of self similarity involves more than just the source level characteristics which are constant. It was found by using the ON/OFF model that the source level characteristics do produce self similar data traffic. Therefore both the network behavior and the traffic source characteristic leads to self similarity.

Simulations of unreliable and reliable protocols in the framework of the ON/OFF model were performed. It was shown that for both of these protocol no change in the self similarity was introduced.

With the model it was also seen that the self similar behavior decreased very fast with the number of active sources making the relative influence of the self similarity smaller for more aggregated traffic. Since the relative size of the bursts decrease with aggregation the main conclusion for the theme of optical networking is that the traffic behavior for wavelengths, assuming that these consists of heavily aggregated traffic, does not change drastically when going from Poisson to Pareto traffic.

Chapter 6

Synchronous Optical Hierarchy

6.1 Abstract

The problems and challenges of a novel transparent optical network solution are introduced and described. We name this solution the synchronous optical hierarchy. It is a form of wavelength routed optical network where the signals occupy fractions of a wavelength through the use of timeslots in frames. Using timeslots for transparent optical networks will solve the capacity granularity problem which is present in the wavelength routed optical network.

We define the problem of assigning wavelengths and timeslots to traffic demands by integer linear programming formulations. We solve the problems by using different routing and coloring algorithms and integer linear programming. For given network, routing, traffic distribution, and parameters describing the synchronous optical hierarchy, we analytically derive the wavelength usage. The accuracy of the analytical model is found to be good when comparing with simulation results, and the model is used to derive optimal choices of timeslots under given conditions, as well as to estimate the gain from applying the synchronous optimal hierarchy.

By solving the integer linear programs for networks with static traffic assumptions we compare the efficiency of synchronous optical hierarchy networks with wavelength routed optical networks. Further, the effect of timeslot and wavelength conversion in synchronous optical hierarchy networks is also studied, as well as the presence of delay of timeslots.

6.2 Introduction

The essence of this chapter has been published in Fenger and Glenstrup (2002b).

As switching cost has become increasingly expensive, Simmons and Saleh (1999) and Roberts (2000), several ideas have been put forward to reduce the switching cost and optical-electric-optical conversion delay by applying optical switching to transit traffic, Veeraraghavan et al. (2001). These suggestions include static and dynamic WRONs (wavelength routed optical networks) Chlamtac et al. (1989); Ramaswami and Sivarajan (1995); Baroni et al. (1999); Cinkler et al. (2000); Glenstrup et al. (2000); Lee et al. (2000); Listanti and Eramo (2000); Pióro et al. (2000) and optical packet switching networks, Guillemot et al. (1998); Hunter et al. (1999); Listanti and Eramo (2000); Hunter and Andonovic (2000). This chapter introduces and studies a practical and efficient alternative to these structures, called the SOH (synchronous optical hierarchy).

The WRON, a circuit switched all-optical network, has long been seen as the solution to drive down cost because electrical processing in large is avoided. The problem with the WRON is that the capacity granularity for connections is in wavelengths, presently up to 40 Gb/s. Traffic demands smaller than this will still occupy a whole wavelength, only making use of a fraction of the available capacity. This is the capacity granularity problem.

Optical packet switched networks could in principle solve the capacity granularity problem, because only the number of packets necessary to accommodate the traffic demands are sent through the network, but unfortunately packet switched optical networks will have to overcome major technological hurdles before they can be deployed. The problems are, among others, a lack of optical buffering and problems of optical label reading and processing Guillemot et al. (1998); Hunter et al. (1998a,b), and as it is a packet switched technology, quality of service requirements are more difficult to fulfill.

The SOH network is seen by the authors as the solution for telecom operators. A similar idea was proposed by Huang et al. (2000) as time shared wavelength channels. Connections in the SOH are circuit switched like in the WRON, but since the wavelengths here consist of frames, which are divided into timeslots, the granularity of a connection is only a fraction of a wavelength, whereby the capacity granularity problem is reduced. Consequently, the technological hurdles which arise in optical packet switched networks are avoided, while the speed and much of the flexibility of optical packet switched networks is preserved.

In the SOH network wavelengths are divided into frames which are composed of timeslots, followed by gaps for synchronization purposes, as illustrated in Figure 6.1. One timeslot per frame is the minimum capacity unit for traffic demands, and a connection can drop in and out of different wavelengths via timeslot add/drops and timeslot cross connects. Bianco et al. (1999) and Kannan et al. (1997) have also considered timeslots, but in configurations where the wavelengths or timeslots were predetermined between specific groups of users, reducing the load flexibility for the individual end-to-end demand.

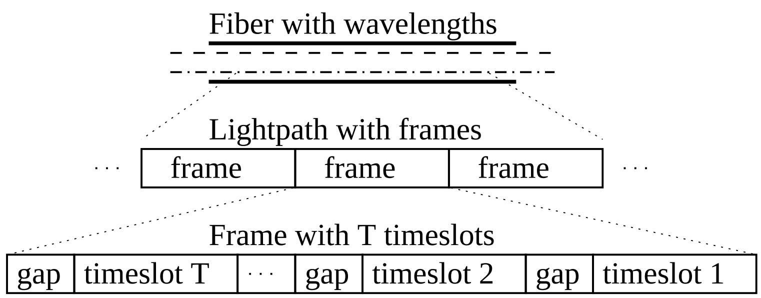

Figure 6.1: Illustration of relation between lightpaths, frames, and timeslots.

The timeslots in the SOH are synchronized, i.e. all switches send a specific number of frames per second, with well-defined positions of timeslots and gaps in the frame. This characteristic and the fact that the network is circuit switched avoids the need for buffering. Further, as a connection is uniquely determined by a timeslot on a wavelength, no label reading is necessary. Thus, the buffering, label reading and processing which are the major hurdles of packet switched optical networks are entirely avoided in the SOH.

A hierarchy is naturally implemented in the SOH, thereby eliminating any granularity problems and saving cost in networks with different traffic levels. There are more ways to introduce the hierarchy: Either a minimum timeslot length is defined, and multiples of this timeslot length would then be available; or a minimum bit rate is defined, and multiples of this bit rate is then available.

In this chapter we formulate and analyze the problems of routing and assigning timeslots and wavelengths in the SOH network. And we study the advantages of using SOH compared to WRON, measured in wavelength usage in the single fiber case, that is, the number of wavelengths needed in the maximum loaded network link to accommodate the offered amount of static traffic. Huang et al. (2000) also considered static traffic, but for the capacitated problem, measuring the percentage of allocated traffic, and only for a fixed number of timeslots per frame, either allocating or rejecting the entire amount of offered traffic between two nodes.

The problem of routing and assigning timeslots and wavelengths in the SOH network is solved both by a heuristic and ILP (integer linear programming). In both circumstances the problem is solved sequentially. I.e. routing is performed independently of the timeslot and wavelength assignment. We will in the very end of Section 6.6.4 comment on why this practice is only negligible worse performing than simultaneous solution of the routing and timeslots and wavelengths assigning problem.

We define uncapacitated network design problems by ILP programs, using formulations where the paths are pre-calculated. These formulations are well-known for WRONs Ramaswami and Sivarajan (1995); Glenstrup et al. (2000); Lee et al. (2000); Pióro et al. (2000) , but here we extend them to include time-slots, with wavelength conversion, timeslot conversion, and delay of timeslots. The advantage of using the formulation with pre-calculated paths instead of formulation where the paths are found by the ILP programming, like that used by Cinkler et al. (2000), is that the problem size can be kept reasonable by restricting the number of pre-calculated paths for each demand.

All our numerical experiments were performed on a Pan-European network with 19 nodes and 39 links, where we vary the number of timeslots per frame and the gap between each timeslot. Due to the novelty of the ideas presented here, the focus is on qualitative results.

6.3 Switching timeslots in SOH networks

When a connection in the SOH network is to be set up, a timeslot can be chosen freely at the source node, as long as the timeslot is empty. At the intermediate nodes, by default the timeslot for the next hop can be determined by that of the preceding hop. Naturally, this timeslot must not be occupied by any other connection—if this is the case, either timeslot conversion must be used, or the entire connection must use a different timeslot.

Timeslot conversion in the SOH is in principle similar to wavelength conversion in the WRON. To do timeslot conversion, the signal in a timeslot must be delayed by a predetermined amount of time. Fixed, predetermined delays are easily achieved optically with FDLs (fiber-optic delay lines). This delay, however short, is a drawback of timeslot conversion.

Due to the switching of packets in timeslots, they must arrive in phase at the node inputs. A simple way to synchronize the timeslots is to arrange all fiber spans connecting nodes in such a way that the time delay is equal to a multiple of the timeslot length. However, due to path variations, e.g. induced by temperature changes, this solution is not sufficiently reliable in practice, and optical synchronizers are necessary Gambini et al. (1998); Guillemot et al. (1998); Huang et al. (2000). To enable exact determination of the timeslot position, gaps between timeslots are needed as illustrated in Figure 6.1.

It is also conceivable to align the frames, such that timeslot 1 from all incident links enter a switch simultaneously, then timeslot 2, etc. However, frames are a virtual concept without any significance for the optical signal; switching does not become any easier for this reason, and aligning frames would cause unnecessary transmission delay.

In the case that the entire frames are not aligned, the packet on timeslot i on an input frame could be switched to a timeslot j on an output frame, where $i \neq j$. In Figure 6.2, the timeslot synchronization and switching is illustrated by an example of two input ports and two output ports with four timeslots per frame. In the figure the frames in the two input links a and b arrive out of phase with a phase shift, after synchronization, of exactly two timeslots. Thus we characterize each link by a delay. In the following we assume that this delay, including the synchronization, is constant and independent of the direction of the traffic on the link.

6.4 Mathematical formulations

In this section we give the integer linear programming (ILP) formulations of the problem of assigning timeslots and wavelengths to traffic demands.

Let a network, where each fiber holds W wavelengths and each frame consists of T timeslots, be represented by a set of L links, and the traffic by a set of D demands. The path for each demand is pre-calculated and expressed as a set of links. The routing aspect is discussed in Section 6.6.2.

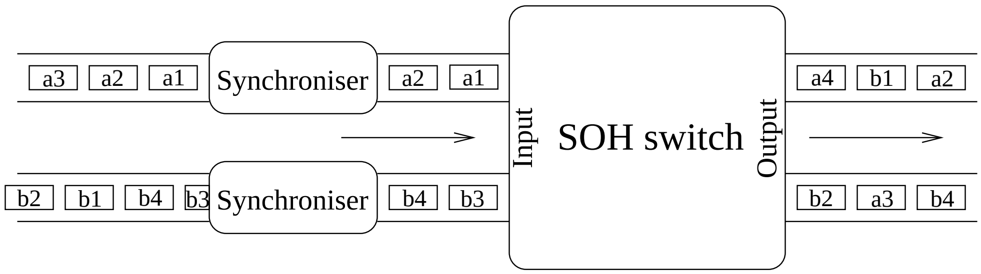

Figure 6.2: Illustration of synchronization and timeslot switching. Here four timeslots per frame are assumed, two input links and two output links with one wavelength per fiber, and one fiber per link.

The main objective is always to minimize the necessary number of wavelengths, W.

In summary, the following indices are used:

d	$= 1,\ldots,D$	traffic demands
w	$= 1,\ldots,\infty$	wavelengths
t	$= 1,\ldots,T$	timeslots
k,l	$= 1,\ldots,L$	links

We introduce constants that describe the volume of the traffic demands, the predefined paths for these demands, including an ordering relation for the path links, and the delay:

h_d	volume of demand d (measured in timeslots)
a_{ld}	1 if link l supplies demand d, otherwise 0
p_{dkl}	1 if link k is the predecessor of link l on the path satisfying demand d, otherwise 0
q_l	the delay in timeslots of a timeslot transported on link l

We present five flavors of the wavelength and timeslot assignment problem for the SOH network and one wavelength assignment problem for the WRON:

SOH: Both wavelengths and timeslots must be assigned, and delays are assumed to be zero (modulo the frame length), i.e. all frames at all switches are in phase. No conversion is present. Optimal result: W_{SOH}.

WRON: Only wavelengths must be assigned (there are no timeslots). No conversion is present. Optimal result: W_{WRON}.

SOH with delay: Both wavelengths and timeslots must be assigned, and delays are given for each link. No conversion is present. Optimal result: W_{delay}.

SOH with wavelength conversion: Both wavelengths and timeslots must be assigned, but wavelengths can change at each node along a path. No timeslot conversion is present. Optimal result: $W_{\lambda\ conversion}$.

SOH with timeslot conversion: Both wavelengths and timeslots must be assigned, but timeslots can change at each node along a path. No wavelength conversion is present. Optimal result: $W_{slot\ conversion}$.

SOH with full conversion: Both wavelengths and timeslots must be assigned, and both can change at each node along a path. Optimal result: $W_{full\ conversion}$.

In the following, we use for each flavor some decision variables to keep track of the assigned flow and wavelengths, and give a list of constraints for describing the particular problem.

6.4.1 ILP formulation for SOH

Variables

x_{dwt}	1 if demand d uses wavelength w, timeslot t, otherwise 0
y_w	1 if wavelength w is used, otherwise 0

Constraints

$\sum_w y_w$	$=$	W		main minimisation objective
$\sum_{w,t} x_{dwt}$	$=$	h_d	$\forall d$	satisfy all demands
$\sum_d a_{ld} x_{dwt}$	$\leq$	1	$\forall l, w, t$	use each wavelength/timeslot on each link at most once
x_{dwt}	$\leq$	y_w	$\forall d, w, t$	compute which wavelengths are used
x_{dwt}, y_w	$\in$	$\{0, 1\}$	$\forall d, w, t$	use only binary decision variables

6.4.2 Transformation of SOH to WRON

By transforming the ILP formulation for the SOH problem to an ILP formulation for the WRON problem we can show that these two problem are equivalent, whereby solving one of them solves both.

To transform the problem, introduce extra variables $y_{wt} = y_w \ \forall t$, whereby the objective becomes to minimize $\sum_{wt} y_{wt} = W \cdot T$. Then replace all occurrences of wt with w', replace all occurrences of w, t with w', and set $W' = W \cdot T$. Finally, replace w' with w and W' with W, to obtain the ILP for the WRON problem:

Variables

x_{dw}	1 if demand d uses wavelength w, otherwise 0
y_w	1 if wavelength w is used, otherwise 0

Constraints

$\sum_w y_w$	$=$	W		main minimisation objective
$\sum_w x_{dw}$	$=$	h_d	$\forall d$	satisfy all demands
$\sum_d a_{ld} x_{dw}$	$\leq$	1	$\forall l, w$	use each wavelength on each link at most once
x_{dw}	$\leq$	y_w	$\forall d, w$	compute which wavelengths are used
x_{dw}, y_w	$\in$	$\{0, 1\}$	$\forall d, w$	use only binary decision variables

The fact that the results for the SOH and WRON problem formulations are equivalent except for a factor T is rigorously stated and proved below.

Theorem 1. *Given identical parameters, h_d and a_{ld}, then*

$$\boxed{W_{SOH} = \left\lceil \frac{W_{WRON}}{T} \right\rceil}$$

Proof: Let the solution to the WRON problem be given, i.e let W_{WRON} and the corresponding values of x_{dw} and y_w be given. As it is an uncapacitated problem, this is always possible.

Without loss of generality we assume that $y_w = 0$ for all $w > W_{WRON}$; this also implies that $x_{dw} = 0$ for all $w > W_{WRON}$ and $y_w = 1$ for all $w \leq W_{WRON}$. Let $W' = \lceil W_{WRON}/T \rceil$, and for $w' = 1, \ldots, W'$ and $t = 1, \ldots, T$ let $x_{dw't} = x_{dw}$, where $w = t + T(w' - 1)$, and let $y_{w'} = \max_t \{ y_{t+T(w'-1)} \}$. This implies that $y_{w'} = 1$ for all $w' \leq W'$. We find that constraints of the SOH formulation are indeed fulfilled with the variables W', $x_{dw't}$, and $y_{w'}$:

$$\begin{array}{rcll} \sum_{w'} y_{w'} & = & W' & \\ \sum_{t,w'} x_{dw't} = \sum_{t=1}^{T} \sum_{w'=1}^{W'} x_{d,t+T(w'-1)} = \sum_{w=1}^{T \cdot W'} x_{dw} = \sum_w x_{dw} & = & h_d & \forall d \\ \sum_d a_{ld} x_{dw't} = \sum_d a_{ld} x_{dw} & \leq & 1 & \forall l, w', t \\ x_{dw't} = x_{dw} \leq y_w & \leq & y_{w'} & \forall d, w', t \end{array}$$

To see that this solution is optimal, i.e. $W' = W_{SOH}$, suppose there exists a better solution $W'' = \lceil W_{WRON}/T \rceil - a$, where a is an integer greater than zero. Again, without loss of generality assume that $y_{w'} = 0$ for $w' > W''$ and thus $x_{dw't} = 0$. Setting $y_{w'} = y_w$ and $x_{dw't} = x_{dw}$ for $w = 1, \ldots, W'' \cdot T$, where $w' = \lceil w/T \rceil$, we find that

$$\begin{array}{rcll} \sum_{w'} x_{dw't} = \sum_w x_{dw} & = & h_d & \forall d \\ \sum_d a_{ld} x_{dw't} = \sum_d a_{ld} x_{dw} & \leq & 1 & \forall l, w' \\ x_{dw't} = x_{dw} & \leq & y_w = y_{w'} & \forall d, w' \end{array}$$

but $\sum_w y_w = \sum_{w'} T \cdot y_{w'} = T \sum_{w'} y_{w'} = T \cdot W'' = T(\lceil W_{WRON}/T \rceil - a) < W_{WRON}$, which contradicts the optimality of W_{WRON}. Therefore $W_{SOH} = \lceil W_{WRON}/T \rceil$. ■

A trivial addition to Theorem 1 is that the wavelength usage for the SOH network in case of timeslot and wavelength conversion, $W_{full\ conversion}$, is related to the wavelength usage in the WRON with conversion, $W_{WRON,\ conversion}$, by the equivalent equation:

$$\boxed{W_{full\ conversion} = \left\lceil \frac{W_{WRON,\ conversion}}{T} \right\rceil}$$

It can be seen that a gain in wavelength usage by using wavelength converters and timeslot converters in the SOH network leads to a gain in the corresponding WRON. The opposite is not true.

6.4.3 ILP formulation for SOH with delay

Variables

x_{dwtl}	1 if demand d uses wavelength w in timeslot t on link l, otherwise 0
y_w	1 if wavelength w is used, otherwise 0

Constraints

$\sum_w y_w$	$=$	W		main minimisation objective
$\sum_{t,w} x_{dwtl}$	$=$	$a_{ld}\, h_d$	$\forall d, l$	satisfy all demands
$\sum_d a_{ld} x_{dwtl}$	$\leq$	1	$\forall l, w, t$	use each wavelength/timeslot on each link at most once
x_{dwtl}	$\leq$	y_w	$\forall l, d, w, t$	compute which wavelengths are used
x_{dwtk}	$=$	$x_{dwt'l}$	$\forall d, w, l, t,$	change timeslot position of demand
			$k{:}\, p_{dkl}=1,$	use the predecessor link to link l
			$t'{:}t'=(t+q_k) \bmod T$	t' is the new timeslot after link k
x_{dwtl}, y_w	$\in$	$\{0,1\}$	$\forall l, d, w, t$	binary decision variables

In this formulation we must keep track of the timeslot used on each link of a path, which requires an extra index l on the flow variable x. We then add a constraint ensuring that if link k is a predecessor of link l on the path of demand d, the timeslots are cyclically delayed q_k timeslots when going from k to l. Note that the modulus operator used differs slightly from the traditional definition. Traditionally, if the left argument is a multiple of the right argument the results is zero, but we have: $k \cdot n \bmod n = n, \forall k \in \mathbb{N}$, because the numbering of timeslots starts with 1.

6.4.4 ILP formulation for SOH with wavelength conversion

Variables

x_{dt}	number of wavelengths used by demand d in timeslot t

Constraints

$\sum_t x_{dt}$	$=$	h_d	$\forall d$	satisfy all demands
$\sum_d a_{ld} x_{dt}$	$\leq$	W	$\forall l, t$	compute number of wavelengths used for each timeslot on each link
x_{dt}	$\in$	$\mathbb{N}_0$	$\forall d, t$	decision variables are non-negative integers

With wavelength conversion the wavelength index w on the x-variable is not needed.

6.4.5 ILP formulation for SOH with timeslot conversion

Variables

x_{dw}	number of timeslots used by demand d on wavelength w
y_w	1 if wavelength w is used, otherwise 0

Constraints

$\sum_w y_w$	$=$	W		main minimisation objective
$\sum_w x_{dw}$	$=$	h_d	$\forall d$	satisfy all demands
$\sum_d a_{ld} x_{dw}$	$\leq$	T	$\forall l, w$	use at most T timeslots on each wavelength of each link
$x_{dw} \geq 1$	$\Rightarrow$	$y_w = 1$	$\forall d, w$	compute which wavelengths are used
x_{dw}	$\in$	$\mathbb{N}_0$	$\forall d, w$	number of timeslots is a non-negative integer
y_w	$\in$	$\{0, 1\}$	$\forall w$	wavelength usage is a binary decision variable

In this formulation we need not keep track of precisely which timeslots are used for each demand, only the total number for each wavelength. As $x_{dw} \leq T$, the implication constraint is simply implemented in the ILP program as $x_{dw} \leq T \cdot y_w$.

6.4.6 ILP formulation for SOH with full conversion

Constraints

$\sum_d a_{ld} h_d$	$\leq$	$T \cdot W$	$\forall l$	each link can carry T timeslots on each wavelength

With full conversion the number of needed wavelengths is determined by the links loaded with the highest volume of traffic.

6.4.7 Relationships between optimal values

We mention without rigorous proof that given the same traffic demands h_d and routing a_{ld}, the following relationships between the optimal values of W found by the various ILP formulations hold:

$$\begin{array}{rcccl} W_{SOH} & \geq & W_{\lambda\ conversion} & \geq & W_{full\ conversion} \\ W_{SOH} & \geq & W_{slot\ conversion} & \geq & W_{full\ conversion} \\ W_{delay} & \geq & W_{slot\ conversion} & \geq & W_{full\ conversion} \\ W_{SOH} & = & \lceil W_{WRON}/T \rceil & & \end{array}$$

In each case, the solution whose value is represented on the left side of one of the inequalities will also be a feasible solution to the problem represented on the right side.

6.5 Gain from using timeslots

In this section we analytically show the capacity savings from using timeslots.

Theorem 2. *Assume zero gap, wavelength conversion, and that the traffic demand volume, A_d, between each node pair, given in granularity of wavelengths (as opposed to h_d which was given in units of timeslots), is chosen from the uniform distribution from 0 to K, where K is a positive integer. Assume further that one link carries a significantly higher number of paths than all other links in the network. Then the number of expected wavelengths is*

$$\boxed{\lambda = \left(\frac{K}{2} + \frac{1}{2T}\right) D}$$

Where T is the number of timeslots per frame, and D is the number of demands on the link, which carries the maximum number of paths.

Proof: The average usage of timeslots for one demand is

$$\sum_{k=1}^{KT} P(k-1 < A_d T < k)\, k = \sum_{k=1}^{KT} \frac{k}{KT} = \frac{(KT)^2 + KT}{2KT} = \frac{KT}{2} + \frac{1}{2}$$

Where $P(\cdot)$ denotes the probability. The average use of timeslots on a link with d demands is then by multiplication by d:

$$\left(\frac{KT}{2} + \frac{1}{2}\right) d$$

The average use of wavelength is then given by the smallest larger integer after division by T:

$$\left(\frac{K}{2} + \frac{1}{2T}\right) d$$

Since one link carries a significantly higher number of paths than all other links in the network then the wavelength usage, λ, is determined by that link, i.e.

$$\lambda = \left(\frac{K}{2} + \frac{1}{2T}\right) D$$

■

With uniformly distributed demand sizes it is seen that the higher the number of timeslots per frame the larger are the savings, but the savings are never more than 50%. The higher the upper bound is in the uniform distribution (determined by K), the smaller are the relative savings by using timeslots.

When we assume non-zero and non-integer parameters, the proof for the average wavelength usage becomes more technical:

Theorem 3. *Assume a gap between 0 and $1/T$ frame length, i.e. $0 \leq g < 1/T$, where T is the number of timeslots per frame. Assume wavelength conversion, and that the traffic demand volume between each node pair in granularity of wavelengths is chosen from the uniform distribution from 0 to K, where K is positive. Assume further that one link carries a significantly higher number of paths than all other links in the network. Then the number of expected wavelengths is*

$$\boxed{\lambda = \frac{1-Tg}{KT^2}\left(\frac{1}{2}\left\lfloor\frac{KT}{1-Tg}\right\rfloor^2 + \frac{1}{2}\left\lfloor\frac{KT}{1-Tg}\right\rfloor + \left\lceil\frac{KT}{1-Tg}\right\rceil\left(\frac{KT}{1-Tg} - \left\lfloor\frac{KT}{1-Tg}\right\rfloor\right)\right) D}$$

Where D is the number of demands on the link, which carries the maximum number of paths, where $\lfloor\cdot\rfloor$ denotes the largest smaller integer, and $\lceil\cdot\rceil$ denotes the smallest larger integer.

Proof: One traffic demand can fill up to $\left\lceil \frac{KT}{1-Tg} \right\rceil$ timeslots. With A_d being the demand volume of demand d in granularity of wavelengths, the average usage of timeslots for one demand becomes

$$\sum_{k=1}^{\left\lceil \frac{KT}{1-Tg} \right\rceil} P\left(k-1 < \frac{A_d T}{1-Tg} < k\right) k =$$

$$\left(\sum_{k=1}^{\left\lfloor \frac{KT}{1-Tg} \right\rfloor} P\left(k-1 < \frac{A_d T}{1-Tg} < k\right) k\right) + \left\lceil \frac{KT}{1-Tg} \right\rceil P\left(\left\lceil \frac{KT}{1-Tg} \right\rceil - 1 < \frac{A_d T}{1-Tg} < \left\lceil \frac{KT}{1-Tg} \right\rceil\right) =$$

$$\left(\sum_{k=1}^{\left\lfloor \frac{KT}{1-Tg} \right\rfloor} \frac{1-Tg}{KT} k\right) + \left\lceil \frac{KT}{1-Tg} \right\rceil \frac{1-Tg}{KT} \left(\frac{KT}{1-Tg} - \left\lfloor \frac{KT}{1-Tg} \right\rfloor\right)$$

Following the same steps as in the proof for Theorem 2, we get the stated expected wavelength usage. ■

6.6 Results and discussion

In this section we first look at the idealized SOH network were the gap is zero and verify the principles of Theorem 2. An ensemble of non-uniform traffic matrices were used for statistical purposes. Secondly, we describe a method to determine the optimal number of timeslots the frame for any gab size. Thirdly, we analyze an example in depth with the traffic generated from the gravity model. The network used in all cases is the The Pan-European network used in the OPEN project Chbat et al. (1998) consisting of 19 nodes and 39 links as displayed in Figure 6.3.

6.6.1 Generation of traffic

We give the traffic demand matrix in units of wavelength, where a wavelength corresponds to a specific bit rate.

Consider the structure of a frame, displayed in Figure 6.4. We let f denote the frame length in time, g the gap length in time, t the timeslot length in time, and T

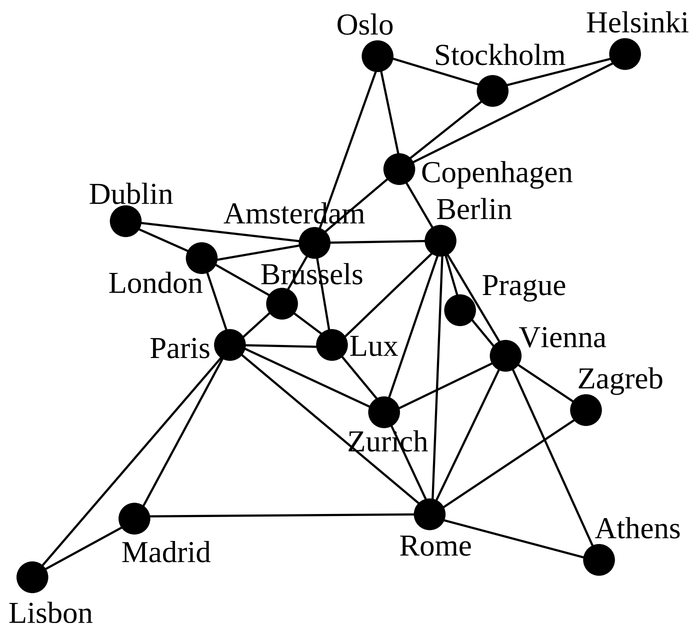

Figure 6.3: The Pan-European network consisting of 19 nodes and 39 links.

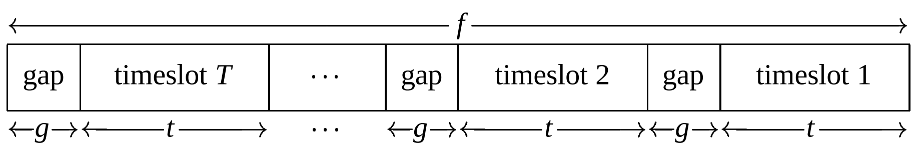

Figure 6.4: Frames are composed of timeslots and gaps. Here 1 frame with T timeslots and gaps is shown.

the number of timeslots in a frame. As each frame consists of T timeslots and T gaps, we have that $f = (t+g)T$, i.e. $t = f/T - g$.

Setting the time unit such that the length of f is 1, then the required number of timeslots, h_d, for satisfying a specific traffic demand, A_d, varies only with T and g. To each d corresponds an element in the traffic matrix. We disallow fractional timeslots—any such values are rounded up to the nearest integer, so the required number of timeslots is $h_d = \lceil A_d/t \rceil = \lceil A_d/(1/T - g) \rceil$. It is seen that if $g = 1/T$ then no number of timeslots can accommodate the traffic demand. In this case the gaps between the timeslots in the frame fill up the entire frame, such that the timeslot length has to be zero, which, of course, is useless.

6.6.2 Routing

We distinguish between what we call simple shortest path routing and optimized shortest path routing. Both routing methods refer to complete routing between all node pairs in the networks between which a traffic demand exists. We define simple shortest path routing as routing using shortest paths without consideration of congestion of the links. Optimized shortest path routing is defined as routing making use of only shortest paths, but where the paths are chosen such that the link with the highest traffic load carries as little traffic as possible. The metric used is number of hops. For simplicity only one path for each demand is considered.

The method for finding the optimized shortest path routing is similar to the one used in Baroni and Bayvel (1997). It is a near optimal method, i.e. we can not guarantee that the most congested link carries as little traffic as possible, but almost. When routing the traffic demands, we employ shortest path routing, using the number of hops as the distance measure. Since usually more than one shortest path exists between each node pair a certain degree of freedom is available and is used to balance, as evenly as possible, the paths among all the links. This contributes to the reduction of number of lightpaths to be rerouted in case of a link failure and to minimize the network wavelength requirement. The path allocation is performed as follows: For each node pair an alternative shortest path substitutes the one previously assigned when the number of channels used on the most loaded link with the alternative path is lower. The process is repeated until no further improvement can be made. Although allowing longer paths than the shortest path between a node pair could lower the the number of channels used on the most loaded link, we do not allow this, since the overall capacity usage would be increased. For simplicity we route all demands between two nodes on the same path. The routing depends on the traffic demands; when the demands change, rerouting must be performed.

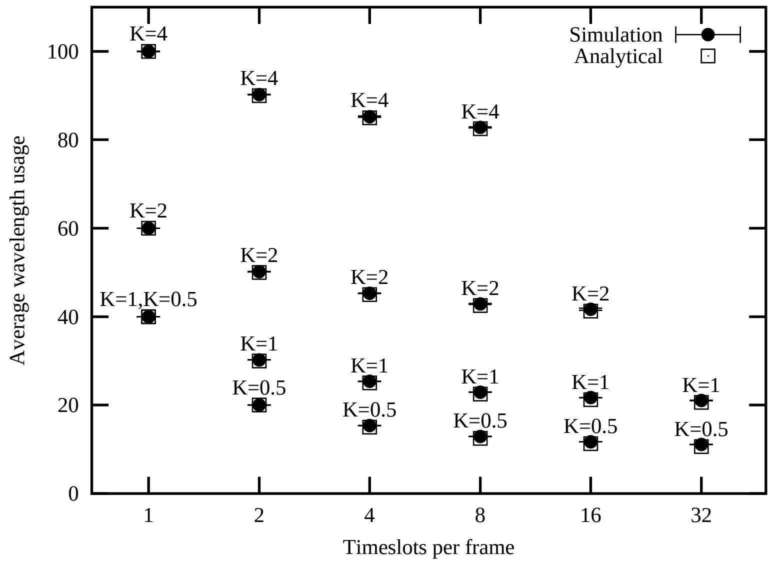

Figure 6.5: Analytically predicted usage of wavelength compared to simulation in case of simple shortest path routing. The 95% confidence interval is shown for the simulation results. Traffic is symmetric uniformly distributed in the interval $[0;K[$. Zero gab.

6.6.3 Verification and consequence of analytical result

To confirm the validity of Theorem 2 in Section 6.5 we have made simulations both for simple shortest path routing and optimized shortest path routing. We have studied traffic from different symmetric uniform distributions in the interval $[0;K[$ for $K = 0.5, 1, 2, 4$ with up to 32 timeslots per frame. To have data material for statistical use, up to 10^5 different traffic matrices have been simulated for each K in case of simple shortest path routing and up to 10^3 different traffic matrices have been simulated for each K in case of optimized shortest path routing. Less experiments have been performed with optimized shortest path routing since this operation is more time consuming.

We have plotted the results as the average wavelength usage as function of number of timeslots per frame. Strictly speaking, the average wavelength usage

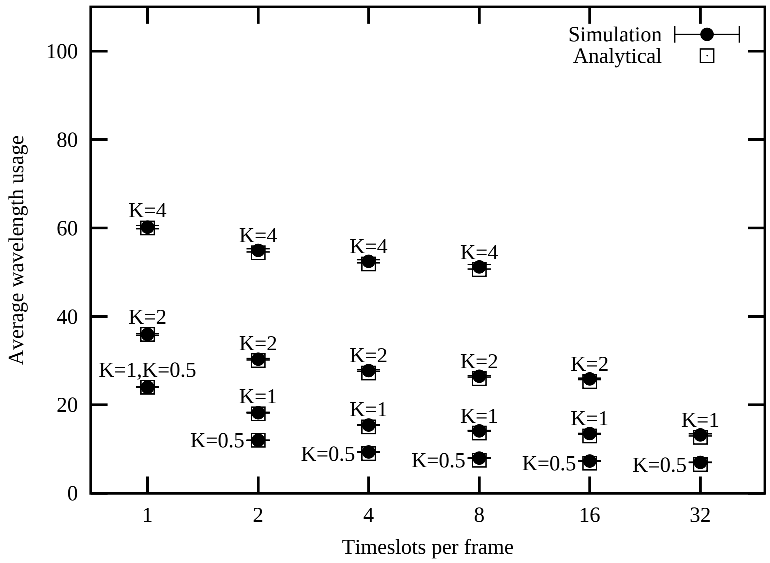

Figure 6.6: Analytically predicted usage of wavelength compared to simulation in case of optimized shortest path routing. The 95% confidence interval is shown for the simulation results. Traffic is symmetric uniformly distributed in the interval $[0;K[$. Zero gab.

is the average load in units of wavelengths for the link carrying the most traffic, i.e. the average wavelength usage in case of wavelength converters. Theorem 1 states the relationship between wavelength usage in SOH networks and WRONs. To find the wavelength usage it therefore suffices to set up the algorithms for the WRON. According to several studies Baroni and Bayvel (1997); Fenger et al. (2000b), the difference in wavelength usage with and without wavelength converters for uniform traffic, i.e. identical traffic demand for all node pairs, is negligible. The values of the elements in the traffic matrix are uniformly distributed, so the entire matrix is in general non-uniform. By using the same methods as in Fenger et al. (2000b) we still find that the difference in wavelength usage with and without wavelength converters is negligible. Therefore the results are in general valid both with and without wavelength converters. This is important since the use of

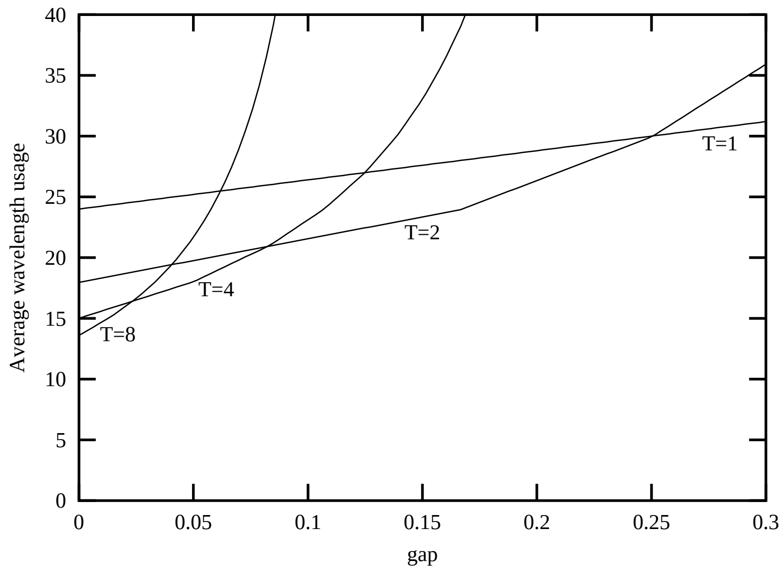

Figure 6.7: Wavelength usage verses gap for different number of timeslots per frame according to Theorem 3. Traffic is symmetric uniformly distributed in the interval $[0;1[$.

timeslot converters would cause unnecessary delay of signal and increase in node complexity.

Since the difference in wavelength usage is almost independent of the presence of wavelength converters, the difference in wavelength usage between the sequential solution to the routing and timeslot and wavelength problem, used here, and the optimal results based on simultaneously solving the routing and timeslot and wavelength problem, is negligible.

The results for simple shortest path routing are shown in Figure 6.5. We have included error bars on the result for the 95% confidence interval. The confidence intervals have the length of four times the estimated spread of the mean value of wavelength usage under the assumption that the error is Gaussian distributed.

In Figure 6.5 it can be seen that in all cases the wavelength usage determined by the theory, Theorem 2, is almost identical to or slightly less the average of the numerical results – the squares lie at or slightly below the circles. This characteristic is due to fact that the assumption that the wavelength usage, λ, is determined by one link only will not hold, since not only the most congested link in terms of demands can have the largest traffic volume. The result obtained theoretically will therefore be a lower bound for the average wavelength usage for the SOH network in case of simple shortest path routing.

The results for optimized shortest path routing are shown in Figure 6.6. We have included error bars on the result for the 95% confidence interval for the average wavelength usage. Although the number of paths on the maximum loaded link varied from traffic matrix to traffic matrix, we did not show the error bars for the analytical result, which depends on the load of the maximum loaded link, since the spread here was smaller, about 50% or less. Both the simulation result and the theoretical results for the wavelength usage varies with the traffic matrix. All the results for average wavelength usage for simulation are higher than or very close to the theoretically expected wavelength usage. Optimized shortest path routing evens out congestion, whereby more links are candidates to be the most congested link in terms of largest traffic volume, which should raise the average wavelength usage compared to the theory more than that in the case of simple shortest path routing. For the results with optimized shortest path routing the theoretical wavelength usage varies as the traffic varies since the routing takes the traffic into account, whereby the number of paths on the most congested link in terms of number of paths varies.

By comparison of the two figures, 6.5 and 6.6, it is seen that the average wavelength usage for simple shortest path routing for all points is about 50% higher than with optimized shortest path routing.

When the gap is zero it is seen from Theorem 2 that the absolute gain in wavelength usage from using SOH is almost independent of K, except for variations in D, when K is an integer. I.e. the absolute difference in wavelength usage between one timeslot per frame and specific large number of timeslots per frame is independent of K. However, the relative gain increases and as seen from Figure 6.5 and Figure 6.6 for large T ($T \gtrsim 8$) the wavelength usage is approximate proportional to K. Just like Theorem 2 predicts, then from Theorem 3 it is also seen that the wavelength usage becomes approximately $\frac{1}{2}KD$ for large T.

With small demand volumes then in case of only one timeslot per frame, many demands will not efficiently fill up a timeslot, i.e. the utilization will be low, and dividing the frames into several timeslots would raise the utilization and lower the wavelength usage as we have seen. When the typical demand volume is several wavelengths then for one timeslot per frame the relative number of inefficiently filled timeslots is smaller. In conclusion, the smaller the demands are, the larger is the gain of using SOH.

Theorem 3 gives the behavior for the wavelength usage for given parameters, K, T, D. In Figure 6.7 we have plotted the behavior for different values of T. For each T the wavelength usage is a growing function and approaches infinite as g approaches $1/T$. In terms of wavelength usage the most efficient choice of T for $T \in \{1,2,4,8\}$ and $K = 1$ for a given g can be derived from Figure 6.7. For given g then the T representing the lowest curve is the optimal choice. For instance, if $g \lesssim 0.02$ then $T = 8$ yields the lowest number of wavelengths, and if $0.02 \lesssim g \lesssim 0.08$ then $T = 4$ is the optimal choice.

The size of the gap is given in units of frame lengths. The length of a frame is therefore important for delay considerations, i.e. there is a trade of between delay and utilization.

6.6.4 Solution to ILP problems

We perform some experiments with the ILP programs to determine the differences between the various formulations. The Pan-European network shown in Figure 6.3 is the basis for the experiments, where the traffic demand matrix is generated from the gravitational model. The point of using this network and traffic is not to guarantee realistic traffic, which we can not. Rather, this is a known network with a traffic demand matrix created by a well known model. Any network with any traffic demand matrix could be used as long as they are not too computationally demanding.

The traffic to be routed is static and symmetric, with each demand A_d between two nodes measured in units of wavelength, i.e. in units of a frame length. To generate the traffic we have used the gravitational model: the traffic demand between two cities is the product of their population sizes, scaled with an appropriate constant (10^{-15}). The traffic demand matrix for the network in Figure 6.3 is shown in Table 6.1. For example the traffic demand between Helsinki and Berlin is 0.43 wavelength. This number is given by multiplying the number of citizens in Finland with the number of citizens in Germany and scaled: $5.2\,10^6 \cdot 8.3\,10^7 \cdot 10^{-15} = 0.43$. If one wavelength corresponds to 40 Gb/s then the traffic between Finland and Germany corresponds to 21.2 Gb/s in each direction. The traffic ranges from 0.0017 to 5 wavelengths.

Table 6.1: Traffic demand matrix in unit of wavelengths.

	Hel.	Sto.	Oslo	Cop.	Ber.	Ams.	Dub.	Pra.	Lux.	Bru.	Lon.	Vie.	Zur.	Paris	Zag.	Ath.	Rome	Mad.	Lis.
Helsinki	0	0.046	0.023	0.028	0.43	0.083	0.02	0.053	0.0023	0.053	0.31	0.042	0.038	0.31	0.022	0.055	0.3	0.21	0.052
Stockholm	0.046	0	0.04	0.048	0.74	0.14	0.034	0.091	0.0039	0.091	0.53	0.072	0.065	0.53	0.038	0.094	0.51	0.36	0.089
Oslo	0.023	0.04	0	0.024	0.37	0.072	0.017	0.046	0.002	0.046	0.27	0.037	0.033	0.27	0.02	0.048	0.26	0.18	0.045
Copenhagen	0.028	0.048	0.024	0	0.44	0.086	0.021	0.055	0.0024	0.055	0.32	0.044	0.039	0.32	0.023	0.057	0.31	0.21	0.054
Berlin	0.43	0.74	0.37	0.44	0	1.3	0.32	0.85	0.037	0.85	5	0.68	0.6	4.9	0.36	0.88	4.8	3.3	0.84
Amsterdam	0.083	0.14	0.072	0.086	1.3	0	0.061	0.16	0.0071	0.16	0.95	0.13	0.12	0.95	0.069	0.17	0.92	0.64	0.16
Dublin	0.02	0.034	0.017	0.021	0.32	0.061	0	0.039	0.0017	0.039	0.23	0.031	0.028	0.23	0.017	0.041	0.22	0.15	0.039
Prague	0.053	0.091	0.046	0.055	0.85	0.16	0.039	0	0.0045	0.11	0.61	0.084	0.075	0.61	0.044	0.11	0.59	0.41	0.1
Luxembourg	0.0023	0.0039	0.002	0.0024	0.037	0.0071	0.0017	0.0045	0	0.0045	0.026	0.0036	0.0032	0.026	0.0019	0.0047	0.026	0.018	0.0045
Brussels	0.053	0.091	0.046	0.055	0.85	0.16	0.039	0.11	0.0045	0	0.61	0.084	0.075	0.61	0.044	0.11	0.59	0.41	0.1
London	0.31	0.53	0.27	0.32	5	0.95	0.23	0.61	0.026	0.61	0	0.49	0.43	3.6	0.26	0.63	3.4	2.4	0.6
Vienna	0.042	0.072	0.037	0.044	0.68	0.13	0.031	0.084	0.0036	0.084	0.49	0	0.059	0.49	0.035	0.087	0.47	0.33	0.082
Zurich	0.038	0.065	0.033	0.039	0.6	0.12	0.028	0.075	0.0032	0.075	0.43	0.059	0	0.43	0.032	0.077	0.42	0.29	0.073
Paris	0.31	0.53	0.27	0.32	4.9	0.95	0.23	0.61	0.026	0.61	3.6	0.49	0.43	0	0.26	0.63	3.4	2.4	0.6
Zagreb	0.022	0.038	0.02	0.023	0.36	0.069	0.017	0.044	0.0019	0.044	0.26	0.035	0.032	0.26	0	0.046	0.25	0.17	0.044
Athens	0.055	0.094	0.048	0.057	0.88	0.17	0.041	0.11	0.0047	0.11	0.63	0.087	0.077	0.63	0.046	0	0.61	0.43	0.11
Rome	0.3	0.51	0.26	0.31	4.8	0.92	0.22	0.59	0.026	0.59	3.4	0.47	0.42	3.4	0.25	0.61	0	2.3	0.58
Madrid	0.21	0.36	0.18	0.21	3.3	0.64	0.15	0.41	0.018	0.41	2.4	0.33	0.29	2.4	0.17	0.43	2.3	0	0.4
Lisbon	0.052	0.089	0.045	0.054	0.84	0.16	0.039	0.1	0.0045	0.1	0.6	0.082	0.073	0.6	0.044	0.11	0.58	0.4	0

Optimization results

The ILP programs have been solved optimally on a 1GB 440MHz HP J7000 using GAMS and CPLEX 7.1.

We have varied the number of timeslots for each of the five flavors of the SOH ILP problems presented in Section 6.4. And we have varied the size of the gap for the SOH ILP. We used optimal shortest path routing, which has been performed separately for each number of timeslots, as the routing depends on the traffic.

In Table 6.2 we give the wavelength usage as a function of the number of timeslots in a frame with a gap of 0.01 frame length between each timeslot. The wavelength usage is given for the five different flavors of the SOH ILP problems presented in Section 6.4. We have 1 to 32 timeslots per frame, where 1 timeslot per frame corresponds to WRON except for a gap on each frame, since a timeslot is followed by a gap.

It can be seen that wavelength conversion, timeslot conversion, or both does not reduce the wavelength usage, which confirms and extends previous results on the routing and wavelength assignment problem for unprotected WDM networks Baroni et al. (1999); Fenger et al. (2000b); Ramaswami and Sivarajan (1995). Furthermore, the introduction of delays, such that connections must use

Table 6.2: Number of necessary wavelengths for the Pan-European network (Figure 6.3) as function of the number of timeslots with traffic demands given in Table 6.1. The gap between timeslots is 0.01 frame length.

timeslots	W_{SOH}	W_{delay}	$W_{\lambda\ conversion}$	$W_{slot\ conversion}$	$W_{full\ conversion}$
1	24	24	24	24	24
2	16	16	16	16	16
4	14	14	14	14	14
8	14	14	14	14	14
16	15	*out of memory*	15	15	15
32	18	*out of memory*	18	18	18

Table 6.3: Number of necessary wavelengths for the Pan-European network (Fig. 6.3) as function of the number of timeslots with traffic demands ten times those given in Table 6.1. The gap between timeslots is 0.01 frame length.

timeslots	W_{SOH}	$W_{\lambda\ conversion}$	$W_{slot\ conversion}$	$W_{full\ conversion}$
1	124	124	124	124
2	122	122	122	122
4	124	124	124	124
8	124	124	124	124

different timeslots on different links of their routes, does not raise the wavelength usage. The delay for each link was chosen randomly uniformly from one to the number of timeslots on a frame. For 16 and 32 timeslots per frame it was not possible to solve the linear problem due to too high memory usage; this could possibly be avoided by using the independent set formulation Ramaswami and Sivarajan (1995) (also called the independent routing configuration formulation Lee et al. (2000)). The minimum wavelength usage is reached with 4–8 timeslots per frame. Compared to 1 timeslot per frame, which corresponds to a WRON with frames, at least 62.5% fewer wavelengths are needed with SOH at the most favorable number of timeslots.

In Table 6.3 results from equivalent ILP runs with ten times the traffic are presented. Still the effect of wavelength and timeslot is negligible. Further it is seen that the savings using SOH is insignificant when the typical traffic demand is more than a couple of wavelengths.

Since neither wavelength conversion nor timeslot conversion improves the wavelength usage then the wavelength usage is determined by the most congested link. Therefore sequentially optimization, first routing and then wavelength and timeslot determination, perform just as well as simultaneous optimization.

6.7 Conclusion

We have described the concept of SOH networks, which we see as an optical solution to alleviate the capacity granularity problem.

Further, we have defined the problem mathematically by ILP formulations in the case of static traffic for various cases of conversion capabilities for wavelengths and timeslots and the presence of delay of timeslots on links.

From the ILP formulation it has been possible to reduce the problem of allocating demands in the SOH network to the simpler problem of allocating demands in the WRON, which we have shown by manipulating the ILP formulation.

Given routing, traffic distribution, and parameters describing the SOH we have analytically derived an approximate result for the expected wavelength usage. We have compared simulation results to the analytical results and found very good agreement for the Pan-European network.

We found that simple shortest path routing has a wavelength usage which is about 50% higher than that of optimized shortest path routing.

From the analytical result we have illustrated a method to determine the optimal number of timeslots per frame as function of the gap size, which has practical importance for determining the tradeoff between delay and utilization. Further, we find the gain from using timeslots as function of the gap size. For optimized shortest path routing the wavelength usage is up to 100% higher without the use of timeslots.

By using ILP we have compared wavelength usage for WRONs and SOH networks with different number of timeslots per frame. The network used was the Pan-European network and the traffic was generated from the gravitational model. We have studied 5 different setups of the SOH: no conversion, conversion for wavelengths, timeslots, and both, and delay of the signal. All setups required the same number of wavelengths for the studied number of timeslots per frame, implying that delay and conversion capabilities of neither wavelengths nor timeslots have any significant effect. The required number of wavelengths was significantly reduced with SOH. In this case more than 60% fewer wavelengths were needed.

We find that it is advantageous to use SOH in all-optical networks; the gain is particularly great when the typical traffic demand between source and destination is less than a few wavelengths.

Chapter 7

Network Design - Part I

This chapter covers much of material in the papers, Pióro et al. (2000); Glenstrup et al. (2000); Fenger et al. (2002).

The chapter is sub divided in two major section. The first section is on network design including duct and fiber deployment, as well as lightpath routing and wavelength assignment for networks with restricted duct placement possibilities. Methods for this purpose are developed, described, and tested.

The second section further includes the cost of switch equipment and neglects the wavelength continuity constraint. Here the duct placement unrestricted which dramatically increases the complexity o fthe optimization task. The computer program is in later chapter refered to as the EXPLAIN application.

7.1 Duct fiber design for all-optical networks

7.1.1 Abstract

We present here a multi fiber optical WDM network design problem formulated as an integer linear problem. The design problem consists in laying out ducts, fibers, routes, and wavelengths, given a set of nodes, the duct and fiber prices, and the traffic demands. We compare different methods for solving the design problem. These are integer linear programming, simulated annealing, and simulated allocation. We find that integer linear programming is useful for benchmarking other algorithms on small networks that consist of less than 7 nodes. For larger networks that cannot be handled by integer linear program solvers, we find that simulated allocation is more promising than simulated annealing. Further we include path protection in the problem formulation and solution. To be able to handle larger networks, we also develop a heuristic, the Path-Selection algorithm, which selects the links most probable to be part of the optimized network topology. Once a set of potential links are chosen the n the metaheuristic *simulated allocation* (SAL), a stochastic algorithm, finds the most optimal placement of the some of these links.

7.1.2 Introduction

As new optical WDM networks are being deployed and competition is increasing, a proper design of the networks is becoming increasingly important. In the mesh network topology design presented here, the task is to determine the position of links between a given set of nodes, satisfying a traffic matrix and minimizing an the deployment cost. In this chapter we treat networks of size up to 73 nodes, but with preimposed restrictions in allowed links between node pairs. The objective function used here is the cost of a link, computed from the deployment cost of ducts and fibers, and the routing and wavelength assignment problem is solved as a side effect. We assume no wavelength converters, whereby the wavelength continuity constraint applies.

We begin by formulating the problem in a integer linear formulation to define it mathematically. This formulation will also be used when the design task is solved by integer linear programming using the Branch and Bound algorithm in the CPLEX-package. However, for larger problems this method becomes too slow, whereby heuristic methods are used. We use simulated annealing and simulated allocation (Pióro and Gajowniczek). We compare all the methods for different networks sizes, for different numbers of wavelengths in a fiber, with and without protection. All three methods work on a set of possible paths between the nodes; this set of paths has been chosen by the Path-Selection algorithm. This preprocessing is essential so to minimize the solution space for the heuristics.

Paths-Selection algorithm

We have developed a heuristics to determine the potential links which is needed for the optimized network. Actually, the links are determined indirectly, by a set of paths for each node pair.

The optimization process is performed in two stages. First the relevant paths are calculated using the Path-Selection algorithm. Then the problem is transformed to a problem of allocating traffic on these paths by a metaheuristic. The metaheuristic will use the cheapest of the available paths.

To describe the Path-Selection algorithm by its pseudocode, the following notation is used:

k_s, k_d, k_b	Desired number of shortest, disjoint, and back paths
adjust	Flag: adjust link costs with new traffic before calculating shortest paths
$c_l^{traffic}$	Cost per traffic unit on link l
c_l^{duct}	Duct cost on link l
t_l	Current volume of assigned traffic on link l
n^S, n^D	Source and destination node
v_d	Volume of demand d
$\mathrm{cost}(l, v)$	Function calculating the cost of v units of traffic on link l
ps^S, ps^D, ps^B	Set of shortest, disjoint, and back paths
ps_d	Total set of shortest, disjoint, and back paths for demand d
$\vec{ps}$	Set of all ps_d's

This is the pseudocode representation of the Path-Selection algorithm:

```
sort(Demands)                              /* Sort according to smallest duct cost     */
for l ∈ Links do c_l^traffic ← c_l^duct    /* Initially, cost is set to duct cost      */
for l ∈ Links do t_l ← 0                   /* Initially, no traffic on any link        */
for d ∈ Demands do
   n^S ← source(d);   n^D ← dest(d)
   if adjust then                          /* Adjust cost as if v_d was put on every link */
      for l ∈ Links do c_l^traffic ← cost(l, t_l + v_d)/(t_l + v_d)
   ps^S ← ∅;   ps^D ← ∅;   ps^B ← ∅
   if k_s > 0 then ps^S ← kshortest(n^S, n^D, c⃗^traffic, k_s)
   if k_d > 0 then ps^D ← kdisjoint(n^S, n^D, c⃗^traffic, k_d)
   if k_b > 0 then ps^B ← kback(n^S, n^D, c⃗^traffic, k_b)
   ps ← ps^S ∪ ps^D ∪ ps^B
   for p ∈ ps do                           /* Update t⃗ and c⃗^traffic as if             */
      for l ∈ p do                         /* v_d are put on every shortest path       */
         t_l ← t_l + v_d
         c_l^traffic ← cost(l, t_l)/t_l
if adjust then                             /* Re-calculate cost if needed              */
   for l ∈ Links do c_l^traffic ← cost(l, t_l)/t_l
for d ∈ Demands do
   n^S ← source(d);   n^D ← dest(d)
   ps^S ← ∅;   ps^D ← ∅;   ps^B ← ∅
   if k_s > 0 then ps^S ← kshortest(n^S, n^D, c⃗^traffic, k_s)
   if k_d > 0 then ps^D ← kdisjoint(n^S, n^D, c⃗^traffic, k_d)
   if k_b > 0 then ps^B ← kback(n^S, n^D, c⃗^traffic, k_b)
   ps_d ← ps^S ∪ ps^D ∪ ps^B
return p⃗s
```

A network with n nodes have $n(n-1)/2$ potential links, and the number of directed potential paths in the network is $\sum_{i=1}^{n-2} \frac{n!}{i!}$ which is prohibitively high. For 30 nodes this is more than 10^{32} non-directed paths, which makes a reduction of paths essential when the optimization problem is transformed to a problem of allocating traffic on the set of paths.

Parameters determining the number of paths and the kind of paths, but typically 5 to 10 paths per node pair will be chosen.

Given the traffic demands, this path generating phase determines for each demand a number of primary and link-disjoint backup paths. The paths are selected to reduce the cost of the links and nodes used, and such that paths between distant nodes share some of the links of paths between intermediate nodes. The idea is similar to that used by Kershenbaum et al. (1991), where an initial "center node" is used as transit node for longer connections, only we start with the shortest link and continually "extend" this "center" each time a new path is allocated. Lee et al. (1998a) present an analogous algorithm called MVA that serves the same purpose.

The pathgenerator uses standard shortest-paths algorithms on internal graphs with vertices and directed edges. Each network node n is represented in the graphs by an input and output vertex $(v_n^{\text{in}}, v_n^{\text{out}})$ and an edge from v_n^{in} to v_n^{out}, while each potential network link connecting node n_1 and n_2 is represented by two edges $v_{n_1}^{\text{out}} \rightarrow v_{n_2}^{\text{in}}$ and $v_{n_2}^{\text{out}} \rightarrow v_{n_1}^{\text{in}}$. This way, the node costs can be represented by weights on the graph edges, allowing the shortest-paths algorithms to take node costs as well as link costs into account.

This path generating phase results in a network where many of the potential links are not used by any path and can thus be eliminated from the optimization phase.

7.1.3 Problem formulation

We consider a network consisting of a number of nodes and E links, cf. Figure 7.1. Each link is assigned a *duct cost* and a *fiber cost;* nodes are assumed to have

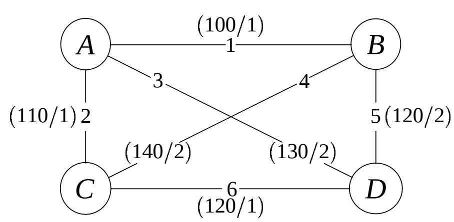

	A	B	C	D
A		70	0	0
B			0	50
C				40
D				

Figure 7.1: WDM network example with 6 links and a traffic demand matrix containing 3 demands. Each links is numbered and labeled with (duct/fiber) cost

infinite switch capacity and is not considered in the cost function. Along each link a number of fibers can be deployed, but only if a duct is constructed. Thus the cost of deploying $x > 0$ fibers is an affine function $cx + f$, where f is the cost of the duct and c is the cost of a fiber.

We assume given D traffic demands, which are assumed symmetric. The traffic demand matrix lists the demand between node pairs in number of *lightpaths*, where a lightpath is a combination of set of links connecting the nodes, and a wavelength to transmit on.

Each fiber can carry C different wavelengths, and as we assume no wavelength conversion in nodes, we impose the wavelength continuity constraint: A path between two nodes traversing several links must use the same wavelength on each of these links. Naturally, if two different paths use the same wavelength on a link, they must use different fibers on this link.

The *nominal design problem* is simply to satisfy the demands by deploying ducts and fibers at minimal cost, whereas the *path protection design problem* additionally requires that if any single link fails, all demands supplied by a lightpath using that link can be supplied by other, spare lightpaths that are otherwise unused.

7.1.4 Integer linear formulations

The purpose of this section is twofold. First it defines the mesh network topology design problems mathematically, that is as integer linear formulations, and second it serves as input for solving the design problems as integer linear programs. A number of articles have been written about these integer linear programs, e.g. Baroni et al. (1999) and Wauters and Demeester (1996).

Nominal design

Below we define the nominal mesh network topology design problem, that is to determine the position of ducts and fibers given the nodes, cost of ducts and fibers, the traffic demand between the nodes, and a set of possible paths between the nodes.

indices:

$d = 1,\dots,D$	demands (between pairs of nodes)
$j = 1,\dots,m(d)$	paths for flows realizing demand d
$c = 1,\dots,C$	colors (wavelengths) available on the fibers
$e = 1,\dots,E$	links

constants:

h_d	volume of demand d to be realized, expressed as the number of light-paths
a_{edj}	link-path incidence coefficient: $a_{edj} = 1$ if link e belongs to path j realizing demand d, $a_{edj} = 0$ otherwise
c_e	cost per fiber of link e
f_e	cost for a duct of link e

variables (all non-negative integers):

φ_{djc}	flow (number of light-paths) realizing demand d in color c on path j
n_{ce}	number of times the color c is used on link e (auxiliary) [1]
y_e	capacity of link e expressed in the number of fibers (auxiliary)
σ_e	binary variable equal one if duct is present at link e, otherwise zero (binary, auxiliary)

objective:

minimize $\quad C(\vec{y},\vec{\sigma}) = \sum_e c_e y_e + f_e \sigma_e$

constraints:

$\sum_j \sum_c \varphi_{djc} = h_d$	$d = 1,\dots,D$	satisfy demands
$\sum_d \sum_j a_{edj}\varphi_{djc} = n_{ce}$	$c = 1,\dots,C,\ e = 1,\dots,E$	compute n_{ce}
$y_e \geq n_{ce}$	$c = 1,\dots,C,\ e = 1,\dots,E$	ensure sufficient capacity
$y_e > 0 \Rightarrow \sigma_e > 0$	$e = 1,\dots,E$	require ducts for fibres

For each demand d between a node pair, we compute $m(d)$ possible paths that connect the nodes. The constants for the example in Figure 7.1 are shown in Figure 7.2. The last constraint, for requiring a duct if any fibers are present, can be

Links

e	between	f_e	c_e
1	$A-B$	100	1
2	$A-C$	110	1
3	$A-D$	130	2
4	$B-C$	140	2
5	$B-D$	120	2
6	$C-D$	120	1

Demands

d	between	h_d	$m(d)$
1	$A-B$	70	2
2	$B-D$	50	3
3	$C-D$	40	2

Paths

d	j	a_{edj}					
1	1	1	0	0	0	0	0
	2	0	1	0	1	0	0
2	1	0	0	0	0	1	0
	2	1	0	1	0	0	0
	3	0	0	0	1	0	1
3	1	0	0	0	0	0	1
	2	0	1	1	0	0	0
	$e=$	1	2	3	4	5	6

Figure 7.2: WDM network example represented by integer linear parameters

stated as $\sigma_e \cdot M \geq y_e$, where M is chosen such that $M > y_e$ for all e, i.e. $M > \sum_d h_d$.

Protection design

Below we define the protection mesh network topology design problem, where the protection method is path protection of single-link failures. In this case limited shared protection (LSP), where the capacity devoted for protection is shared for the different failure situations. We have chosen to use this protection method because the protection paths do not necessarily become longer than the primary paths, which besides the advantages of short paths also leads to less spare capacity usage than for example link protection of single-link failures. The drawback of using path protection is that all links in the protection path and primary path must be different, which constrains the choices of paths.

We introduce $S = E + 1$ *failure situations*, which in this case correspond to all the situations where one link is broken, and the normal situation.

indices:

$d = 1,\dots,D$	demands (between pairs of nodes)
$j = 1,\dots,m(d)$	paths for flows realizing demand d
$c = 1,\dots,C$	colors (wavelengths) available on the fibers
$e = 1,\dots,E$	links
$s = 0,\dots,S$	failure situations, $s = 0$ corresponds to the nominal state.
$k = 1,\dots,l(d,j)$	backup paths for protecting nominal flow realizing demand d on path j
$g = 1,\dots,C$	backup colors

constants:

h_{ds}	volume of demand d to be realized in situation s, expressed as the number of light-paths
a_{edj}	link-path incidence coefficient: $a_{edj} = 1$ if link e belongs to path j realizing demand d, $a_{edj} = 0$ otherwise
α_{es}	binary link failure coefficient: $e_s = 0$ if link e is failed in situation s, $e_s = 1$ if it works
$\delta_{djs} = \prod_{e:a_{edj}=1} \alpha_{es}$	path failure coefficient: $\delta_{djs} = 0$ if path j of demand d is failed in situation s, $\delta_{djs} = 1$ otherwise
b_{edjk}	link-path incidence coefficient: $b_{edjk} = 1$ if link e belongs to backup path k protecting path j of demand d, $b_{edjk} = 0$ otherwise
c_e	cost per fiber of link e
f_e	for a duct of link e

variables (all non-negative integers):

φ_{djc}	flow (number of light-paths) realizing demand d in color c on path j
ψ_{djkcg}	backup flow on path k in color g protecting nominal flow φ_{djc} on path j
ε_{djkcg}	protection flow allocation variable: $\varepsilon_{djkcg} = 1$ if color c on path j supplying demand d is backed up by color g on path k (binary)
n_{ces}	number of times the color c is used on link e in situation s (auxiliary)
y_e	capacity of link e expressed in the number of fibers (auxiliary)
σ_e	variable equal one if duct is present at link e, otherwise zero (binary)

objective:

minimize $\quad C(\vec{y},\vec{\sigma}) = \sum_e c_e y_e + f_e \sigma_e$

constraints:

$\sum_j \delta_{djs} \sum_c \varphi_{djc} = h_{ds}$	$d = 1,\dots,D,\ s = 0,1,\dots,S$	satisfy demands
$\sum_k \sum_g \varepsilon_{djkcg} = 1$	$d = 1,\dots,D,\ j = 1,\dots,m(d)$ $c = 1,\dots,C$	one path per backup path
$\psi_{djkcg} > 0 \Rightarrow \varepsilon_{djkcg} > 0$	$d = 1,\dots,D,\ j = 1,\dots,m(d)$ $k = 1,\dots,l(d,j),\ c,g = 1,\dots,C$	compute ε_{djkcg}
$\sum_k \sum_g \psi_{djkcg} = \varphi_{djc}$	$d = 1,\dots,D,\ j = 1,\dots,m(d)$ $c = 1,\dots,C$	satisfy backup demands
$\sum_d \sum_j \left(\delta_{djs} a_{edj} \varphi_{djc} + (1-\delta_{djs}) \sum_k \sum_g b_{edjk} \psi_{djkcg}\right) = n_{ces}$	$e = 1,\dots,E\ c = 1,\dots,C$ $s = 1,\dots,S$	compute n_{ces}
$y_e \geq n_{ce}$	$c = 1,\dots,C,\ e = 1,\dots,E$ $s = 1,\dots,S$	ensure sufficient capacity
$y_e > 0 \Rightarrow \sigma_e > 0$	$e = 1,\dots,E$	require ducts for fibres

Again, the constraint $y_e > 0 \Rightarrow \sigma_e > 0$ can be rewritten as $\sigma_e \cdot M \geq y_e$, where M is chosen such that $M > y_e$ for all e, i.e. $M > 2\sum_d h_d$, and $\psi_{djkcg} > 0 \Rightarrow \varepsilon_{djkcg} > 0$ can be rewritten as $\psi_{djkcg} \leq \varepsilon_{djkcg} h_d$.

Problem size

By looking at the variables and equations above, we find that the complexity of the problems are given by

Problem	*Variables*	*Equations*
Nominal design	$O(CE + CDJ)$	$O(CE + D)$
Protection design	$O(CE^2 + C^2DJ^2)$	$O(C^2DJ^2 + CE^2)$

where J is the maximum number of paths for any demand. In practice, J can be considered constant (usually 8 or less).

7.1.5 Heuristic Design Methods

The complexity of the problem causes the integer linear program to grow quickly to sizes which the standard solvers (CPLEX) cannot solve to optimality within reasonable time. If we want to optimize practical networks, we have to rely on heuristics of some sort.

As in the integer linear programs, a solution consists of simple choices of which paths and wavelengths to use for each demand. Each pair of nodes demands a number of connections, which is established through lightpaths. Given a (possibly partial) solution with one or more lightpaths assigned, corresponding to the solution variables φ_{djc} or ψ_{djkcg} and ε_{djkcg}, the corresponding layout of the network can calculated as the auxiliary variables $\vec{y}$ and $\vec{\sigma}$ are calculated for the nominal design problem and the protection design problem.

In this section we will describe the two types of metaheuristics:

- Simulated annealing, a well known metaheuristic which is widely used and hence will only be briefly described.

- Simulated allocation, a lesser known metaheuristic which has been applied to similar optimization problems. This algorithm will hence be more throughly described.

Simulated annealing

The standard layout of a simple simulated annealing algorithm for minimizing solution cost is given in Figure 7.3. We choose start and stop temperatures T_0, T_{stop}, and time limit t_{stop}, and then let constant $\gamma = t_{stop}^{-1} \log(T_0/T_{stop})$ such that $T_{stop} = T_0 \cdot e^{-\gamma t_{stop}}$.

choose a random x in solution space
$cost_{min} := cost(x)$
$x_{min} := x$
$T := T_0$ /∗ *temperature* ∗/
$t := 0$ /∗ *real time timer variable* ∗/
repeat
  for $i := 1$ **to** *Markov length* **do**
    choose an x' in the neighborhood of x
    $\delta := cost(x') - cost(x)$
    choose a random $r \in [0, 1[$
    if $\delta < 0$ **or** $r < e^{-\delta/T}$ **then**
      $x := x'$
      if $cost(x) < cost_{min}$ **then**
        $cost_{min} := cost(x)$
        $x_{min} := x$
  $T := T_0 \cdot e^{-\gamma t}$
until $t \geq t_{stop}$

Figure 7.3: Simulated annealing core algorithm

Choosing the initial x in the solution space is a simple random (with linear distribution) allocation of the necessary lightpaths. For each temperature, T, value the parameter, *Markov length*, determines how many solutions will be searched. In all the Simulated Annealing runs we have used the value 60. The procedure for selecting x' from the neighborhood of x is somewhat more complicated. Two types of neighborhoods have been tested:

- Removal of one single lightpath and random re-assignment.

- Removal of all lightpaths through one link and random re-assignment.

The first procedure turns out to give unsatisfactory results, because of the high duct costs which have a strong influence on the overall cost of a solution. For this reason, the second type performs better.

Simulated allocation

Simulated allocation is a new metaheuristic, invented by Pióro Pióro and Gajowniczek for use in optimization of telecommunication networks. The basic simulated allocation algorithm is shown in Figure 7.4.

let x be an unallocated network
$cost_{min} := \infty$
$t := 0$ /* *real time timer variable* */
repeat
  choose a random $r \in [0,1[$
  if $r < q(x)$ **then**
    allocate and add one or more lightpaths to x
  else
    disconnect a lightpath or link in x
  if x is fully allocated **and** $cost(x) < cost_{min}$ **then**
    $cost_{min} := cost(x)$
    $x_{min} := x$
  if x is fully allocated **or** $cost(x) > cost_{min}$ **then**
    bulk disconnect many links in x
until $t \geq t_{stop}$

Figure 7.4: Simulated allocation core algorithm

Contrary to simulated annealing, simulated allocation starts with an empty solution. Instead a solution is gradually constructed. Inside the main loop, a probabilistic choice is made whether to allocate a lightpath or disconnect one or more lightpaths. Allocation simply means adding to the current partial solution x one lightpath, and disconnection is the opposite, i.e. removing one or more lightpaths from the solution. In order to reach a complete solution, the probability for choosing allocation $q(x)$ should be sufficiently high. Whenever a complete solution is reached, it is compared with the current best solution. If the solution is complete or the partial solution is worse than the current best (i.e. it can never improve the current best), a large number of lightpaths are disconnected so that a different part of the solution space can be reached. The algorithm is terminated after a predetermined number of seconds, t_{stop}.

The problem dependent procedures are:

Allocation of one single lightpath to the current solution. It chooses the best single lightpath from a group of these.

Disconnection of all lightpaths passing through a certain link, or of only one lightpath.

Bulk disconnection of all lightpaths through a certain set of links. The set of links are chosen at random with equal probability.

Simulated allocation is not as widely applicable as simulated annealing or other metaheuristics; it requires the possibility of evaluating partial solutions, i.e. solutions which are not feasible. In some ways it resembles an iterated construction algorithm, which is restarted from different partial solutions. The point is though, that these restarts are not random, but are based on parts of previously discovered solutions.

7.1.6 Results and Discussion

Experimental design

The networks used in experiments are two real-world examples of networks in Denmark, and a small, 5-node network:

network	*nodes*	*links*	*average duct cost*	*average fiber cost*	*demands*	*demand volume*
A	5	10	152.0000	1.535000	10	71
B	23	29	213.5862	1.999310	21	844
C	73	165	31692.84	316.9284	279	1824

For each network, up to 3 mutually disjoint shortest paths and up to 5 shortest paths are generated for each pair of demand nodes. Each (task–network–wavelengths–method) configuration was run five times for 10 minutes. The results are shown in Table 7.1. Figures 7.5 and 7.6 show examples of progress for

Task	*Net*	*w*	*Simulated allocation*		*Simulated annealing*		*ILP solving*	
			average	*std.dev.*	*average*	*std.dev.*	*result*	*status*
nominal	A	4	444.00	0.00	444.60	1.79	444.00	optimal
		16	413.00	0.00	415.20	0.89	413.00	optimal
		256	404.00	0.00	404.00	0.00	—	timeout
	B	4	4384.40	1.49	4453.50	19.12	4377.68	optimal
		16	3035.02	3.26	3103.25	13.33	3010.46	timeout
		256	2605.78	1.01	2674.70	6.96	—	timeout
	C	4	2053019	19371	2089457	144781	2847760	timeout
		16	1898782	4598	1979889	97755	—	timeout
		256	1842618	4984	1954155	55768	—	timeout
protection	A	4	579.00	0.00	589.00	1.41	—	timeout
		16	531.00	0.00	537.00	1.41	—	timeout
		256	515.00	0.00	516.80	1.67	—	memout
	B	4	9614.92	7.15	9667.46	11.70	—	timeout
		16	6074.30	3.74	6083.91	4.15	—	memout
		256	4935.40	0.96	4948.83	3.11	—	memout
	C	4	3604097	32069	3705365	28938	—	timeout
		16	3341704	14458	3409685	48311	—	memout
		256	3246105	33566	3315111	65634	—	memout

Table 7.1: Experimental results

the current best solution during optimization (point wise averages over the multiple runs).

The results indicate that simulated allocation is in general slightly better than simulated annealing. Furthermore, simulated allocation obtains almost optimal results in the cases where the ILP solver reaches a result within the time limit. We have also conducted experiments for 15-minute runs, and they indicate that only small improvements are gained when the heuristics are run for more than 5 minutes on these network problems. The inclusion of protection raised the cost of

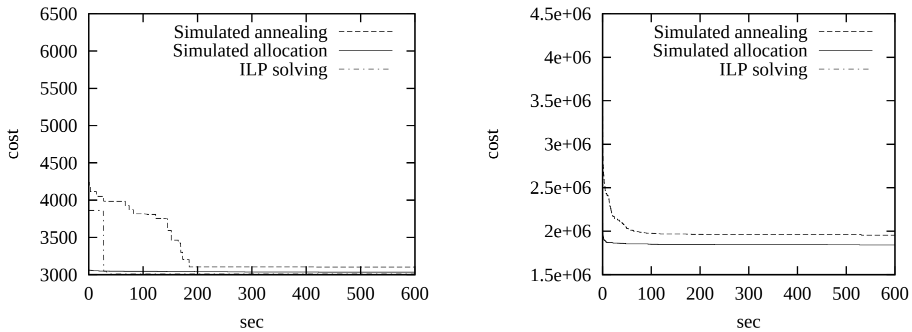

(a) Network B, 16 wavelengths (b) Network C, 256 wavelengths

Figure 7.5: Nominal case

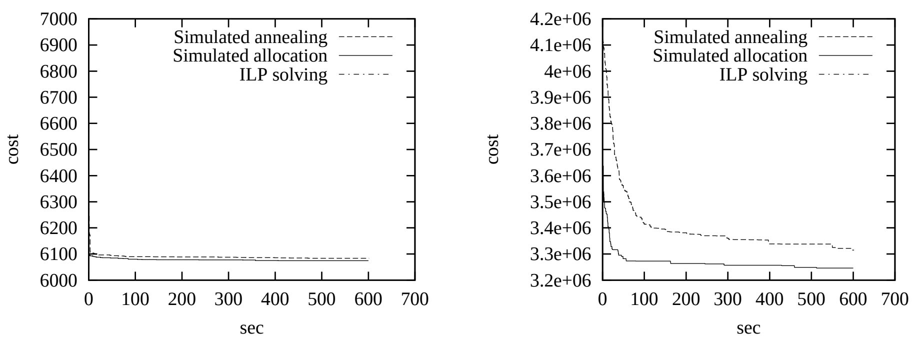

(a) Network B, 16 wavelengths (b) Network C, 256 wavelengths

Figure 7.6: Protection case

the net by 30% to 120%.

7.1.7 Conclusion

In this paper we have presented methods to solve the mesh network topology design problem for deployment of ducts and fibers and the routing and wavelength assignment problem both in the case of nominal design and for protection. We formulated the problems as integer linear formulations and solved them using a self developed heuroistic, Path-Selection algorithm, the metaheuristics, simulated annealing and simulated allocation, and integer linear programming. For larger networks we found that integer linear programming was useless due to its exponential rise in demand of time and memory. Simulated annealing and simulated allocation were always able to find solutions, however, simulated allocation was always able to find the better solution.

In the next section we include the cost of nodes, where switching and termination takes place. This type of cost takes up a major part of the budget when deploying networks and is therefore essential to include. Inclusion of node cost complicates the problem significantly, since extra choices with respect to node capacity and functionality must be taken.

7.2 Duct Fiber and switch design for optical networks

7.2.1 Abstract

We expand the optimization task of the previous section and reformulate the linear programs used. The optimization task here is green-field network optimization – non restricted optimization including cost os ducts, fiber, and cost of switching equipment in nodes. We use the Path-Selection algorithm, defined in Section, 7.1.2, together with simulated allocation and integer linear programming. We show that it is feasible to use this method on networks of realistic sizes, and that inclusion of node costs in the optimization is superior to simple postdeployment of switching equipment in driving down the cost of deploying a new optical network. We compare integrated optimization of ducts, fibers and nodes and compared this results to the result of separated optimization where first the network is optimized with respect to ducts and fibers, whereupon switch equipment are placed according to the traffic.

7.2.2 All-optical network design

Enabling the backbone network. Backbone telecommunication networks are characterized by having relatively few nodes (less than 100) but supporting large communication channel bandwidths. Such large bandwidths are transported most cost-efficiently on optical fibers, which have been deployed in telecommunication networks through the past couple of decades. At first, simple point-to-point fiber links using just one wavelength were deployed; later, they were upgraded to exploit the fiber optical capacity by attaching wavelength division multiplex (WDM) equipment at the ends, enabling simultaneous communication in the same fiber using different wavelengths. This helps to satisfy the faster increase in communication demand seen lately, and optical fibers can provide reliable communication over long distances with low delay. While delays are low in fibers, this is not so in the conventional digital cross-connect (DXC): When the path from source to destination node involves several hops, the optical signal is at each DXC converted into electrical form before it is switched and converted back into an optical signal for the next hop. This optical-electrical-optical (O-E-O) conversion is a delay bottleneck in current optical backbone networks, which has spurred the development of the all-optical network (AON).

The all-optical network. The all-optical network (AON) utilizes the low delay in optical fibers by keeping the signal in the optical domain from source to destination node. Each node of the AON is equipped with an optical cross-connect (OXC) or an optical add/drop multiplexer (OADM), both of which are able to pass on the optical signals without O-E-O conversion, thus eliminating processing delay. A good overview of WDM and AON is given by Sengputa and Ramamurthy (2001).

Static and dynamic traffic demands. Designing an AON usually means that traffic demands—i.e., connection requests between pairs of nodes—must be satisfied by specifying how much capacity in the form of fibers and switches must be used in the AON links and nodes. If there are given limits on the number of fibers on each link or the switch size in each node, the network design problem is said to be *capacitated,* otherwise it is *uncapacitated.*

Research into AON design has considered dynamic traffic demands (Chlamtac et al., 1992; Mohan et al., 2001; Zhang and Acampora, 1995; Zang et al., 2000), in which connection requests arrive and a routed one at a time, as well as static traffic demands (Baroni et al., 1999; Chlamtac et al., 1992; Cwilich et al., 1999; Doshi et al., 1999; Garnot and Perrier, 1998; Kershenbaum et al., 1991; Lee et al., 1998a; Nagatsu et al., 1996; Saniee, 1996; Sinclair, 1999; Varela and Sinclair, 1999), in which the demands are given as a fixed set. Dynamic traffic demands may experience *blocking*: if there are not sufficient network resources to accommodate the request when it arrives, it is blocked and lost.

Network design goals. When considering dynamic traffic, arrival intensities are given for each node pair demand, and the design goal is to determine the capacities of the network links and nodes, minimizing the blocking probabilities. In most cases, if it was not given as input, the *routing* of each connection is also a result of the design process. Alternatively, Jan et al. (1993) present an algorithm for maximizing the network reliability, which is a average measure for the probability that two nodes are able to communicate with each other, given a certain reliability for each link.

The design goals for a network with static traffic demands in a capacitated setting include maximization of the total network flow (Saniee, 1996) or number of accepted demands (Chlamtac et al., 1992) or minimization of network congestion (Dutta and Rouskas, 1999). In the uncapacitated setting, the design goals include minimization of the maximum number of required wavelengths on any link (Baroni et al., 1999; Chlamtac et al., 1992; Varela and Sinclair, 1999), minimization of total network cost (Doshi et al., 1999; Kershenbaum et al., 1991; Lee et al., 1998a; Sinclair, 1999), minimization of the number of hops (Garnot and Masetti, 1997) or maximization of wavelength utilization (Nagatsu et al., 1996).

Protection and restoration. Given the importance of telecommunication networks today, operators are increasing their focus on reliable networks, which continue to provide service even when some network elements fail, for example due to cable cuts or power blackouts.

Proactive measures to ensure reliable connections include *protection* by deploying spare capacity in the network, and also precomputing static backup paths (Baroni et al., 1999; Cinkler, 2002; Cwilich et al., 1999; Doshi et al., 1999; Garnot and Masetti, 1997; Huang and Copeland, 2001; Lee et al., 1998b; Nagatsu et al., 1996; Saniee, 1996). Protecting primary paths by dedicating backup capacity to each path is called $1+1$ *protection* or $1:1$ *protection*, depending on whether the signal is sent over the backup path during normal operation or not. When one backup path is shared between n primary paths we have $1:n$ *protection*, so the general case of a network with n primary paths and m backup paths should be termed $m:n$ *protection*. Reactive measures include *restoration*, the act of finding a backup path when a primary path is broken (Shami and Sinclair, 1999).

Two major protection methods are distinguished by the extent of the backup routing: In *link protection*, all traffic of the broken link is routed around the failure, between the two link nodes. *Path restoration* reroutes the entire path of any path that is broken for the given failure; if the non-broken links of the primary path cannot be reused—e.g., due to the management systems—we call it *limited shared protection* (LSP), since the sharing is only among the protection capacity.

In recent years the ring network architecture called MS-SPRing has to some extent replaced the general mesh network architecture. MS-SPRing has become popular among network operators because it is able to switch quickly and automatically to backup paths based just on local decisions, that is, without the need for centralized failure control. The entire network is constructed from rings where each link in a ring has twice the maximal capacity needed on any of its links. When a link fails, a link protection scheme reroutes all traffic the long way round the ring. The major drawback with MS-SPRing is that it requires at least 100% spare capacity.

Greenfield network design. Even in the uncapacitated scenario it can be natural to speak of a predeployed capacity on each link and node. This capacity then has zero cost, and the task is the *network extension design* problem, where *additional* capacity must be deployed. In contrast, the *green-field network design* starts from scratch: there is no “capacity for free” at the outset.

Link costs are often taken to be proportional to the number of deployed fibers, but for the green-field model where also ducts must be constructed, it can make good sense to include an opening cost for each link (Pióro et al., 2000; Glenstrup et al., 2000), or simply that it is an increasing, concave function of their length (Kershenbaum et al., 1991).

Finally, if all link costs are set to 1, the resulting design will tend to comprise paths with few hops—at the cost of longer link lengths—which can be appropriate if node costs dominate (Garnot and Perrier, 1998; Hjelme and Andersen, 1999).

Wavelength conversion. WDM can be used in the AON in which case we obtain the *wavelength routed optical network* (WRON). Individual connections are accommodated by *lightpaths*, identified by their route and wavelength because each path must use the same wavelength on all its links—this is called the *wavelength continuity constraint.* The constraint restricts the number of multi hop paths that can be accommodated: two different demands cannot use lightpaths that share a fiber if they use the same wavelength. This gives rise to the *routing and wavelength assignment* (RWA) problem, where all traffic demands must be assigned lightpaths; solving this to optimality is an NP-complete problem (Chlamtac et al., 1992), but Ramaswami and Sivarajan (1995) devised an LP program to calculate an upper bound on the mount of carried traffic that *any* RWA algorithm would be able to accommodate. Various theoretical resource bounds for WDM networks are given by Aggarwal et al. (1996), and a good survey of the RWA problem is presented by Zang et al. (2000).

Network design methods. Optimal solutions to small network design problems (up to about 15 links) can be found by integer linear programming (ILP) tools (Baroni et al., 1999; Cwilich et al., 1999). In general, the network design problems are variants of the *multicommodity flow problem*, which can be stated in an *arc-flow* formulation in which input and output flow is balanced for all nodes (Cinkler et al., 2000; Doshi et al., 1999; Dutta and Rouskas, 1999; Lee et al., 1998a), or a *link-path* formulation, where each traffic demand can be satisfied by a limited set of precomputed paths, which thus limit the optimality of the solution (Glenstrup et al., 2000; Pióro et al., 2000; Saniee, 1996).

Doshi et al. (1999) give detailed algorithms for solving some ILP programs, based on Lagrangian relaxation and subgradient optimization techniques, and Jan et al. (1993) develop a branch and bound algorithm. Planning just backup capacity, Lee et al. (1998b) used a branch and cut algorithm for finding the optimum in a 42 link network. Removing the integrality constraints and thus relaxing the problem to an LP program, Saniee (1996) was able to optimize the layout of a 150 link network with 29 switches. By designing a protection path finding algorithm based on local bypasses along primary paths, Cwilich et al. (1999) were able to find backup paths for a network of 1974 links and 1050 nodes satisfying 679 demands by running column-generation based ILP solvers for 60 hours.

However, for networks of realistic sizes, solving these network design problems optimally using ILP tools is not possible within reasonable computing time and memory, so either the problems must be decomposed (Dutta and Rouskas, 1999), or reduced—for example by restricting the length of the paths for each demand (Baroni et al., 1999)—or *heuristics* must be applied.

Finally, various optimization heuristics based on *stochastic algorithms* have been developed for network design problems (Sinclair, 1999; Varela and Sinclair, 1999).

Network design tools. As network operators are beginning to see a decrease in the exponential growth in bandwidth demand, the manual and rule-of-thumb network deployment strategies of the past decade are being augmented with computer aided network planning. As a recent study shows (Stidsen and Glenstrup, 2002), manual planning does not a priori lead to the most cost-efficient network designs. Several software packages for various design and analysis tasks are commercially available—some examples of photonic network planning tools are COMPOSIS® (AixCom, 2002), LightPlan™ (Lightscape Networks, 2002), OPNET Modeler® (OPNET Technologies, Inc., 2002), StarNet Planner (Tellium, 2002) and VPItransportMaker (VPIsystems™, 2002).

This work. In this paper, which is an extension of previous work (Pióro et al., 2000; Glenstrup et al., 2000), we present ILP formulations of two uncapacitated green-field AON design problems for static traffic demands: *Nominal design* (ND) where traffic demands are only assigned primary paths, and *protection design* (lsp) where additionally each primary path is assigned a backup path in the case of a single link failure.

We use a link cost model which is the sum of the fiber cost and an opening cost for duct construction. As Kershenbaum et al. (1991) note, this can also model any node costs that are proportional to the number of fiber ports. Hjelme and Andersen (1999) found that the overall network costs scale with different network parameters—hop length, link length, node degree—according to whether duct, fiber or node costs dominate. However, which factor is dominating may not necessarily be clear before the network is designed, so instead of optimizing specifically for reducing hop length, link length or node degree, we *include* the node cost in the optimization process. Furthermore, we also add a quadratic fiber port factor, which allows modeling more precisely switches whose costs are proportional to the size of the switch matrix. Cinkler et al. (2000) also consider node costs for several different node components (OXCs, DXCs, OADMs etc.) in their optimization, but that is done indirectly by separating the network into W layers (one for each wavelength) and converting the nodes into small subgraphs according to their functionality and incorporating them in the layered network. This layering method has also been used by Sun et al. (2001), but the layers increases dramatically the complexity of the problem, and the method does not in itself allow for the quadratic cost factor. Furthermore, although the nodes are included in the optimization, the *kind* of node must be selected by the user before optimization starts.

As our main concern is the network element costs rather than wavelength assignment, we assume that all nodes are equipped with wavelength converters.

7.2.3 Network model

We consider a green-field scenario in which a telecommunication operator has decided where to locate the network nodes, and has estimated the costs of constructing ducts and deploying fibers between the nodes. We refer to these estimates as (potential) links; it is up to the optimization process to select which links should actually be constructed, and how many fibers to deploy in each duct. Although we do not require estimates for *all* node pairs, the intention is that there should be sufficiently many potential links for the optimization process to choose between.

The traffic which the network must be designed to support is given as a static set of traffic demands (a traffic matrix), where each demand consists of a source node, a destination node and a traffic volume, measured in units of wavelengths, which is to be realized. Each fiber supports a fixed number of wavelengths, W.

Links can contain as many fibers as is necessary. When fibers are deployed along a link, there must also exist a duct, so the cost model for a link l is given by

$$cost_l(f) = \begin{cases} C_l^{\text{fibre}} f + C_l^{\text{duct}}, & f > 0 \\ 0, & f = 0, \end{cases} \tag{7.1}$$

where f is the number of fibers deployed, and C^{fibre} is the estimated cost of deploying one fiber in the duct which has an estimated construction cost of C^{duct}. Typically, C^{duct} is much larger than C^{fibre}.

Each node is equipped with an optical switch which we assume has no bounds on the number of fiber ports it can handle, and is able to perform strictly non-blocking switching between all input and output ports. The node cost for any node n in the network is modeled as a second order polynomial:

$$cost_n(f) = \begin{cases} C^{\text{switching}} f^2 + C^{\text{port}} f + C^{\text{core}}, & f > 0 \\ 0, & f = 0, \end{cases} \tag{7.2}$$

where f is the number of fiber ports required in the node. This allows for modeling switches where the cost is proportional to the switching matrix size. We require $C^{\text{switching}} \geq 0$ and $C^{\text{port}} \geq 0$, as the node cost function must be increasing for positive f to avoid “getting stuck” in non-global minima during the optimization process; similar requirements are made in other work on network design optimization (Kershenbaum et al., 1991).

7.2.4 Network design optimization

The objective of the network design task is to satisfy all the traffic demands, minimizing the total network cost given as the sum of the link and node costs. We note that as the number of fibers and switch ports in not bounded, we are considering an *uncapacitated* network design problem.

We consider two variants of the design problem:

Nominal design (ND), which is just to satisfy all the traffic demands, and

Protection design (LSP), in which additional capacity must be deployed in the network to be able to also satisfy the traffic demands in the event of single link failures. We consider just single link failures, in which case any demands whose primary paths are affected must be rerouted along backup paths which are precomputed before the network is constructed. As the name suggests, any working links of a failed primary path cannot be reused for backup paths. However, the *backup* capacity deployed is shared between all backup paths in an $m:n$ protection style.

Orthogonal to this is the choice of how to optimize the different components of the network—the nodes and links. We focus on two ways of optimizing the network design:

Staged optimization, in which we first optimize the links, that is, decide where to construct ducts and how many fibers to deploy on them. This is followed by a second stage where the node equipment is optimized, given the fixed fiber deployment. Given the quadratic node model described in Section 7.2.3, this simply corresponds to postprocessing, calculating the cost of each node, but one could envisage other node models in which switching functionality or port restrictions would leave room for further optimization by choosing between a set of node architectures.

Integrated optimization, in which both nodes and links are optimized in the same stage, which allows the node costs to influence the layout of the ducts and fibers.

The choice between these two optimization strategies is a main focus point of this work, and it depends among other things on the relative sizes of the node and link costs and the traffic volumes, as well as the effect of the added complexity of integrated optimization, which could slow down the optimization process significantly.

Optimization by integer linear programs

In this section we cast the network design problems in mathematical formulations as ILP (integer linear programming) programs. ILP programs consist of an objective and a list of constraints, all parameterized by *decision variables* x_i which are the free variables whose optimal values are to be determined. ILP constraints are written in the basic form $\sum_i a_i x_i \leq b$, but for presentation purposes we will also use forms like $\varphi = 0 \Rightarrow \sum_i a_i x_i \leq b$, where φ is a binary variable. These expressions can be rewritten into the basic form by a straightforward rewriting rule, given that $M \neq 0$ is an upper bound on $\sum_i a_i x_i - b$:

Implication	*is implemented as*
$\varphi = 0 \quad \Rightarrow \quad \sum_i a_i x_i \leq b$	$\sum_i a_i x_i \quad \leq \quad b + \varphi M$

ILP programs can act as rigorous definitions of the problems, but are especially useful as benchmarks for optimized network design heuristics because they can be passed directly to ILP optimizers. The optimizers we use here are GAMS (Brooke et al. (1992)) and CPLEX (ILOG Cooperation (2000)) : GAMS is a preprocessor which takes the formulations we give, re-casts them in a shape that CPLEX can handle and performs some simple preoptimizations, before passing them to CPLEX which is the real optimization tool.

We present in the following an ILP formulation of the network design problems we are considering in this work.

Approximating the polynomial node cost model

As the node cost function $cost_n(f)$ is not linear, we cannot express it directly in the ILP framework. Instead we approximate the non-constant part, $\widehat{cost}_n(f) = C^{\text{switching}} f^2 + C^{\text{port}} f$ with the piecewise linear function $\widehat{cost}_n^{\text{ILP}}(f) = \max_i\{K_i f + C_i^0\}$ as sketched in Figure 7.7. Note that $C^{\text{core}} + \widehat{cost}_n^{\text{ILP}} \leq cost_n$ because $C^{\text{switching}} \geq 0$.

The coefficients for the set of linear functions $\{K_i f + C_i^0 \mid i = 1, \ldots, I\}$ are determined by selecting I points $\left(f_0, \widehat{cost}_n(f_0)\right), \ldots, \left(f_I, \widehat{cost}_n(f_I)\right)$ on the graph for $\widehat{cost}_n(f)$ and finding the tangential slope $K_i = 2C^{\text{switching}} f_i + C^{\text{port}}$ by differentiation. The cost offset C_i^0 is determined by solving $\left(\widehat{cost}_n(f_i) - C_i^0\right) \big/ \left(f_i - 0\right) = K_i$, which yields $C_i^0 = -C^{\text{switching}} f_i^2$. Naturally, the accuracy of the approximation is better when then number of points is large, but for our purposes we expect that $I = 5$ points are sufficient if we make sure that the largest point is greater than the number of ports expected at any node.

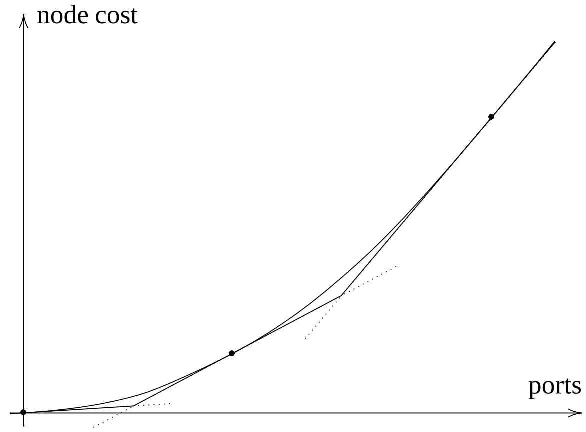

Figure 7.7: Approximating the node cost function by a piecewise linear function.

ILP program in the arc-flow formulation

Next we shall describe the components of the ILP program for the arc-flow formulation of the ND network design task. In this formulation, the input and output flow at each node, including locally added and dropped flow, must be balanced. Additionally, we use the K_i and C_i^0 parameters described in Section 7.2.4 to calculate the node costs, based on the total input and output flow at the node. In the constraints the quantification "$m : (nm) \in \mathcal{E}$" denotes "all nodes m for which there exists an edge (nm) from node n to node m in $\mathcal{E}$."

Indexes:

$d \in \{1,\ldots,D\}$	Traffic demands
$m,n \in \{1,\ldots,N\}$	Network nodes
$(nm) \in \mathcal{E} \subseteq \{1,\ldots,N\}^2$	Directed edges
$\{n,m\} \in \mathcal{L} \subseteq \mathcal{P}(\{1,\ldots,N\})$	Undirected links
$i \in \{1,\ldots,I\}$	Function approximation point indexes

Constants:

$W \in \mathbb{N}$	Number of wavelengths in any fiber
$V_d \in \mathbb{N}$	Volume of wavelengths to be realized for demand d
$n_d^{\text{src}} \in \{1, \ldots, N\}$	Index of the source node for demand d
$n_d^{\text{dst}} \in \{1, \ldots, N\}$	Index of the destination node for demand d
$K_i \in \mathbb{R}_+$	Coefficient for approximation function i
$C_i^0 \in \mathbb{R}_+$	Offset for approximation function i
$C_{\{n,m\}}^{\text{duct}} \in \mathbb{R}_+$	Cost of constructing the duct on link $\{n,m\}$
$C_{\{n,m\}}^{\text{fiber}} \in \mathbb{R}_+$	Cost of deploying a fiber on link $\{n,m\}$

Variables:

$x_{dnm} \in \mathbb{N}_0$	Flow of demand d along edge (nm)
$u_{\{n,m\}} \in \mathbb{N}_0$	Number of required fibers on link $\{n,m\}$
$\delta_{\{n,m\}} \in \{0,1\}$	Number of required ducts on link $\{n,m\}$
$z_n \in \mathbb{R}_+$	Number of required ports in node n
$\gamma_n \in \{0,1\}$	Number of required cores in node n
$v_n \in \mathbb{R}_+$	Cost of ports and switching at node n

Objective: Minimise $\sum_{\{n,m\}} (C_{\{n,m\}}^{\text{duct}} \cdot \delta_{\{n,m\}} + C_{\{n,m\}}^{\text{fibre}} \cdot u_{\{n,m\}}) + \sum_n (C^{\text{core}} \cdot \gamma_n + v_n)$,
subject to

Constraints:

$\sum_{m:(nm)\in\mathcal{E}} x_{dnm} - \sum_{m:(mn)\in\mathcal{E}} x_{dmn} = \begin{cases} V_d, \text{ if } n = n_d^{\text{src}} \\ -V_d, \text{ if } n = n_d^{\text{dst}} \\ 0, \text{ otherwise} \end{cases}$	$\forall d, n$	Flow conservation for paths: what goes into node n must come out again
$\sum_d x_{dnm} + x_{dmn} \leq W u_{\{n,m\}}$	$\forall \{n,m\}$	Calculate the required number of fibres on $\{n,m\}$
$\delta_{\{n,m\}} = 0 \Rightarrow u_{\{n,m\}} = 0$	$\forall \{n,m\}$	Without a duct, there can be no fibers on link $\{n,m\}$
$\sum_{\{n,m\}} u_{\{n,m\}} = z_n$	$\forall n$	The required number of ports at node i is the sum of connected fibres
$\gamma_n = 0 \Rightarrow z_n = 0$	$\forall n$	Without a core, there can be no ports at node n
$K_i z_n + C_i^0 \leq v_n$	$\forall i, n$	The port and switching cost of a node n with a core is bounded from below by linear approximation function i

We note that if a node is a source or destination for at least one demand then $\gamma_n \neq 0$, so for networks with demands from or to all nodes we can eliminate γ_n from the ILP program.

ILP program in the link-path formulation

We shall now describe the components of the link-path formulation of the ILP program for the two network design variants, ND and LSP. They are based on the concept of a set of network *states* $s = 0, \ldots, S$, each of which is characterised by a set of failed paths. We only consider the case where paths fail due to a single link failure, but the framework can readily be extended to handle more complex equipment errors like node failures. Conventionally, state 0 is considered to correspond to a fully functioning network, so the ILP program for the ND and LSP network design variants are identical, except that for ND we only use one state, $s = 0$.

In the link-path formulation a number of primary paths have been precalculated for each demand, represented by a three-dimensional binary matrix A which indicates which links are used by which paths. The paths are here found by the

Path-Selection algorithm. For each primary path a number of backup paths—failure disjoint with the primary path—have also been precalculated and represented in a four-dimensional binary matrix B.

Indexes:

$d \in \{1,\ldots,D\}$	Traffic demands
$s \in \{0,\ldots,S\}$	Network states
$n \in \{1,\ldots,N\}$	Network nodes
$l \in \{1,\ldots,L\}$	Network links
$p \in \{1,\ldots,P_d\}$	Primary paths realising demand d
$q \in \{1,\ldots,Q_d^p\}$	Backup paths protecting demand d, path p
$i \in \{1,\ldots,I\}$	Function approximation point indexes

Constants:

$W \in \mathbb{N}$	Number of wavelengths in any fibre
$V_d \in \mathbb{N}$	Volume of wavelengths to be realised for demand d
$A_{ldp} \in \{0,1\}$	Primary link-path coefficient: 1 if path p for demand d uses link l
$B_{ldpq} \in \{0,1\}$	Backup link-path coefficient: 1 if path p for demand d can be protected by backup path q that uses link l
$G_{dp}^s \in \{0,1\}$	Path survival coefficient: 1 if path p of demand d works in state s
$J_{ln} \in \{0,1\}$	Node-link incidence coefficient: 1 if node n is incident with link l
$K_i \in \mathbb{R}_+$	Coefficient for approximation function i
$C_i^0 \in \mathbb{R}_+$	Offset for approximation function i
$C_l^{\text{fibre}} \in \mathbb{R}_+$	Cost of deploying a fibre on link l
$C_l^{\text{duct}} \in \mathbb{R}_+$	Cost of constructing the duct on link l

Variables:

$x_{dp} \in \mathbb{N}_0$	Primary flow of demand d on path p
$y_{dpq} \in \mathbb{R}_+$	Backup flow on path q protecting primary flow x_{dp}
$\beta_{dpq} \in \{0,1\}$	Backup indicator: 1 if path p supplying demand d is backed up by path q
$u_l \in \mathbb{N}_0$	Number of required fibres on link l
$\delta_l \in \{0,1\}$	Number of required ducts on link l
$z_n \in \mathbb{R}_+$	Number of required ports in node n
$\gamma_n \in \{0,1\}$	Number of required cores in node n
$v_n \in \mathbb{R}_+$	Cost of ports and switching at node n

Objective: Minimize $\sum_l (C_l^{\text{duct}} \cdot \delta_l + C_l^{\text{fibre}} \cdot u_l) + \sum_n (C^{\text{core}} \cdot \gamma_n + v_n)$, subject to

Constraints:

$\sum_p x_{dp} = V_d$	$\forall d$	Total volume of demand d is supplied by various paths
$\sum_q y_{dpq} = x_{dp}$	$\forall d,p$	Satisfy backup demands
$\sum_q \beta_{dpq} = 1$	$\forall d,p$	Each path must have exactly one backup path
$\beta_{dpq} = 0 \Rightarrow y_{dpq} = 0$	$\forall d,p,q$	Ensure that x_{dp} uses only one backup path
$\sum_d \sum_p \begin{pmatrix} A_{ldp}x_{dp} + \\ (1-G^s_{dp})\sum_q B_{ldpq}y_{dpq} \end{pmatrix} \leq Wu_l$	$\forall l,s$	Calculate required number of fibres on link l in state s
$\delta_l = 0 \Rightarrow u_l = 0$	$\forall l$	Without a duct, there can be no fibres on link l
$\sum_l J_{ln}u_l = z_n$	$\forall n$	The required number of ports at node i is the sum of connected fibres
$\gamma_n = 0 \Rightarrow z_n = 0$	$\forall n$	Without a core, there can be no ports at node n
$K_i z_n + C_i^0 \leq v_n$	$\forall i,n$	Cost of node n is bounded by linear approximation function i

Optimization by simulated allocation

While the ILP programs are concise representations of the network design tasks, they are not useful when solving design problems for networks of realistic sizes: Running ILP optimizers on networks with more than approximately 15 nodes does not finish within reasonable time. For this reason we turn to heuristics which cannot guarantee to find an optimal solution, but turn out to yield good results in practice without running for an excessively long time.

We have constructed a *simulated allocation* (SAL) metaheuristic, whose design was invented by Pióro (1997) for use in optimization of telecommunication networks. It is similar to the GRASP metaheuristic (Feo and Resende, 1995) in that it is restarted from different partial solutions. The point is though that for

SAL these restarts are not random, but are based on parts of previously discovered solutions. Simulated allocation is not as widely applicable as GRASP or other metaheuristics because it requires the possibility of evaluating partial solutions; that is, solutions which are not feasible.

The basic SAL algorithm is shown in Figure 7.8. Contrary to most other metaheuristics, simulated allocation starts with an empty solution and then gradually constructs a solution. Inside the main loop a probabilistic choice is made whether to allocate a lightpath or disconnect one or more lightpaths. Allocation simply means adding to the current partial solution x one lightpath, and disconnection is the opposite; that is, removing one or more lightpaths from the solution. In order to reach a complete solution, the probability for choosing allocation $q(x)$ should be sufficiently high. Whenever a complete solution is reached, it is compared with the current best solution: If the solution is complete or the partial solution is worse than the current best (i.e., it can never improve the current best), a large number of lightpaths are disconnected so that a different part of the solution space can be

```
let x be an unallocated network
cost_min := ∞
t := 0     /* real time timer variable */
repeat
   choose a random r ∈ [0,1[
   if r < q(x) then
      allocate and add one lightpath to x
   else
      disconnect a lightpath or a link in x
   if x is fully allocated and cost(x) < cost_min then
      cost_min := cost(x)
      x_min := x
   if x is fully allocated or cost(x) > cost_min then
      bulk disconnect many links in x
until t ≥ t_stop
```

Figure 7.8: Simulated allocation core algorithm.

reached. The algorithm is terminated after a predetermined number of seconds, t_{stop}.

The problem dependent procedures are:

Allocation of one single lightpath: Allocate the best from a (small, random) group of candidate lightpaths.

Disconnection of a single lightpath: Remove a random lightpath.

Disconnection of a link: Remove all lightpaths passing through a certain link.

Bulk disconnection : Remove all lightpaths going through a set of links. The set of links are chosen using a uniform distribution.

Integrated link and node optimization

Integrating optimization of both link and node costs is relatively easy when working with Simulated Allocation. Actually the above algorithm is not changed at all! The only difference is that when evaluating a (partial) solution, besides calculating the cost of the fibers and ducts, the number of incoming fibers to the node is calculated by summing the fiber count on all incident links. In the heuristic, we can easily calculate the node costs as a second degree polenomium in the number of incoming fibers. The cost of the links, the fiber and duct costs, are calculated as in Formula 7.1. The node costs are then calculated as specified in Formula 7.2.

Notice that in the above formula each of the terms may be calculated for just a partial solution. Further, the value of $cost(x)$ is a strictly non-decreasing function, that is, whenever a lightpath is added, $cost(x)$ increases. This is important since poorly performing partial solutions can be detected early (in the pseudo code): $cost(x) > cost_{min}$ and the search direction can then be changed by a bulk disconnect.

7.2.5 Evaluating optimization method quality

In this section we will report the results of some experiments with running the ILP programs and the heuristic on various network and traffic examples.

Networks and traffic demands

We use the following fully connected networks of various sizes:

Network	*Links*	*Nodes*
1	10	5
2	45	10
3	105	15
4	190	20
5	300	25
6	435	30

The networks are created by randomly placing the respective number of nodes on a 1000 times 1000 quadrant. The duct construction costs equal the euclidean distance, and the fiber deployment costs are $1/20$th of the duct cost. The node cost is given by equation (7.2), where the parameters, $C^{\text{switching}}$, C^{port}, and C^{core} is varied in the chapter.

Traffic is uniform, that is, the same demand volume for all node pairs. One unit traffic demand, i.e. one wavelength, between each node pair is used.

Estimating green-field optimization tool quality

We now perform some experiments to get an estimate of the quality of the tools for optimizing green-field network design where both fiber deployment and node deployment is optimized.

Given the network and traffic demand examples described in Section 7.2.5, we fix the node cost parameters $C^{\text{switching}} = 0.2$, $C^{\text{port}} = 10$, $C^{\text{core}} = 100$, and then determine what the total network cost is for the two network design tasks, ND and LSP, and three different network optimization methods:

- Path-Selection / simulated allocation
- Path-Selection / ILP solver, link-path
- ILP solver, arc-flow   (only without protection)

The Path-Selection algorithm used up to 10 minutes. Each experiment is run with the SAL optimizer 3 times for 30 minutes, using between 5 and 10 shortest paths per traffic demand, and the average total network cost is calculated.

The ILP programs and simulated allocation are run for up to 30 minutes on a 440MHz HP Series 9000 Model J7000 with 1Gb RAM per optimization process. Each experiment with simulated allocation was run three times to reduced the confidence interval.

The results are shown in Figures 7.9 and 7.10. 95% confidence intervals for

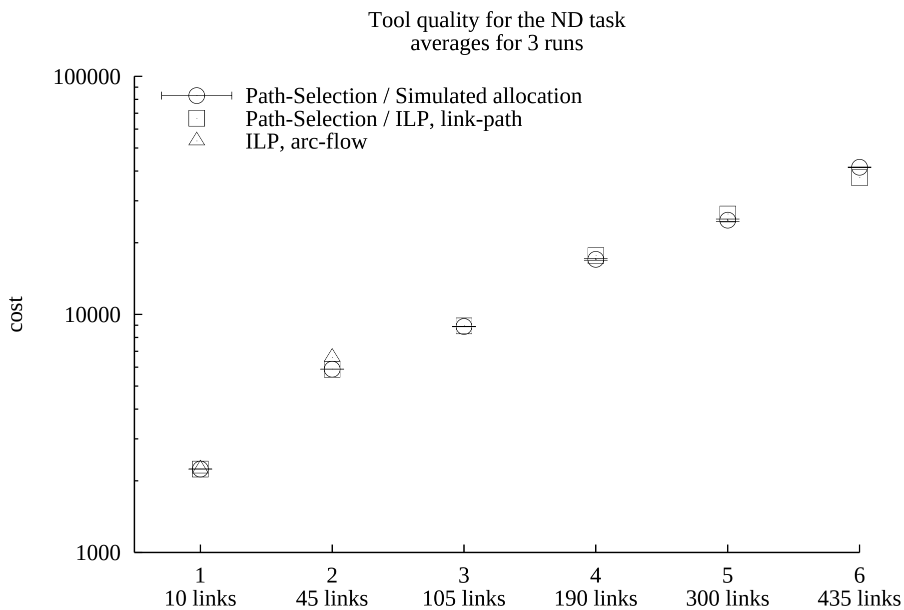

Figure 7.9: Optimization tool quality for the ND design task.

the Path-Section algorithm / simulated allocation results are shown with two horizontal lines.

From the Figure 7.9 it is seen that the ILP solver with the arc-flow formulation only reaches a result for the two smallest network. This is due to the very high complexity of this formulation. For the 10 link network the arc-flow reached the optimal result. For the 45 link network arc-flow reached a result, but not an optimal one. For larger networks arc-flow did not reach any results.

The the link-path formulation, with paths form the Path-Selection algorithm, reaches results for all the networks, but only optimality for the two smallest net-

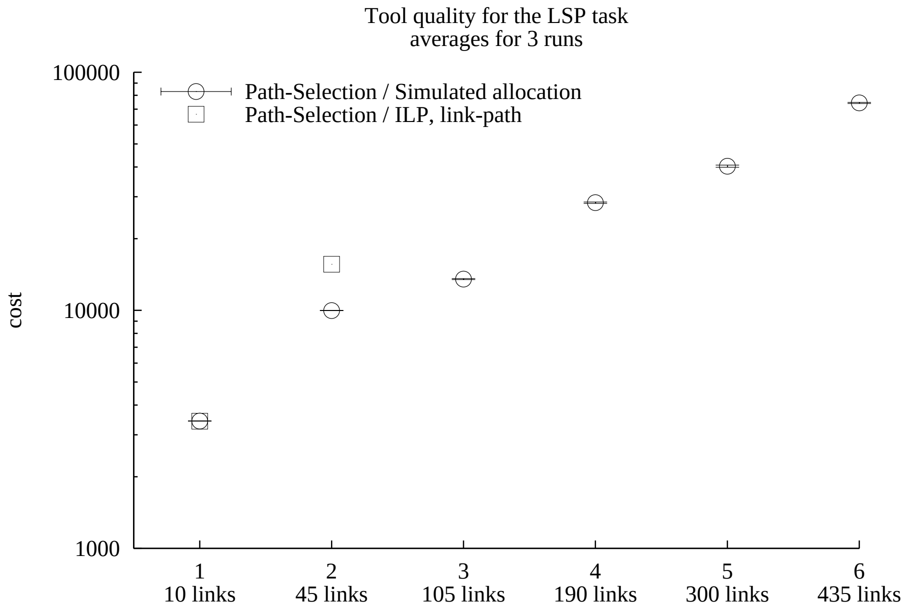

Figure 7.10: Optimization tool quality for the LSP design task.

works. Although link-path doesn't reach optimality the solution is very close to the results generated from simulated allocation. This together with the fact that the confidence intervals are very narrow for the results for simulated allocation indicates that the paths from the Path-Selection yields one obvious solution.

The results with protection are displayed in Figure 7.10. We achieve solution with Path-Selection / Simulation allocation for all the networks. But due to the increased complexity of the problem with protection and the integer linear programs in particular, then the link-path model only finds an optimal solution for the 10 link / 5 node network. For the 45 link / 10node network an feasible but non-optimal solution is found. For larger network no feasible solution is found. This illustrates the importance of heuristics/metaheuristics which is optimized for finding a good but not necessaryly optimal solution.

Staged versus integrated optimization

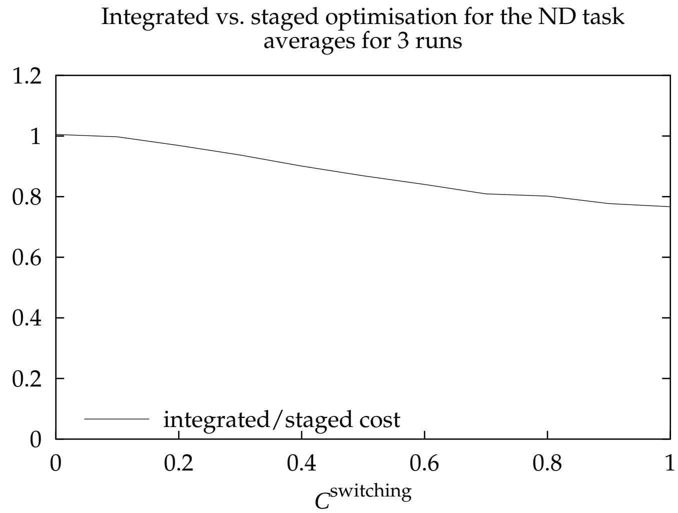

Figure 7.11: Staged versus integrated optimization for the ND task on the 300 link network.

Next, we compare staged optimization, where node costs are calculated in a postprocessing stage after link-based optimization, with integrated node and link optimization. The objective is to estimate the importance of integrated optimization. Obviously this optimization depends on the values of the parameters $C^{\text{switching}}$, C^{port} and C^{core}. Since it is far from obvious which values these obtain and since the first of these is the dominating factor, we fix the values $C^{\text{port}} = 10$ and $C^{\text{core}} = 100$. The value of $C^{\text{switching}}$ is now varied between $C^{\text{switching}} = 0.0$ and $C^{\text{switching}} = 1.0$.

This setting was tested for the nominal design case, and the result is shown in Figure 7.11. It is seen that the higher the switching cost the the more expensive is staged optimization compared to integrated optimization. The fraction of node cost relative to the total network cost is given in Figure 7.12 for solutions for both integrated and staged optimization.

In Figures 7.13 and 7.14 a visual of networks are given for integrated and

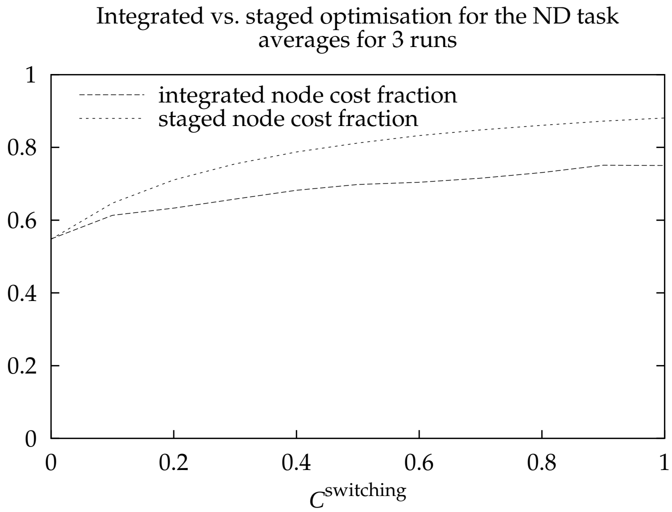

Figure 7.12: Fraction of switch equipment cost for both staged and integrated optimization for the ND task on the 300 link network.

staged optimization, respectively. It is noticed that with intregrated optimization the network is much more connected than the network, which is a results of staged optimization which resembles the minimum spanning tree. Integrated and staged optimization use the same paths generated from the Path-Selection algorithm.

The networks produced by the heuristic look intuitively right—an example of the 300 link network designed by integrated optimization is shown in Figure 7.13.

Overall, the network looks similar to what a human network planner would produce based on common sense and experience. The heuristic chose 47 links to connect the 25 nodes, yielding an average node degree of 3.76.

Optimizing node switch deployment

The final experiments we perform to determine how good the tools are at handling a *non*-green-field network design task: Given the nodes and the actual links (i.e., not all the potential links) of a network, we consider the task of routing the traffic demands to minimize node equipment costs. The pan-European network with

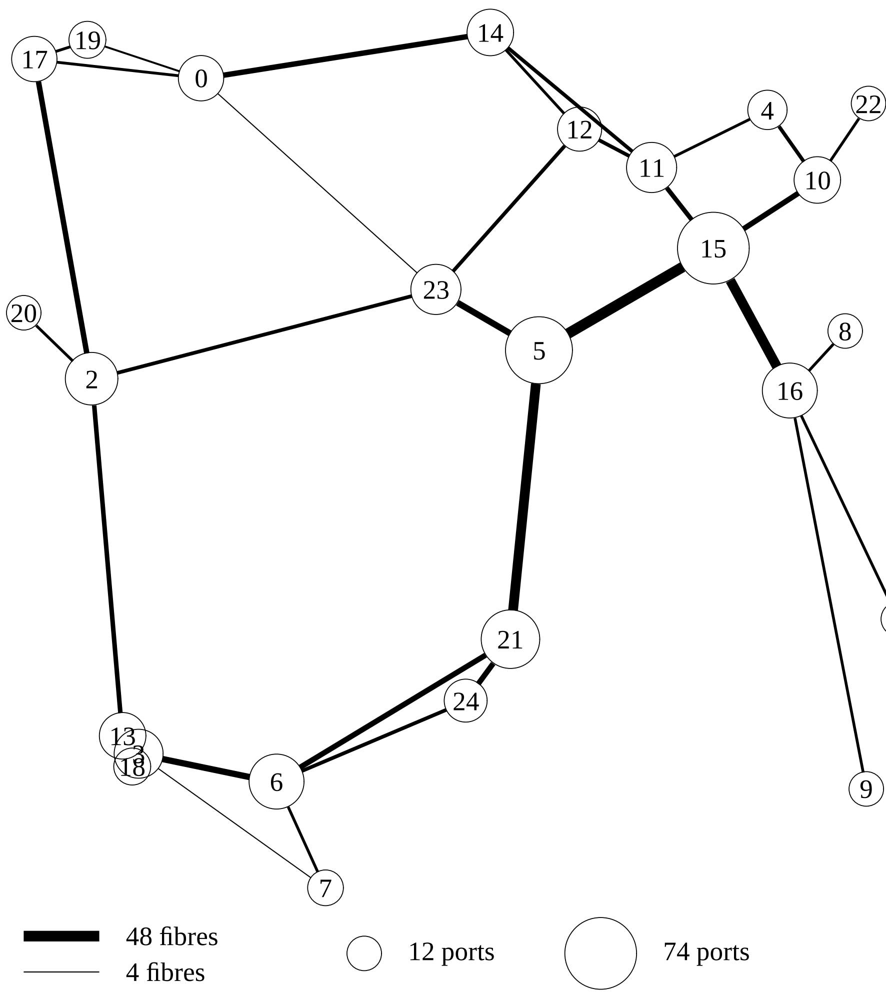

Figure 7.13: Example network result for the ND task on the 300 link network designed using the SAL heuristic with integrated optimization and $C^{\text{switching}} = 0.2$, $C^{\text{ports}} = 10, C^{\text{core}} = 100$.

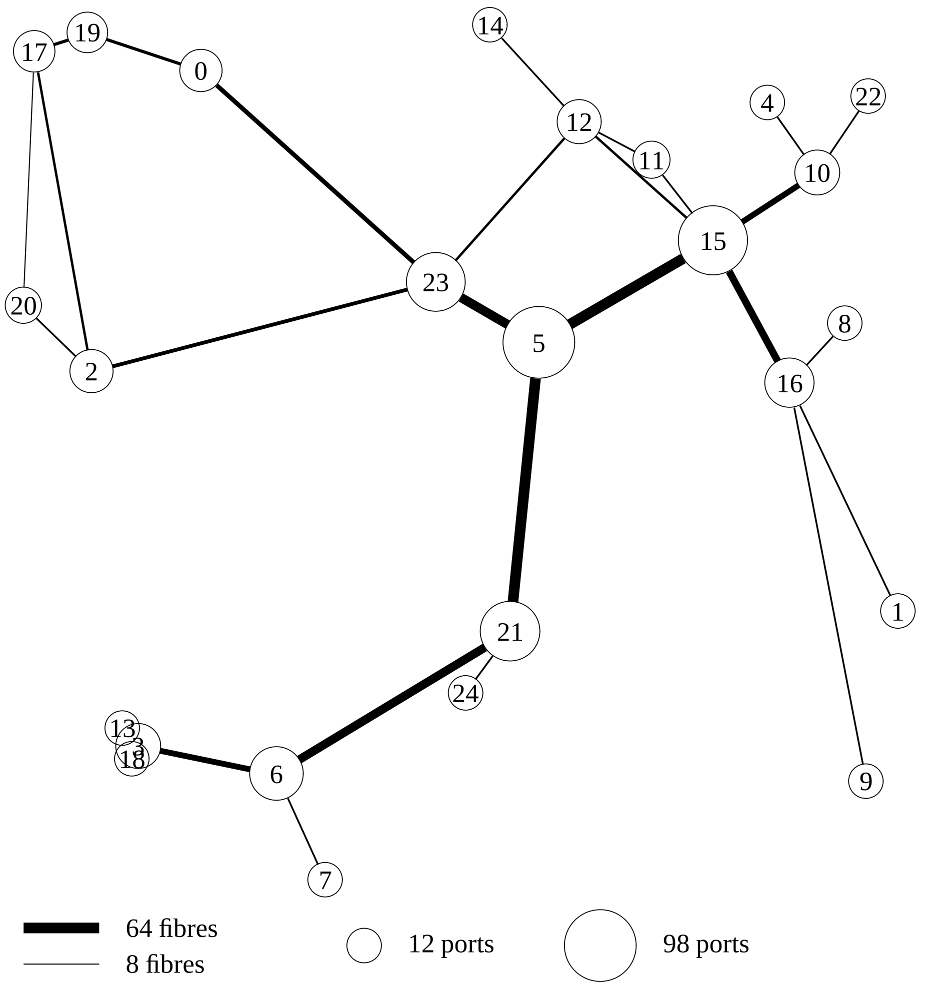

Figure 7.14: Example network result for the ND task on the 300 link network designed using the SAL heuristic with staged optimization and $C^{\text{switching}} = 0.2$, $C^{\text{ports}} = 10$, $C^{\text{core}} = 100$.

actual links is shown in Figure 7.15. The traffic is non-uniform and created with gravity model (see also Section 6.6.4).

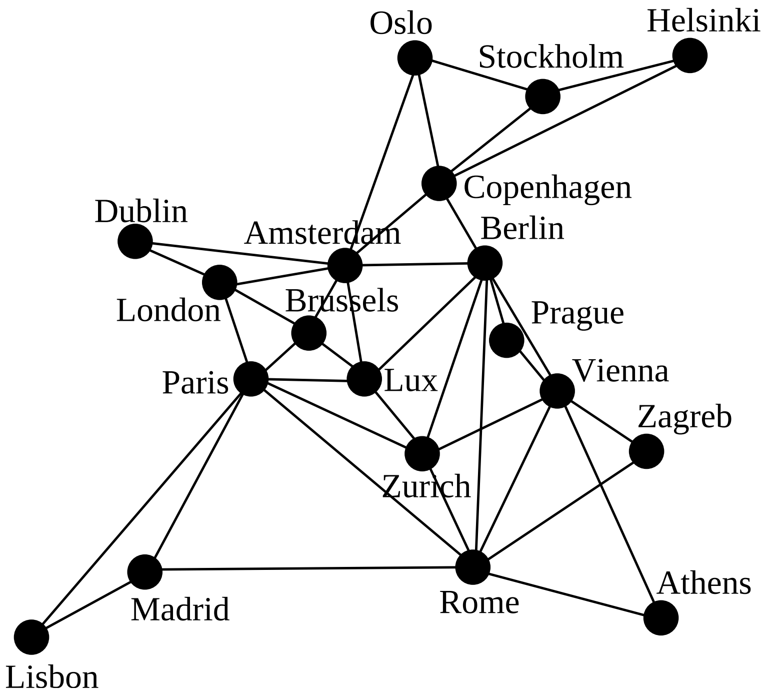

Figure 7.15: A Pan-European network consisting of 19 nodes and 39 actual links.

Fixing $C^{\text{port}} = 10$, $C^{\text{core}} = 100$, $C_l^{\text{duct}} = 0$, and letting C_l^{fibre} be $1/20$th of the euclidean distance, we consider the Pan-European optical network for the gravitational traffic demands shown in Table 7.2. Note that we model symmetric connections, so only demands from the upper triangular matrix are used.

The results are given in the graphs in Figure 7.16. The trend is the same as in the tests in section 7.2.5: Integrated optimization is increasingly important as the node costs increases. The results for a specific setting ($C^{\text{switching}} = 0.2$) is shown in Figure 7.17.

	Helsinki	Stockholm	Oslo	Copenhagen	Berlin	Amsterdam	Dublin	Prague	Luxemburg	Brussels	London	Vienna	Zurich	Paris	Zagreb	Athens	Rome	Madrid	Lisbon
Helsinki	0	1	1	1	3	1	1	1	1	1	2	1	1	2	1	1	2	2	1
Stockholm	1	0	1	1	4	1	1	1	1	1	3	1	1	3	1	1	3	2	1
Oslo	1	1	0	1	2	1	1	1	1	1	2	1	1	2	1	1	2	1	1
Copenhagen	1	1	1	0	3	1	1	1	1	1	2	1	1	2	1	1	2	2	1
Berlin	3	4	2	3	0	7	2	5	1	5	26	4	4	25	2	5	24	17	5
Amsterdam	1	1	1	1	7	0	1	1	1	1	5	1	1	5	1	1	5	4	1
Dublin	1	1	1	1	2	1	0	1	1	1	2	1	1	2	1	1	2	1	1
Prague	1	1	1	1	5	1	1	0	1	1	4	1	1	4	1	1	3	3	1
Luxemburg	1	1	1	1	1	1	1	1	0	1	1	1	1	1	1	1	1	1	1
Brussels	1	1	1	1	5	1	1	1	1	0	4	1	1	4	1	1	3	3	1
London	2	3	2	2	26	5	2	4	1	4	0	3	3	18	2	4	18	12	4
Vienna	1	1	1	1	4	1	1	1	1	1	3	0	1	3	1	1	3	2	1
Zurich	1	1	1	1	4	1	1	1	1	1	3	1	0	3	1	1	3	2	1
Paris	2	3	2	2	25	5	2	4	1	4	18	3	3	0	2	4	18	12	4
Zagreb	1	1	1	1	2	1	1	1	1	1	2	1	1	2	0	1	2	1	1
Athens	1	1	1	1	5	1	1	1	1	1	4	1	1	4	1	0	4	3	1
Rome	2	3	2	2	24	5	2	3	1	3	18	3	3	18	2	4	0	12	3
Madrid	2	2	1	2	17	4	1	3	1	3	12	2	2	12	1	3	12	0	2
Lisbon	1	1	1	1	5	1	1	1	1	1	4	1	1	4	1	1	3	2	0

Table 7.2: Traffic demand matrix for the Pan-European optical network in units of wavelengths.

7.2.6 Conclusion

Network design as an optimization problem of duct, fiber, and switch equipment deployment has been considered.

The problem of network optimization is defined mathematically both without and with protection.

We have used more optimization methods. Integer linear programming as a stand-alone; and integer-linear programming together with a inhouse developed heuristic to reduce the solution space, the Path-Selection algorithm; and the Path-Selection algorithm together with the metaheuristic simulated allocation.

The different optimization methods are compared, and it is found that the

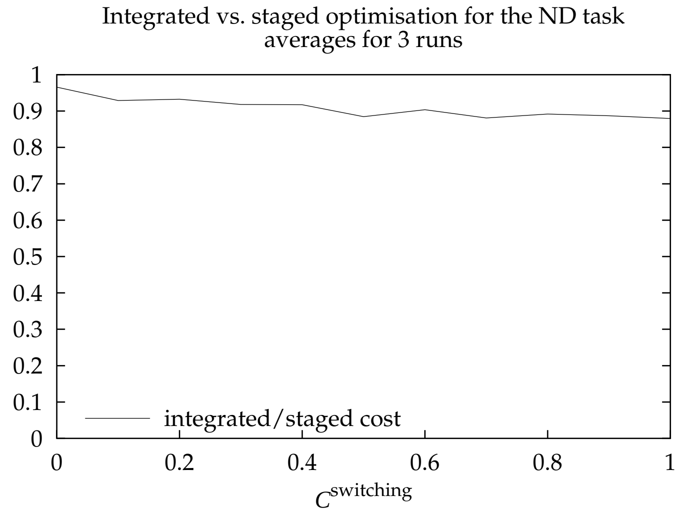

Figure 7.16: Using the optimization tool to route static traffic demands, considering node switch deployment, for the ND design task in the Pan-European optical network.

problem complexity increases quickly with network size, such that the integer linear programming as a stand-alone optimization tool breaks down for networks larger than 45 links / 10 nodes in the nominal design case. For the protection case no feasible solution at all can be found with the integer linear programming as a stand-alone optimization tool. Integer linear programming together with the Path-Selection break down for the protection case at 45 links / 10 nodes, where it finds a feasible but very expensive solution.

Optimizations with and without node cost are considered. It is found that the larger the node cost the more important is it to include thenode cost in the optimization.

The above consideration have been for green-field optimization. For the Path-Selection / simulated allocation tool has been demonstrated as a routing and deployment of fiber and switch equipment tool in a network with a predeployed set of ducts. The gain of including the cost of switch equipment has been quantified.

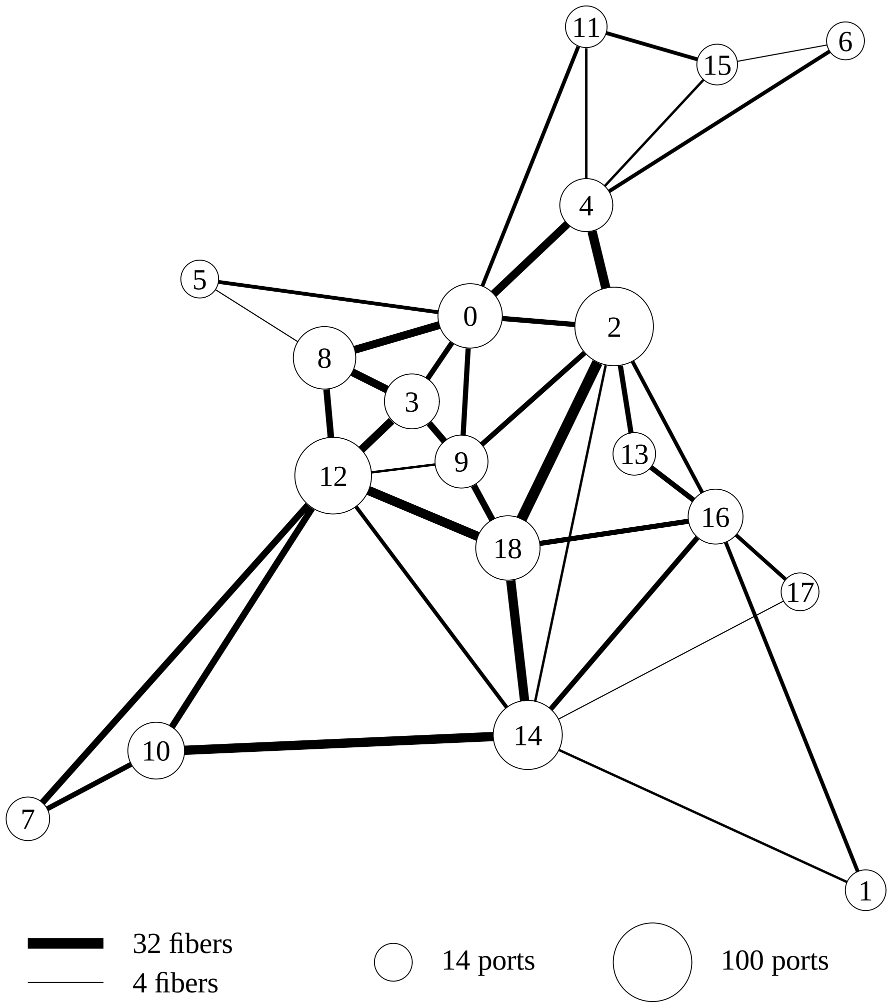

Figure 7.17: Resulting network using the optimization tool to route static traffic demands for the ND design task in the Pan-European optical network where $C^{\text{switching}} = 0.2$, $C^{\text{ports}} = 10$, $C^{\text{core}} = 100$.

7.3 Conclusion

This chapter have looked at several methods for network design.

Network planning is a very difficult problem due to the fast increase in complexity for larger networks. We have therefore made a sequential type of optimization, where a set of potential path first are found between the not yet connected nodes. When this has been done then only the best of these paths are used.

We have proposed and described an algorithm for finding the possible paths in a network not yet connected. The paths found will then be basis for further optimization. The further optimization process is then performed by the meta-heuristic, simulated allocation.

In the design process both duct, fiber, and node cost are considered. The problem, where the traffic demands should be allocated is considered. In addition the problem of allocating protection demands is considered.

We have formulated the network design problems using the exact formulation method of mathematical programming. We have also solved the design problem using integer linear programming. However, integer linear programming is not a scalable method, and this method therefore breaks down for larger networks.

We compare results from the different methods used and find similar performance.

We compare the cost integrated and staged network design. In staged design the node cost is neglected during the optimization process, where it is included in integrated design. We find that the higher the node cost the higher is the advantage of integrated design.

We illustrate the usage of the optimization tool for routing in a network where the a set of duct are already deployed.

Chapter 8

Network Design - Part II

8.1 Introduction

This chapter is devoted to the study how genetic algorithms perform in network optimization. In Addition different path protections methods are compared. Genetic algorithms (GAs) are computational models inspired by the idea of evolution, Whitley (1994), and introduced by Holland (1975) and his student DeJong (1975).

In this chapter the concept of GAs will be introduced. The focus will not be on the techniques of using GAs, but on the results that can be achieved in network planning by using GA.

GAs have been used to solve telecommunication network problems in a variety of contexts. Dengiz et al. (1997a,b) optimizes the reliability of networks. Narula and Ho (1980) and Chou et al. (2001) minimizes cost in a degree-constrained minimum spanning tree network problem. Kapsalis et al. (1993) optimizes Steiner trees. Cuppini (1994) uses GAs for allocation of channels. Palmer and Kershenbaum (1995) solves the optimal communication spanning tree problem. Sinclair (1999) used genetic algorithms for routing and wavelength assignment in all-optical networks.

GAs are adaptive heuristic search algorithms based on the evolutionary ideas of natural selection and genetics. The pseudocode of a GA in shown in Figure 8.1. The first step in a GA is to select a pool of individuals, i.e. a population. In this case of network optimization each individual will represent one network topology.

1) Select pool of individuals
2) repeat until best individual is good enough
   a) crossover of individuals
   b) mutate individuals
   c) evaluate individuals according to cost model
   d) selection: remove individuals from population

Figure 8.1: Pseudocode of genetic algorithms

The gene string representing a network is in this case an array of zeroes and ones. Next step is to mate individuals to create offspring which crossover of genes from each of the parents. Then mutation is performed by randomly swapping elements in the gene strings with a low probability. After this all the individuals are evaluated, and individual are removed, such that less fit individual have a higher risk of removal. Here the least fit individuals are the most expensive networks. This process of crossover, mutation, evaluation, and removal of least fit individuals are repeated until the solution represented by the best individual is good enough - each repetition called a generation. Other stop criteria could be a time limit or when the best solution has not improved in a given period of time. But there is no way of knowing how close the best solutions to an optimal solution. In Figure 8.2

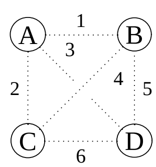

Figure 8.2: Illustration of link positions in a network

the correspondence between the network and the gene string is illustrated. A gene string expresses weather or not node pairs are connected. If N nodes are present in the network, then the gene string has the length $N(N-1)/2$, since there are that many possible link positions. Each position in the gene string describes if a specific link is present in the network. Figure 8.3 illustrate two networks with their respective gene strings. The network to the left has two links and therefore two 1s in the gene string. In Figure 8.2 it is seen that the two link is placed at

Figure 8.3: Illustration of two network with the respective gene string.

the link positions 2 and 3. Figure 8.4 illustrates crossover. Two individuals mate

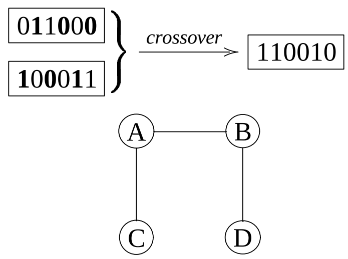

Figure 8.4: Illustration of crossover. The genes involved are displayed in bold face. The resulting offspring is shown as a network.

to create an offspring. The genes of the new individual is randomly chosen from each of the parents. For each generation all individuals are mated randomly, such that each individual produce one offspring in average. The new individuals are then added to the population.

Figure 8.5 illustrates mutation. The last gene is swapped from 0 to 1, which has the consequence that a link is added to the network. In the simplest version genes in the gene string are randomly swapped with a low blocking probability. By the use of network knowledge, specific combinations of genes can be swapped such that the chance of a random improvement is raised. The purpose of mutation is to maintain diversity within the population and inhibit premature convergence and to reach a better solution by random walk. Mutation alone induces only a random walk through the search space.

In the selection process the more fit individuals are selected with a higher probability than less fit individuals. Selecting using a probabilistic method pre-

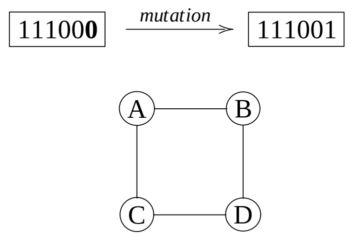

Figure 8.5: Illustration of mutation. The genes involved are displayed in bold face.

serves genetic variation in the population and inhibit premature convergence.

Mutation and selection (without crossover) create a parallel, noise-tolerant, hill-climbing algorithm. The operations of mating, mutation, and selection produce a useful and robust technique, i.e. noise-tolerant and hill-climbing, which is largely due to the fact that GAs combine direction and chance in the search in an effective and efficient manner. Since a population implicitly contain much more information than simply the individual fitness scores, GAs combine the good information hidden in a solution with good information from another solution to produce new solutions with good information inherited from both parents, inevitably (hopefully) leading towards optimality.

8.2 Computer program

I have written a computer program in C++ using the method of GAs to optimize networks. The network size, location of nodes, duct, fiber and node cost are read from files into the program. Options like controlling population size, mutation rate, and the selection method has been implemented. Further the island model has been implemented as an option to preserve genetic variation. In the island model subpopulations are kept separate with less crossover between subpopulations. Having implemented the island model makes the program structure ready for parallel implementation for execution on a cluster. The interface of the program is shown in Figure 8.6. The input is either read from files or given at the command line (or default values are used).

The network used for the experiments presented in this chapter have their nodes located in the 1000x1000 quadrant. The duct price between two nodes is the distance between the two nodes. The fiber price is chosen as a fraction of the duct price. The traffic is uniform, i.e. one wavelength (or channel or connection) between every node pair in each direction. The node cost is determined by the three parameters in a second order polenomium, see equation (8.5).

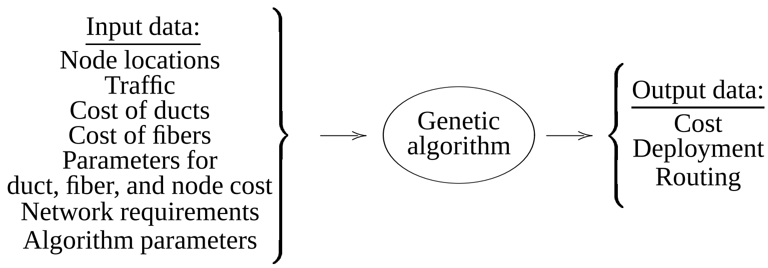

Figure 8.6: Program interface.

8.3 Network model

A network consists of nodes, which are connected by duct in which fibers are put. Lightpaths travel in the fiber. Depending on what is chosen then one or more lightpaths can be allocated to a fiber. Although bidirectional fibers have the advantage of easier upgradability, unidirectional fibers is used here, because of the lower signal distortion and that the advantage in upgradability becomes negligible for larger networks The fiber are unidirectional, i.e. all lightpaths in a fiber must run in the same direction. If between two nodes lightpaths are required in each direction then one and only one duct is required, but at least two fiber. If multiple lightpaths are allowed on one fiber then multiplexers are assumed in the cross connects, such that the switching will be on the wavelength level. The cross connect can have any size, but the larger the more expensive. Only one type of cross connect is assume. This type takes care of both the switching of transit traffic and adding and dropping traffic from the sources and to the destinations.

The wavelength continuity constraint does not apply. In wavelength routed optical networks without wavelength converters then the wavelength of a lightpath traveling through the network must remain the same. If the wavelength continuity constraint was assumed the this would have a negligible influence on the result, see for example Section 6.6.4.

8.4 Cost model

The cost of a network is the cost is the cost of the different equipment types which is classified into ducts, fibers, and nodes:

$$\text{total cost} = \text{duct cost} + \text{fiber cost} + \text{node cost} \tag{8.1}$$

The cost of all ducts is:

$$\text{duct cost} = \sum_{ij, i<j} C_{d,ij}\, \delta(U_{ij}) \tag{8.2}$$

where $C_{d,ij}$ is the cost of the non-directed duct between node i and j; U_{ij} is the load on the link between the node i and j. If no link is present then that will have the consequence that $U_{ij} = 0$. And where

$$\delta(x) = \begin{cases} 1 & \text{for } x > 0 \\ 0 & \text{otherwise} \end{cases} \tag{8.3}$$

The cost of the fibers is the sum of the cost of all fibers in the network:

$$\text{fiber cost} = \sum_{ij} C_{f,ij} \lceil \frac{U_{ij}}{W} \rceil \tag{8.4}$$

The cost of a fiber between node i and j is $C_{f,ij}$, which typically is set to a fraction r of the duct cost, i.e. $C_{f,ij} = rC_{d,ij}$. $\lceil \cdot \rceil$ represents the ceiling operator.

To model the cost of a node the following cost model has been chosen:

$$\text{node cost} = \sum_{i} \left(C^{core} + C^{port} \cdot f_i + C^{switching} \cdot f_i^2 \right) \tag{8.5}$$

where the sum is over all nodes, and where f_i is the total number of input and output fibers to node$_i$ including dropped and added traffic. C^{core}, C^{port}, and $C^{switching}$ are constants. Any model could have been chosen, but this is general in that it contains a constant part, a linear part, and a non-linear part of higher order than linear. The constant term represents the basic cost of setting up the node and necessary equipment. In case that $r = 0$, then the node is not needed at all and the node cost should therefore be zero. It is, for simplicity, assumed that every node will switch traffic. The linear term represents a cost increase proportional to the number of channels. The square term represents the quadratic increase in complexity a node experiences as the number of switch possibilities increase.

The number of fibers switched by node i is

$$f_i = \sum_j \lceil \frac{U_{ij}}{W} \rceil + \lceil \frac{T_{add,i}}{W} \rceil + \lceil \frac{T_{drop,i}}{W} \rceil \tag{8.6}$$

where U_{ij} is the utilization measured in number of channels on the link directed from node i to node j; $T_{add,i}$ is the number of channels added by node i; $T_{drop,i}$ is the number of channels dropped to node i; and W is the maximum number of channels per fiber.

8.5 Network types

When a network is to be optimized it can be characterized by its physical and functional requirements. By physical requirements is meant number of nodes, cost of equipment, and traffic demands. By functional requirements is meant weather or not the network should be connected, biconnected, and weather or not the traffic should be protected, and what type of protection is required. A network is connected if routes through allocated ducts can be made between all node pairs. A network is biconnected if two link disjoint routes through allocated ducts can be made between all node pairs. I.e. the network will still connected after one removal of any duct. Three types of protection is provided: *shared protection*, *limited shared protection*, and *non shared protection*. When a network is protected then fiber and switch capacity must be available to accommodate traffic that is rerouted in case of link failure. Implicitly this, as a minimum, requires the network to be biconnected. When a link failure occurs then traffic using that link is removed from other links. In *shared protection* this free capacity can be used by protection paths. In limited shared protection only protection capacity from one failure can be used as protection capacity for other failures since only single link failure are assumed. With *limited shared protection* the capacity can be shared among protection paths, but already used capacity that is freed when the link failure occurs cannot be reused. The name M:N protection is used in the literature for both these types of shared protection. *Non shared protection* (1:1 protection) is protection without any sharing. It is the simplest but by far the most expensive. Shared protection is the most complicated since free capacity from removed traffic is reused, but, as we shall see, the most efficient. Limited shared protection is the kind of protection used in Chapter 7.

8.6 Results

In this section the genetic algorithm program will be evaluated and compared to results from the EXPLAIN application (described in Chapter 7) and, in simpler cases, VPI TransportMaker and optimal results. This is done by testing the ability to optimize network with connectivity requirements and biconnectivity requirements, where the only cost is duct cost, i.e. fiber and duct costs are neglected. Secondly the ability to do full network design is tested both in the case of nominal design (no protection) and in the case of protection design.

The three different kinds of protection provided and compared to each other and to solutions without protection requirements.

8.6.1 Connectivity and biconnectivity tests

In this section basic tests of the GA program is made. The ability to find the least costly connected network and the least costly biconnected network is tested. In a connected network at least one route must be available between all node pairs. This task is also called the minimum spanning tree problem, which minimizes the cost of ducts between a number of cities, such that the cities are all connected. This problem differs from the optimal communication minimum spanning tree problem, which is to find a tree such that the sum of all routes weighted by the traffic on the route is minimized. This latter problem is studied by Palmer and Kershenbaum (1995) using a genetic algorithm and by Fischetti et al. (2002) using the branch and price algorithm.

In a biconnected network at least two link disjoint routes must be available for all node pair. The problem of finding the least costly biconnected network is different from the task of solving the *traveling salesman problem*: Given *N* cities and the distance between each pair of them, the task of the salesman is to visit each and every city once so that the overall tour length is minimal, Sena et al.

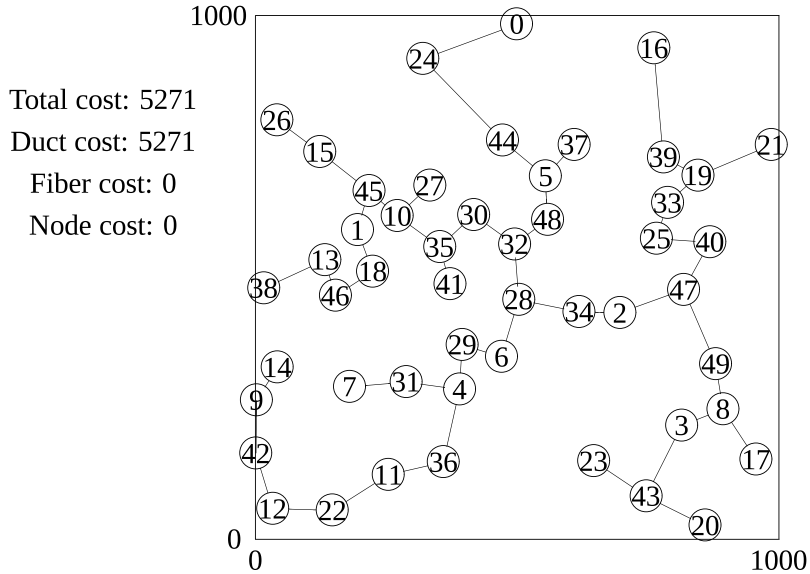

Figure 8.7: Solution by GA program for a connected 50 node network.

(2001). Only duct cost are considered. Fiber and node cost are not considered. And no capacity limitation exist. GAs have been applied on the traveling salesman problem in Goldberg (1989) and in Michalewicz (1996).

Finding the minimum spanning tree can be done by a polynomial greedy algorithm, i.e. an algorithm which from local information is capable of finding the global optimum. For example the Prim's algorithm, Weiss (1997), can be used. The time complexity for the Prim's algorithm for finding the minimum spanning tree is $O(N^2)$. The traveling salesman problem is on the other hand a NP-hard problem, Garay and Johnson (1979b), i.e. only algorithms with exponential time complexity have been shown to exist. The task of finding the the least costly biconnected network requires a global overview, and this is the fundamental difference that makes the latter problem much more difficult. The networks and results from using VPI and the optimal results is supplied by Panagiotis Saltsidis from LM Ericsson in Sweden. The network sizes span from 6 to 60 nodes.

In Figure 8.7 is shown the minimum spanning tree solution found by the GA

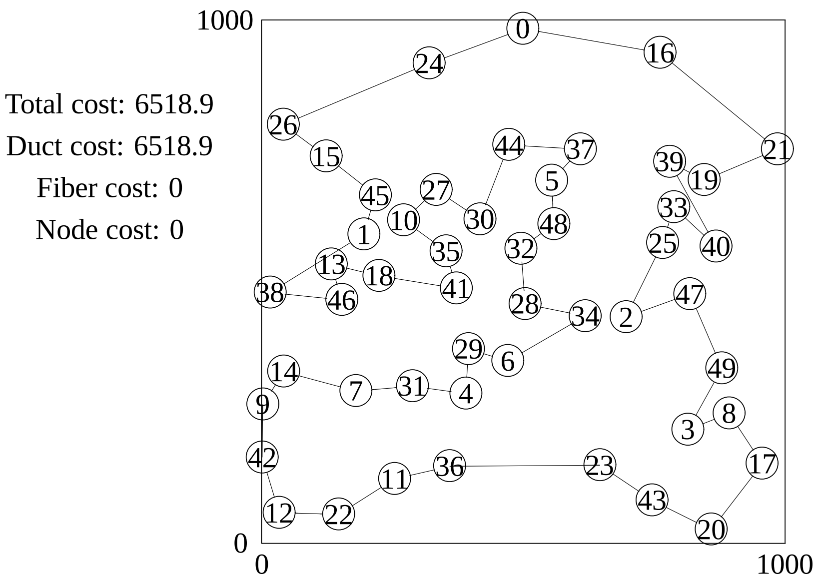

Figure 8.8: Solution by GA program for a biconnected 50 node network.

program. In this case the optimal results is presented but in general guarantee that the optimal solution is found. In Figure 8.8 the least costly biconnected network found is shown. Finding the minimum spanning tree could been found by a polynomial greedy algorithm, i.e. an algorithm which from local information is capable of finding the global optimum. The task of finding the the least costly biconnected network requires a global overview, and this is the fundamental difference that makes the latter problem much more difficult.

In Table 8.1 we have compared the ability of finding the minimum spanning tree in a network for the genetic algorithm to VPI TransportMaker, EXPLAIN, and the optimal results. It is seen that the genetic algorithm performs perfect in all cases, i.e. the minimum spanning tree has been found. For 15 and 40 nodes one node did not have any traffic demand, whereby VPI, EXPLAIN, and the optimal solution have missed that node. In the genetic algorithm it has been chosen to

[1] The better than optimal results is caused by rounding error in input data

[2] The minimum spanning tree includes a node with no traffic demand

Nodes	GA	VPI	EXPLAIN	Optimum
6	1894.0	1894.0	1894.0	1894.0
9	2014.7[1]	2046.7	2014.7	2014.9
12	3050.9	3050.9	3050.9	3050.9
15	2936.3[2]	2806.7	2806.8	2806.7
20	3424.4	3441.2	3424.4	3424.3
25	4003.8	4226.6	4003.8	4003.7
30	4019.0	4169.6	4019.0	4019.1
40	4963.7[2]	4909.7	4848.8	4843.4
50	5271.0	5439.3	5390.7	5271.1
60	6091.4	6118.7	6091.4	6091.7

Table 8.1: Comparison on minimum spanning tree solutions. Only duct costs are considered.

Nodes	GA	VPI	EXPLAIN	Optimum[4]
6	2630.0	2630.0	2630.0	2630.0
9	2460.6	2691.7	2734.4	2460.6
12	3685.9	3915.7	3685.9	3686.0
15	3851.8[3]	4597.2	6320.6	3712.4
20	4557.6	4715.6	6865.5	4557.7
25	4696.4	6087.8	5913.3	<5669.6
30	4716.9	6129.2	6125.7	<5201.1
40	5940.4[3]	6889.4	7949.3	<6322.5
50	6704.8	6761.0	9764.5	<6586.1
60	8316.2	8357.0	10557.4	<7362.8

Table 8.2: Comparison for biconnected networks. Only duct costs are considered.

include all node.

In Table 8.2 results for optimization of biconnected networks are presented. The genetic algorithm performs better than VPI and EXPLAIN in all cases, but

[3] The best traveling salesman route includes a node with no traffic demand

[4] Optimum solution for the traveling sales man problem

for the largest networks the result from the genetic algorithm deviates from the optimal result, which displays the difficulty of NP-hard problems and in particular large network optimization. Longer run time would not necessarily result in a significant lower cost. If the population had converged prematurely longer runtime would only be a steepest descent method, i.e. work like a greedy algorithm. Premature convergence occurs when the best networks extinguish the more expensive network, whereby valuable genetic material is lost. When increasing the run time one should at the same make sure that the genetic diversity is kept for a longer time. The optimum results is for the traveling salesman problem, which is theoretically more costly than the least costly biconnected network. The optimal solution to the traveling salesman problem must be one big cycle in the network. This is not the case for the least costly biconnected network. The solutions to all the networks are visualized in Appendix A. For all networks, except the 40 and 60 nodes network, the least costly biconnected network solution is indeed the minimum spanning tree solution. And the cost is less than the cost given by the upper bound for the optimum result, except for the 15 nodes network[2], and the 60 nodesnetwork.

This has been a qualitative test of the ability to perform some graph exercises, which does not necessaryly reflect the ability to perform network optimization. Further the time usage is not included. Partly because many the time usage was only available for some experiments and partly because of the very large costs that can be saved with network optimization, whereby time usage becomes relative.

8.6.2 Full network design - multiple wavelengths

In full network design both duct, fiber, and node cost are considered. In this section the case with multiple wavelengths on each fiber is considered. In the next section the case of a single wavelength per fiber is considered. The reason for this unusual order is that the case of multiple wavelengths on each fiber were considered in the previous chapter and will be the starting point for full network design in this chapter.

The networks were created by randomly placing the respective number of cities on a 1000 times 1000 square. The duct cost between two cities is set to the euclidean distance between them. The cost per fiber between a node pair is set to $1/20$th of the distance between them. Uniform traffic is chosen with the demand of one wavelength between all node pairs in each direction. Each fiber

Nodes	GA ND	EXPLAIN ND
5	2240.59	2240.9
10	5398.55	5885.61
15	8266.02	8929.24
20	15444.6	17096.29
25	21588.7	24660.62
30	32268.3	41082.47

Table 8.3: Comparison for full network design - no protection. ND – nominal design. $W = 8$, $C^{core} = 100$, $C^{port} = 10$, and $C^{switching} = 0.2$.

Nodes	GA SP	GA LSP	GA NSP	EXPLAIN LSP
5	3425.7	3425.7	3925.13	3425.70
10	7500.7	7651.41	11174.5	9974.44
15	11915.8	12027.1	19216.7	13513.77
20	20802.1	20967.8	38981.6	28015.82
25	29308.2	29691.9	58262.6	40370.70
30	42423.7	42681.3	88554.5	75662.30

Table 8.4: Comparison for full network design for protected networks. $W = 8$, $C^{core} = 100$, $C^{port} = 10$, $C^{switching} = 0.2$, and $f = 0.05$. SP – shared protection, LSP – limited shared protection, NSP - non shared protection.

is directed and has the capacity of eight wavelengths. The cost of a node follows equation (8.5) with the parameters, $C^{core} = 100$, $C^{port} = 10$, and $C^{switching} = 0.2$. The network sizes span from 5 to 30 nodes.

In Table 8.3 the ability to do full network design is compared to results from EXPLAIN. The results of the two programs, the genetic algorithm and EXPLAIN application, reached the same result for 5 nodes. As the network size rise so does the difference in quality of the two methods with the genetic algorithm program reaching a very low cost relatively to the EXPLAIN application. In Table 8.4 the ability to do full network design with protection is compared to results from EXPLAIN. The results for all three kinds of protection is given. In the second column shared protection, in the third column limited shared protection, and in the fourth column non shared protection. In the last column the EXPLAIN results for limited shared protection is given.

Just like in the nominal design case it is seem the cost difference between EXPLAIN and the genetic algorithm with limited shared protection rises as the network size increases indicating the relatively good scaling properties of the genetic algorithm program.

To much surprise the cost of shared protection is only slightly less expensive than the cost of limited shared protection. This is partly due to the routing algorithm and partly due to the fact that a lot of empty protection capacity is available close to failed links, whereby the used capacity which is freed is of no need.

It is also seen that non shared protection is much more expensive than the two other types of protection. For 30 nodes the cost is the double of shared protection.

In Figure 8.9 the cost of the three protection methods is compared the cost of nominal design. I.e. the cost of protection of divided by the cost of nominal design. As previously seen, the curves for and shared and limited shared protection divided by nominal design (SP/ND and LSP/ND) are almost identical. Also very interesting the curves drop from 1.5 to 1.3. I.e. the relative cost of protection becomes less for larger network. That is, shared and limited shared protection does not display any scaling problems. The third protection method non shared protection becomes relatively more expensive for larger networks. The cost rises from 1.8 times the cost of nominal design to 2.8 times the cost of nominal design. In Figure 8.10 the absolute cost of nominal design and the three protection types are plotted. In Table 8.5 the method of quick protection is introduced. Quick protection is a temporary method, where some tricks are used such that the optimization is much faster, and therefore more applicable for larger networks. The quick protection method will be used in the next section for larger networks, and is here compared to the slower method of protection to evaluate the quality. Compared to the slower protection method in Table 8.4 it is seen that the quick protection method is 0-8% more expensive than the slower form of protection. However, GA LSPQ is still significantly better than the EXPLAIN method.

In Figure 8.11 the relative cost of network equipment is displayed for the nominal design and in Figure 8.12 for shared protection design. In the case nominal design then for the smallest network of 5 nodes almost 60% of the total network cost is for ducts, with about 7% for fibers, and about 35% for nodes. Both in the nominal design case and in the protection design case then as the network size is increased then the distribution of the relative of equipment is changed. The duct

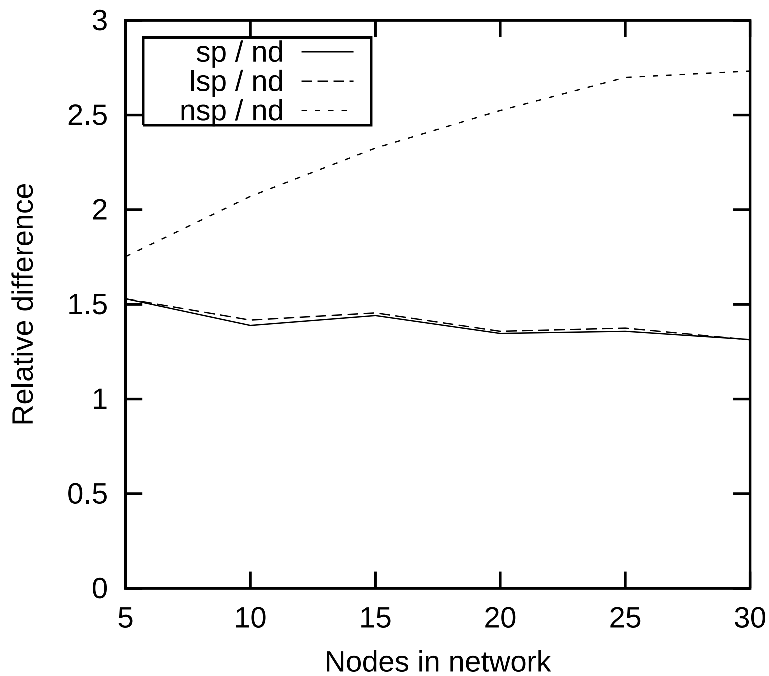

Figure 8.9: Relative cost difference between network with protection design and nominal design. ND – nominal design, SP – shared protection, LSP – limited shared protection, NSP - non shared protection. $W = 8$, $C^{core} = 100$, $C^{port} = 10$, $C^{switching} = 0.2$, and $f = 0.05$.

cost drops, which is partly due to the fact that the geographical distribution of all networks is in the same area, i.e. the nodes are closer together for larger networks. Both the fiber cost and and node cost is increased due to more traffic. Contrary to what could be expected then a larger part of the cost is for switching for nominal design. But because of the increased capacity demand in protection design then more ducts are deployed, which again requires less switching.

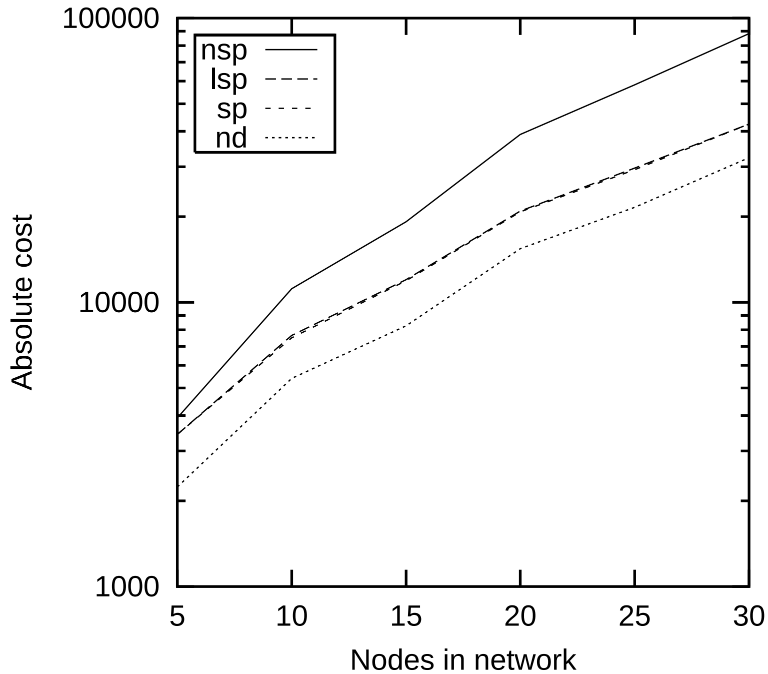

Figure 8.10: Absolute cost for networks with protection design and nominal design. ND – nominal design, SP – shared protection, LSP – limited shared protection, NSP - non shared protection. $W = 8, C^{core} = 100, C^{port} = 10, C^{switching} = 0.2$, and $f = 0.05$.

8.6.3 Full network design - single wavelength

In this section one wavelength per fiber is assumed. This is to avoid the discreteness in fiber prices, which to some extend randomize the cost of the network. The network used in this section is the same as those in Section 8.6.2. In addition networks with 40, 50, and 60 nodes have been included, such that also larger networks are considered. The fiber price has been kept the same, i.e. $1/20$th of the duct price. The parameters for expression (8.5), determining the node prices, have been changed to $C^{core} = 100$, $C^{port} = 0.5$, and $C^{switching} = 0.0005$. I.e. except for the core part of the node cost, the node prices per wavelength is reduced. Since

Nodes	GA SPQ	GA LSPQ	GA NSPQ
5	3425.7	3425.7	3925.13
10	7500.7	7651.41	11917.8
15	12503.8	12607.3	20966.1
20	22323.3	22546.5	43464.2
25	30628.6	31085.1	65554.6
30	45153.9	45784.5	99677.4

Table 8.5: Comparison of the quick protection method with real method for full network design. $W = 8$, $C^{core} = 100$, $C^{port} = 10$, $C^{switching} = 0.2$, and $f = 0.05$. SPQ – shared protection, LSPQ – limited shared protection, NSPQ - non shared protection.

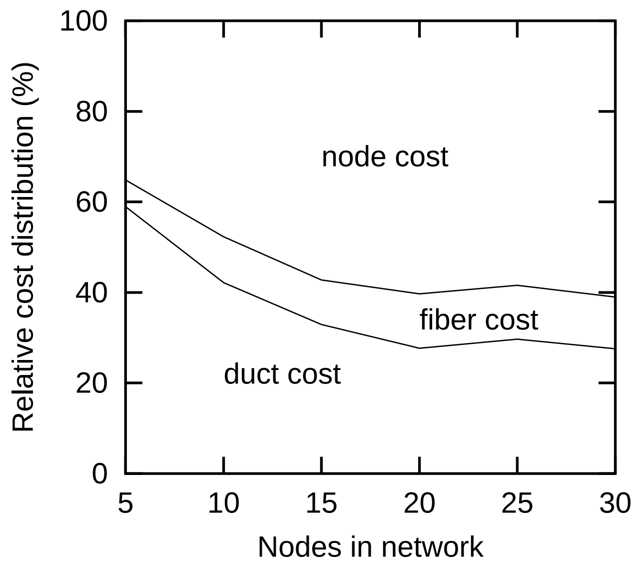

Figure 8.11: Relative equipment cost for connected networks. $W = 1$, $C^{core} = 100$, $C^{port} = 10$, $C^{switching} = 0.2$, and $f = 0.05$.

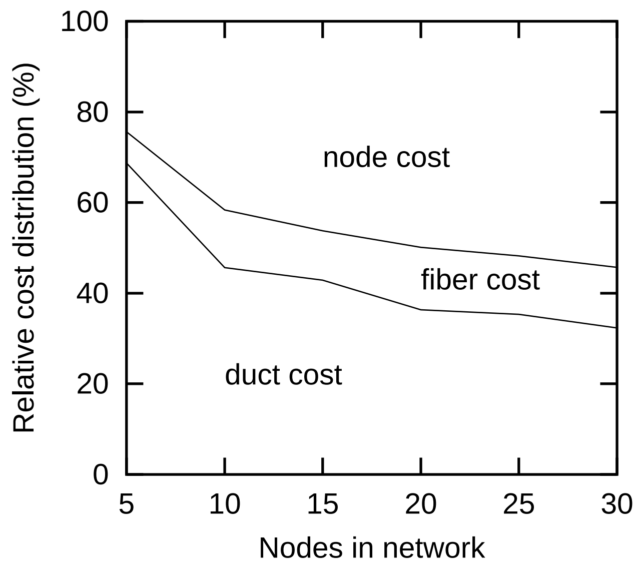

Figure 8.12: Relative equipment cost for protected networks with full sharing. $W = 1$, $C^{core} = 100$, $C^{port} = 10$, $C^{switching} = 0.2$, and $f = 0.05$.

the fiber price is identical to the price in the previous section, then the price per wavelength has increased 8 times.

In Table 8.6 the genetic algorithm is compared with EXPLAIN for the nominal design optimization. For the 5 node network. For up to 30 nodes the genetic algorithm finds solutions which are 4-10% less expensive. For larger networks it seems that the EXPLAIN program breaks down in the sense that the GA ND solution is 6 - 8 times less expensive. In Table 8.7 the results for protection are presented and compared with those from EXPLAIN. As described in Section 8.6.2 the form of quick protection is used. The slower, but more optimal, form of protection also used in Section 8.6.2 would not be applicable for more than about 30 nodes due to the time constraint. As mention previously the genetic algorithm program lacks a bit in the routing capabilities, and therefore the result for 5 nodes LSPQ is slightly larger than the EXPLAIN results. The 5 nodes SPQ result is by coincidence identical to EXPLAIN. The 5 node NSPQ is again the most expen-

Nodes	GA ND	EXPLAIN ND
5	2566.42	2566.42
10	7469.11	7718.40
15	10782.6	11698.66
20	20682.1	22233.19
25	29238.2	31247.08
30	40356.1	44875.16
40	71952.9	461501.68
50	109827	780099.13
60	159280	1260865.43

Table 8.6: Comparison for full network design - no protection. $W = 1$, $C^{core} = 100$, $C^{port} = 0.5$, $C^{switching} = 0.0005$, and $f = 0.05$.

Nodes	GA SPQ	GA LSPQ	GA NSPQ	EXPLAIN LSP
5	4349.4	4459.91	5459.63	4349.40
10	12135	12197.8	19402	12673.64
15	17650.9	17753.8	28730.3	17423.09
20	33809.2	33986.7	61991.7	36686.08
25	46416.2	47038.4	89773.3	48180.40
30	63736.8	64148.7	123748	76393.43
40	113979	115092	233632	825256.13
50	170319	171703	355378	1353234.05
60	240110	241136	517160	*not obtainable*

Table 8.7: Comparison for full network design for protected networks. $W = 1$, $C^{core} = 100$, $C^{port} = 0.5$, $C^{switching} = 0.0005$, and $f = 0.05$. SPQ – shared protection quick , LSPQ – limited shared protection quick, NSPQ - non shared protection quick.

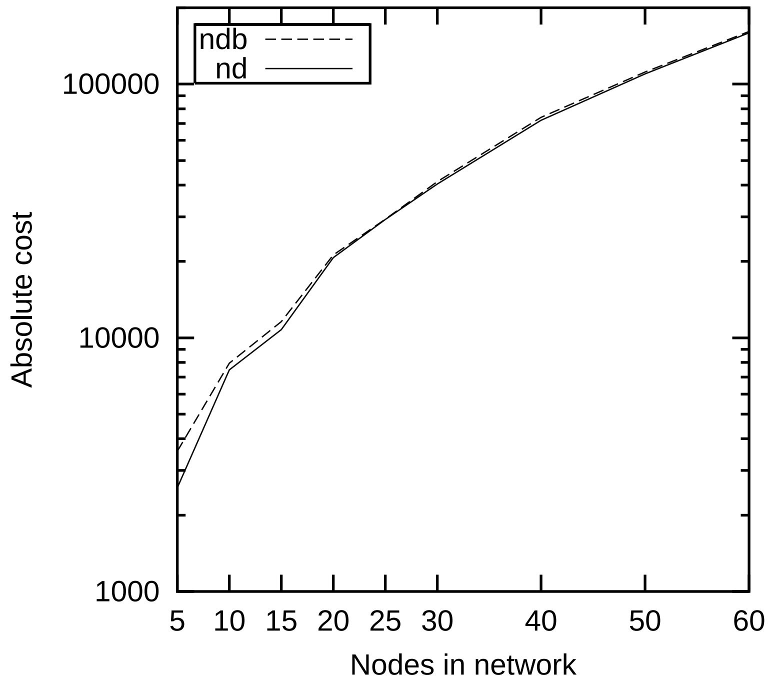

Figure 8.13: Absolute cost for networks with nominal design (W=1). ND – nominal design, NDB – nominal design with biconnectivity constraint. $C^{core} = 100$, $C^{port} = 0.5$, $C^{switching} = 0.0005$, and $f = 0.05$.

sive, and this difference increases with the network size as fiber and node cost make up a relatively larger part of the total network cost. Just like in the nominal design case then for more than 30 nodes the solution form EXPLAIN deteriates quickly. It is seen that the gain of using shared protection instead of limited shared protection is ony insignificantly better. This is partly due to the routing algorithm and partly due to the fact that a lot of empty protection capacity is available close to failed links, whereby the used capacity which is freed is of no need.

In Figure 8.13 the cost of the biconnectivity requirement is compared the the cost with only the connectivity requirement. Fiber and node cost are still present. It is seen that only for small network is there any extra cost by the biconnectivity requirement. For larger network most of the nodes will with the requirement be

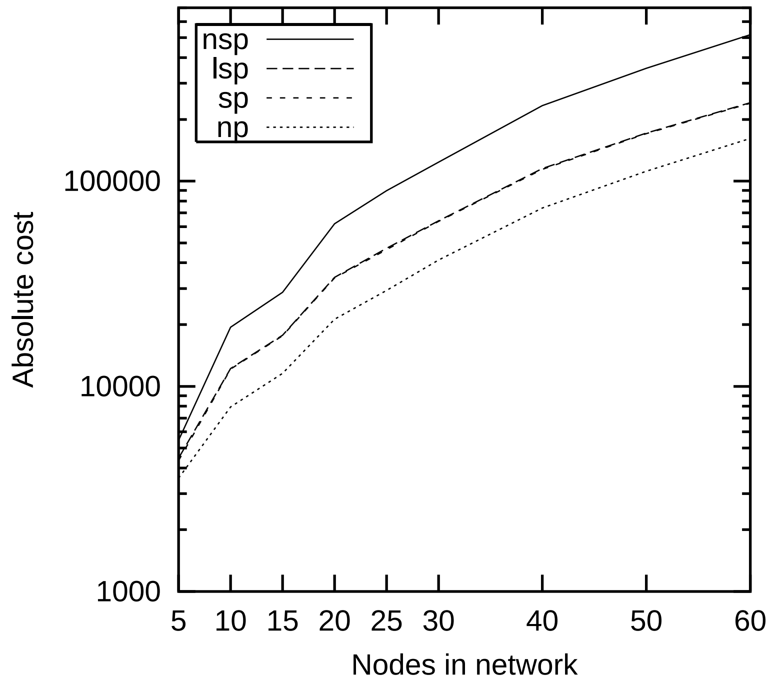

Figure 8.14: Absolute cost for networks with protection (W=1). SP – shared protection, LSPQ – limited shared protection, NSP – non shared protection. $C^{core} = 100$, $C^{port} = 0.5$, $C^{switching} = 0.0005$, and $f = 0.05$.

biconnectet anyway to minimize switching. In Figure 8.14 the absolute cost of nominal design and the three protection design types are compared. Somewhat Contrary to what seen in Section 8.6.2 then the extra cost of introducing shared or limited shared protection does not decrease but approaches a constant extra cost relatively as the network size increases, but the protection is still scaleable. The extra cost of non shared protection increases relatively to the nominal design cost and is therefore not scalable.

The Figures 8.15 and 8.16 is very interesting due to the behavior for larger networks. Just like in Section 8.6.2 the cost related to traffic, i.e. fiber and switching cost increases relatively for up to 30 nodes. But from 30 nodes the cost distributions are constant, indicating an optimal distribution of equipment cost.

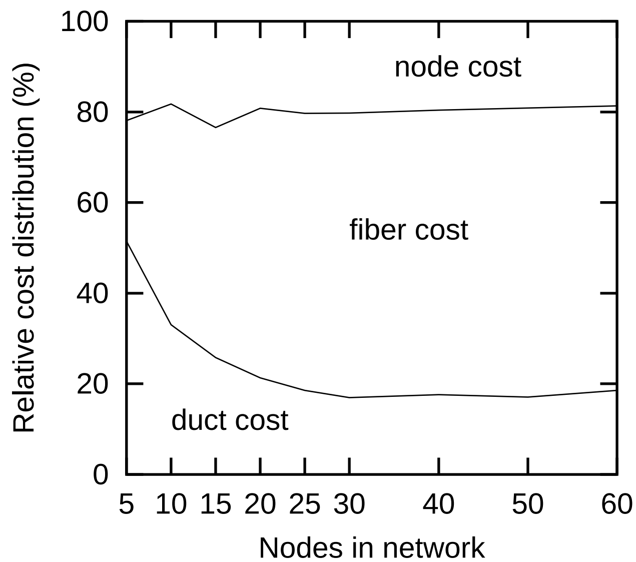

Figure 8.15: Relative equipment cost for connected networks (W=1). $C^{core} = 100$, $C^{port} = 0.5$, $C^{switching} = 0.0005$, and $f = 0.05$.

In Figure 8.17 and Figure 8.18 the results of optimization of two 40 nodes networks with the functional requirements nominal design and shared protection quick design, respectively. The total cost and the equipment cost is given to the left of the figure. The thicker the link size the the more fiber run over the link. And the larger the circle around the node number the higher is the number of nodes switched in the node. The teh left of the figure is given the extremes of the node and fiber sizes. The non protected network in Figure 8.17 has several nodes which are not biconnected, but the reason that most parts of the network is actually heavyly connected is that the high connectivity yields more routing possibilities, which reduce node and fiber cost. Where the nominal design network contain 76 link, then the protected network in Figure 8.18 contains 112 links. It obviously pays of have a higher connectivity when the capacity demand is higher. It is somewhat surprising that the largest nodes are larger in the nominal design network than in the protected network – almost double the size, but with a higher

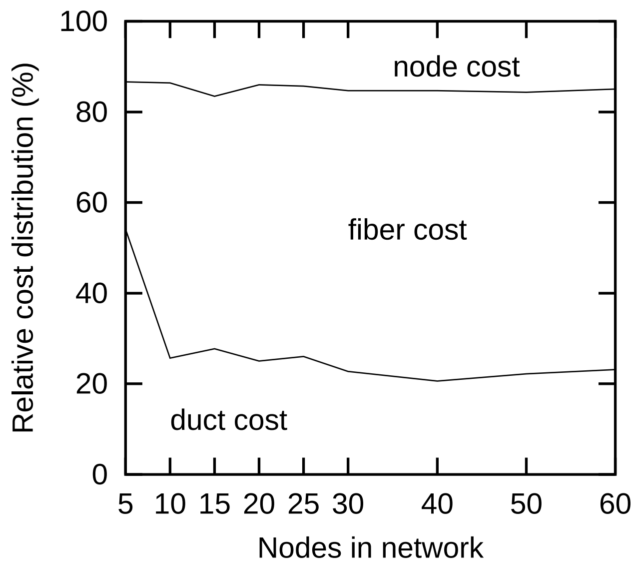

Figure 8.16: Relative equipment cost for networks with shared protection(W=1). $C^{core} = 100$, $C^{port} = 0.5$, $C^{switching} = 0.0005$, and $f = 0.05$.

capacity demand all over the network, it must pay off to many middle sized nodes.

8.7 Future work

This design program has not been fully developed and several improvements can be made.

For larger network the design algorithm becomes very time consuming, but since GAs are inherently parallel (Mitchell (1997)),

whereby parallel execution can be made on parallel computers and clusters. A special scheme for implementing GAs on clusters is proposed by Sena et al. (2001), who also used the TSP as case study.

Due to insufficient time for programming, then the Floyd routing algorithm (Floyd (1962)), which route all routes, has been chosen. This makes it a difficult task to take the switch sizes into acount when routing, and further it makes it

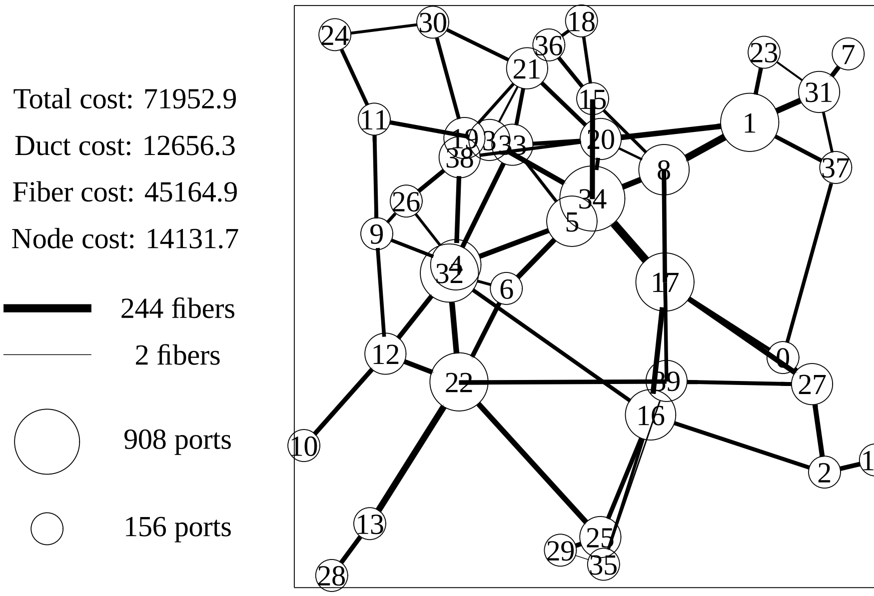

Figure 8.17: Illustration of a 40 node network with no protection. $W = 1, C^{core} = 100, C^{port} = 0.5, C^{switching} = 0.0005$, and $f = 0.05$.

difficult to chose a route with a low fiber utilization in stead of a route where a new fiber might be needed to accomodate the traffic. Using the Dijkstra algorithm, Dijkstra (1959), with marginal cost would solve the problem.

Especially for large networks (more than 30 nodes) much time is spent on ruting in the process of evaluation of networks with protection requirements. For faster evaluation a hierarchy in two or more layers must be introduced. The hierarchy would naturally be coded as part of the genestring. Alternatively routing should be included in the genestring, but this

The results in this chapter are qualitative results, because data points are drawn from one run on one network. Should the quantitative results, which is also of importance for practical purposes, be obtained then more run on more equally sized networks should be performed. That qualitative results is obtained is because of clear trends and that run are performed on many networks of different sizes.

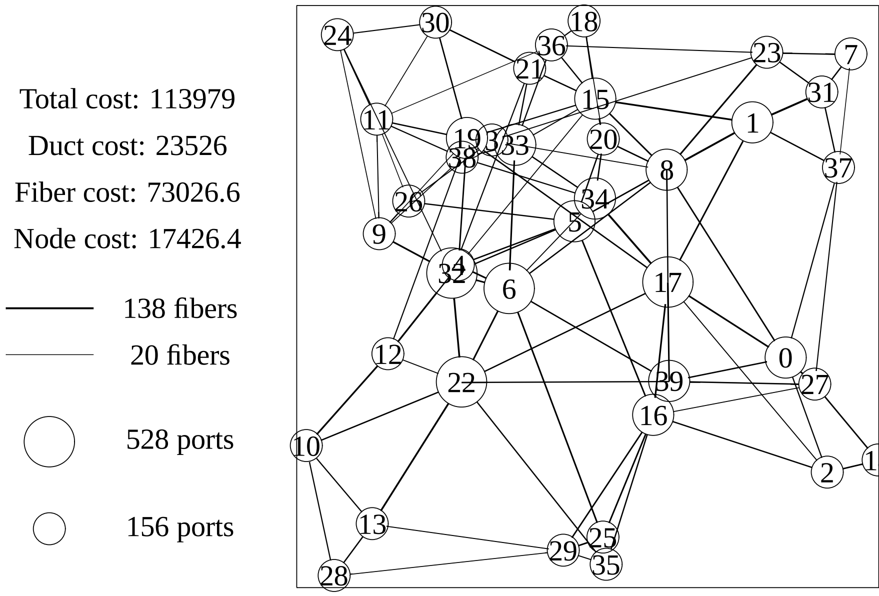

Figure 8.18: Illustration of a 40 node network with shared protection quick. $W = 1$, $C^{core} = 100$, $C^{port} = 0.5$, $C^{switching} = 0.0005$, and $f = 0.05$.

8.8 Conclusion

In this chapter genetic algorithms have been introduced with focus on the application in network design. A genetic algorithm has been tailored for this purpose. Performance is measured by comparision with results from the EXPLAIN project, VPI TransportMaker, and optimal results for theoretical graph problems. The genetic algorithm find solution at optimum or close to optimum for the theoretical graph problems, and significantly better than VPI and EXPLAIN.

Using genetic algorithms for full network design is completely new. The performance shown here is up to 8 times better compared to results from EXPLAIN. I.e. the network optimized from the genetic algorithm have down to $1/8$th of the price.

New comparison of three different protection methods has compared. It was shown that the gain of reusing freed capacity, when a link failure occurs, has a negligible effect, but protection capacity must be shared. It was also shown that the cost spent on protection scales well with the network size.

The drawback of the genetic algorithm is that it is relatively slow on a serial computer, but it is easily paralisable for execution on clusters. And due to the large investment network deployment is the processing power is spent well. Therefore time usage is not an issue.

The conclusion is that genetic algorithm is very promising for full network design. The work performed for this chapter only covers a fraction of the possibilities.

Chapter 9

Conclusion

This thesis has had its focus on wavelength routed optical networks with respect to planning, performance, and management. New knowledge and results have been generated and new methods and algorithms have been implemented. The thesis deals with subjects needed for planning, performance, and management of all-optical network. These subjects have or might have very promising prospects in particular concerning future broadband networking, nationally and regionally.

In short the following results have been achieved:

- Developed computer program for routing and wavelength assignment for static wavelength routed optical networks
- Studied capacity needs verses topology parameters for static wavelength routed optical networks
- Developed simulation computer program for dynamic wavelength routed optical networks
- Studied management, routing methods, etc. for dynamic wavelength routed optical networks
- Proposed and studied a new all-optical network architecture (Synchronous Optical Hierarchy), which is circuit switched, but without some of the problems and with most of the advantages of wavelength routed optical networks and optical packet switched networks

- Proposed and studied analytical methods for determining the blocking probability in dynamic circuit switched networks for fixed routing and alternate fixed routing
- Discussed the possible sources of self similarity in networks with theoretical and experimental validation.
- Co-developed methods and computer program for planning of networks including duct, fiber and switching placement. Studied different network planning strategies.
- Developed alternative method and computer program for planning of networks including duct, fiber and switching placement. Studied relative cost of different protection methods.

Appendix A

Figures from Genetic Algorihtm optimization

A.1 Connectivity and biconnectivity tests

In this section is displayed the figures from the optimization of the connectivity and biconnectivity tests in Section 8.6.1. Only duct costs are included in the network costs. Network sizes range for 6 to 60 nodes.

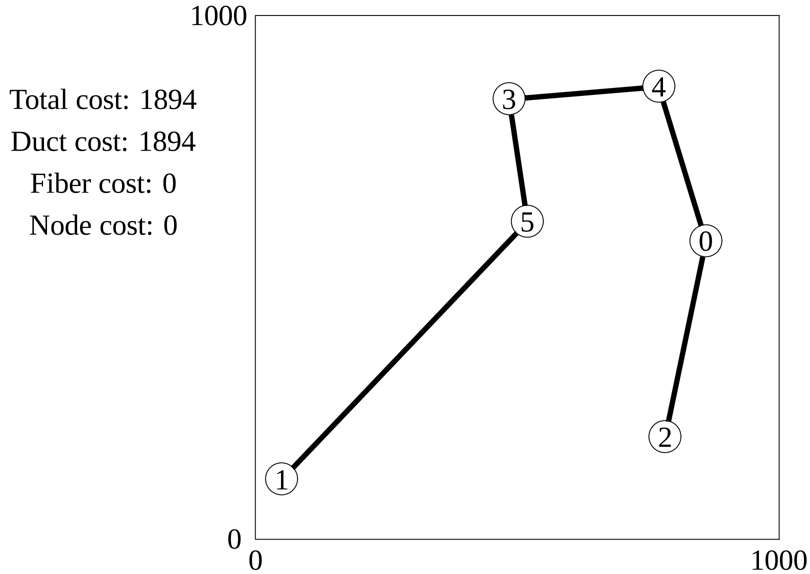

Figure A.1: Design solution for a connected 6 node network.

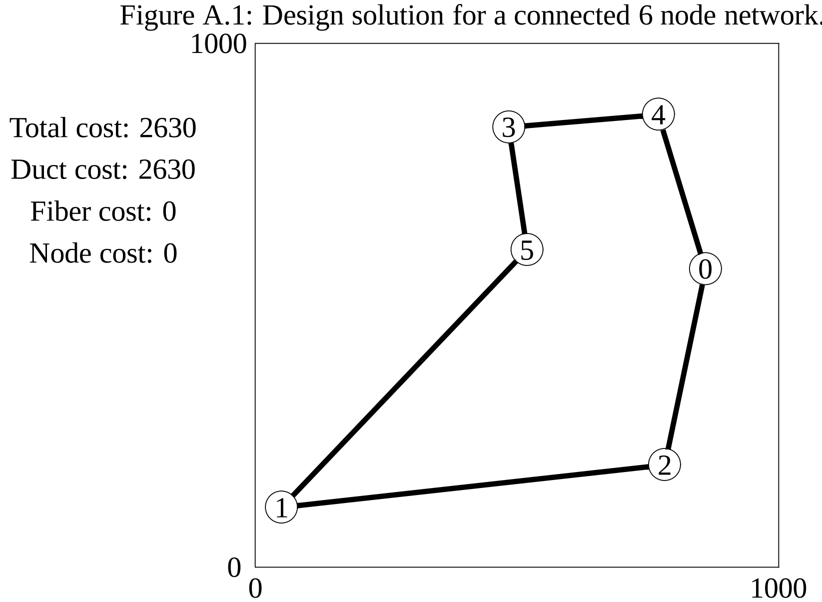

Figure A.2: Design solution for a biconnected 6 node network.

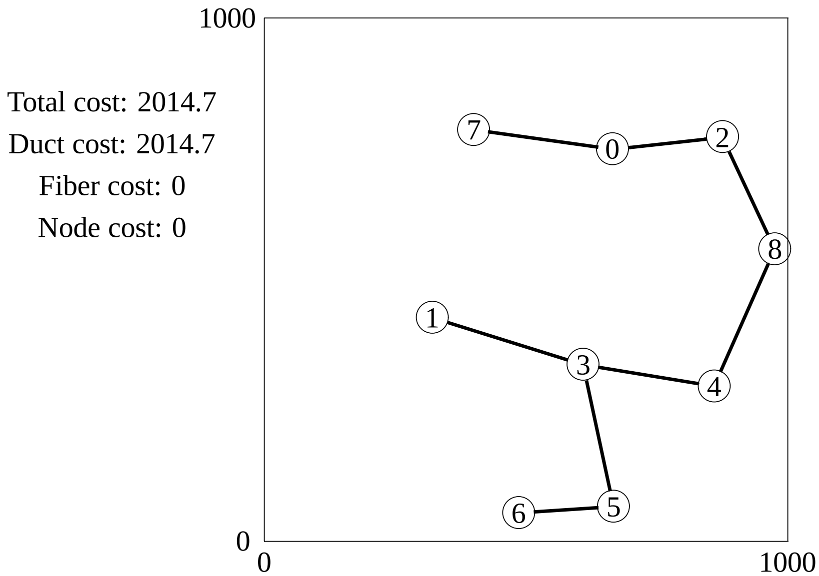

Figure A.3: Design solution for a connected 9 node network.

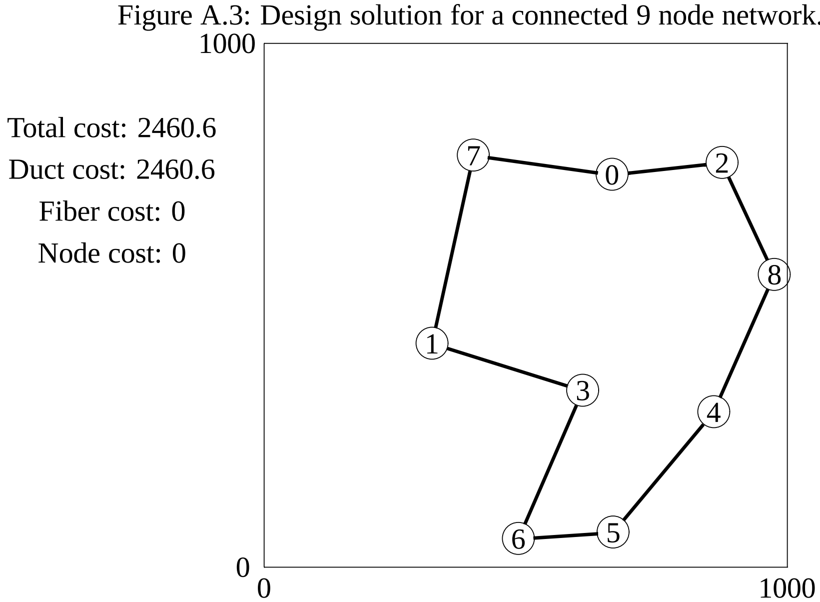

Figure A.4: Design solution for a biconnected 9 node network.

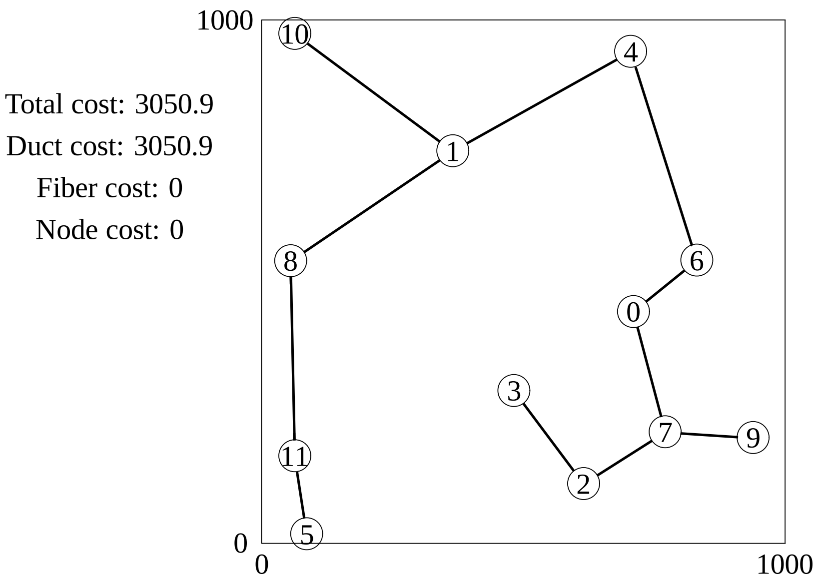

Figure A.5: Design solution for a connected 12 node network.

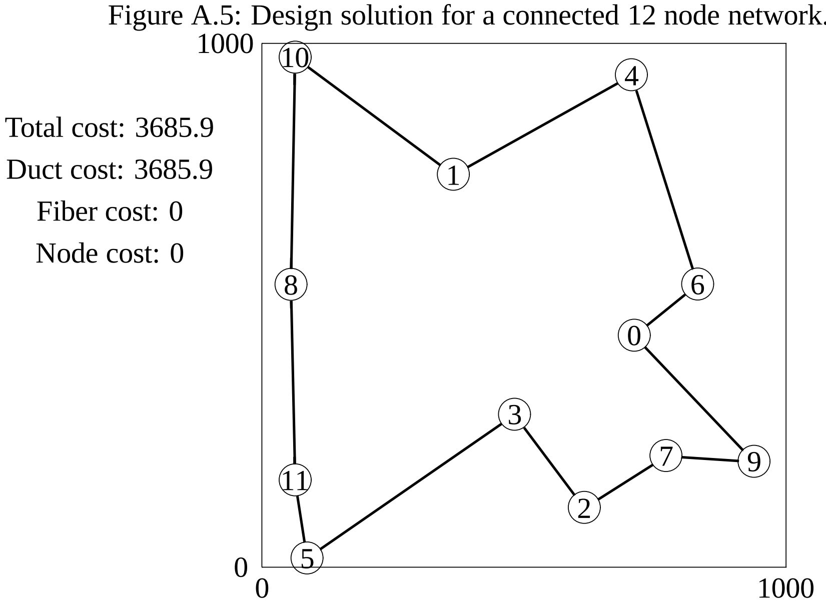

Figure A.6: Design solution for a biconnected 12 node network.

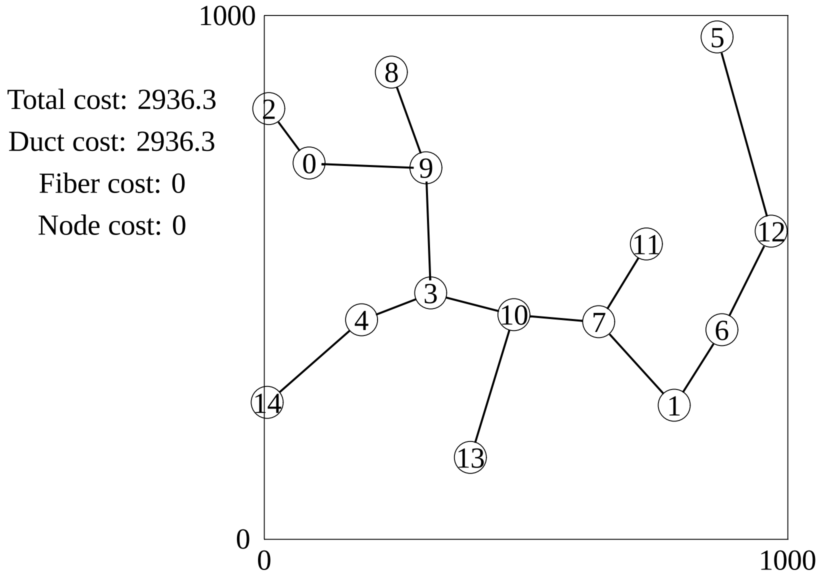

Figure A.7: Design solution for a connected 15 node network.

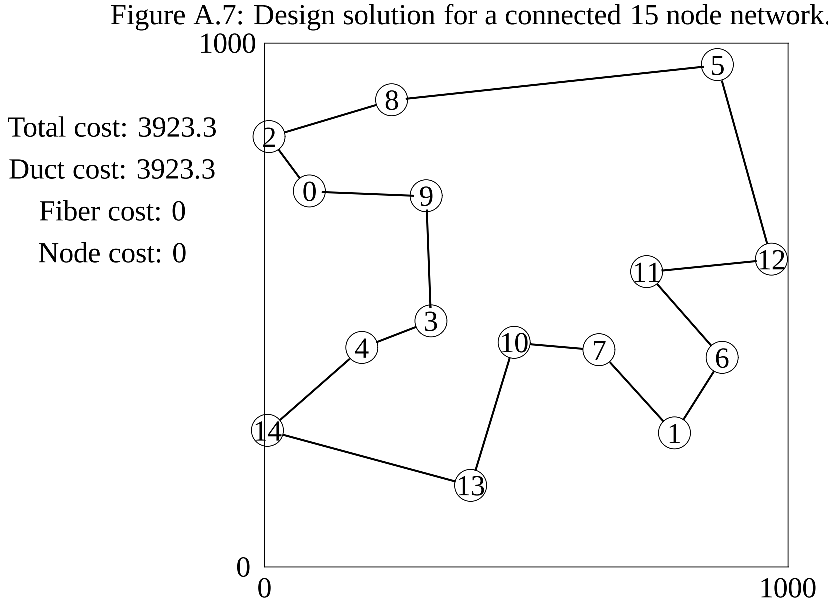

Figure A.8: Design solution for a biconnected 15 node network.

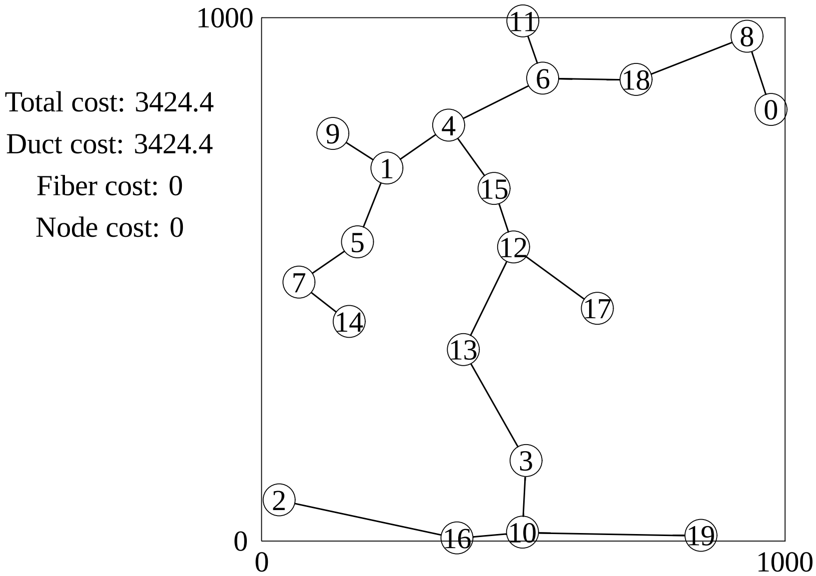

Figure A.9: Design solution for a connected 20 node network.

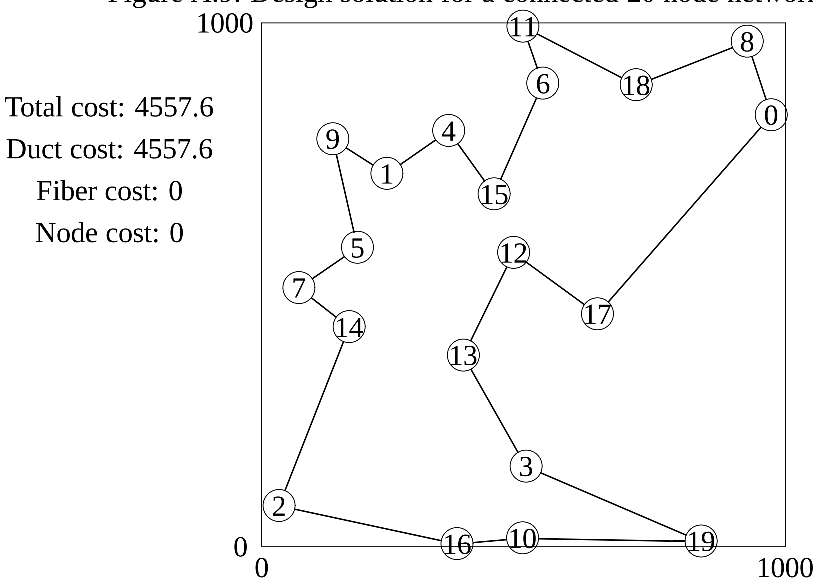

Figure A.10: Design solution for a biconnected 20 node network.

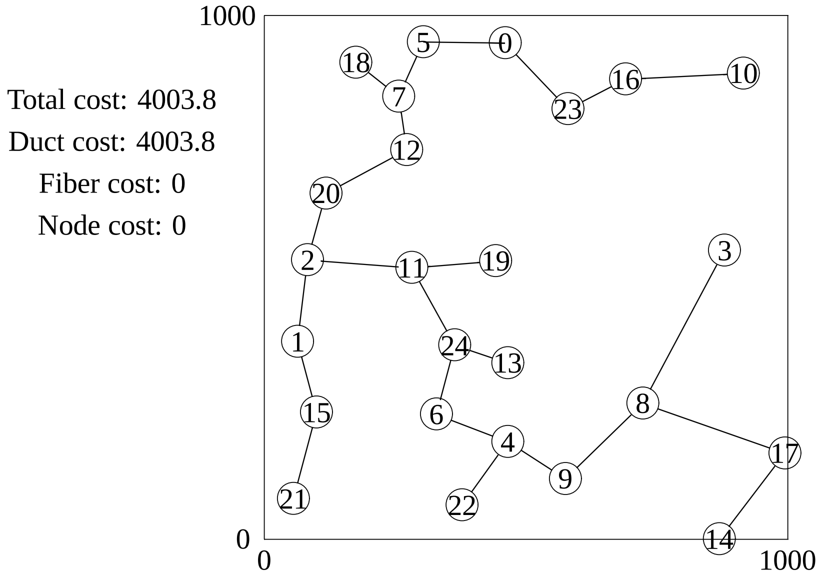

Figure A.11: Design solution for a connected 25 node network.

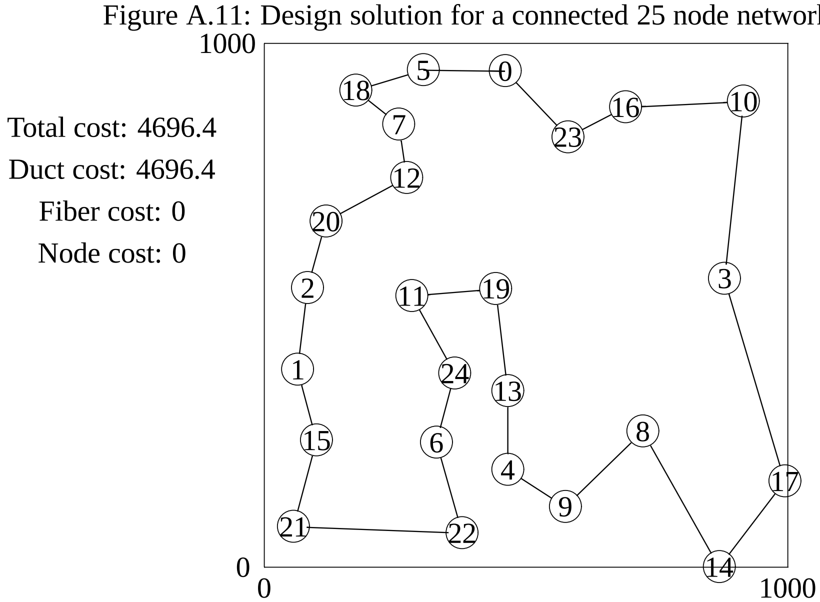

Figure A.12: Design solution for a biconnected 25 node network.

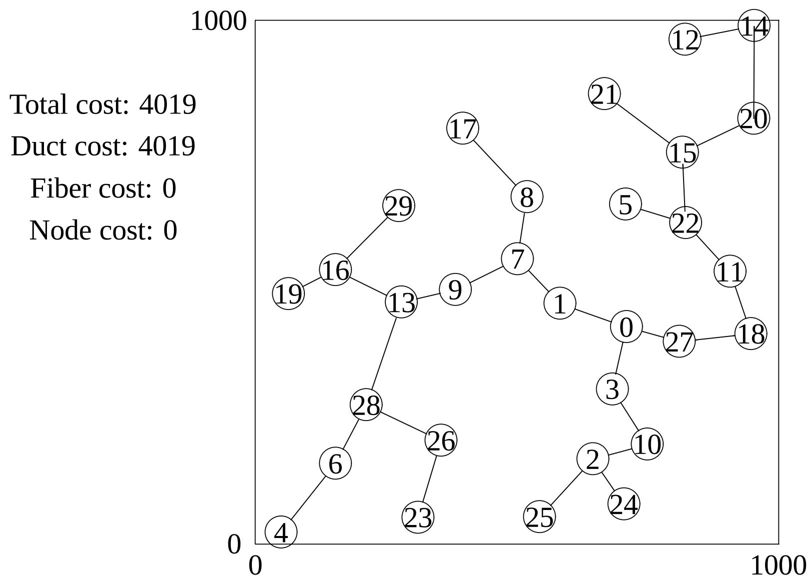

Figure A.13: Design solution for a connected 30 node network.

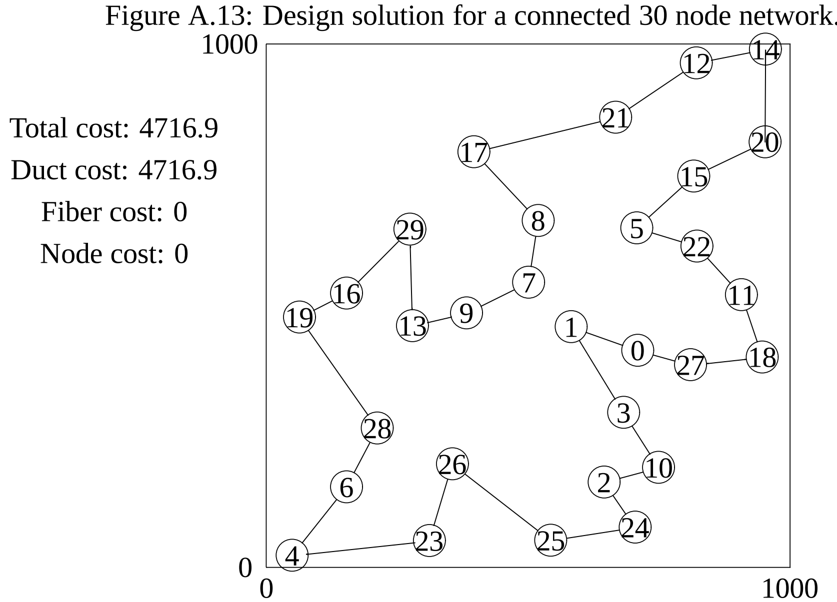

Figure A.14: Design solution for a biconnected 30 node network.

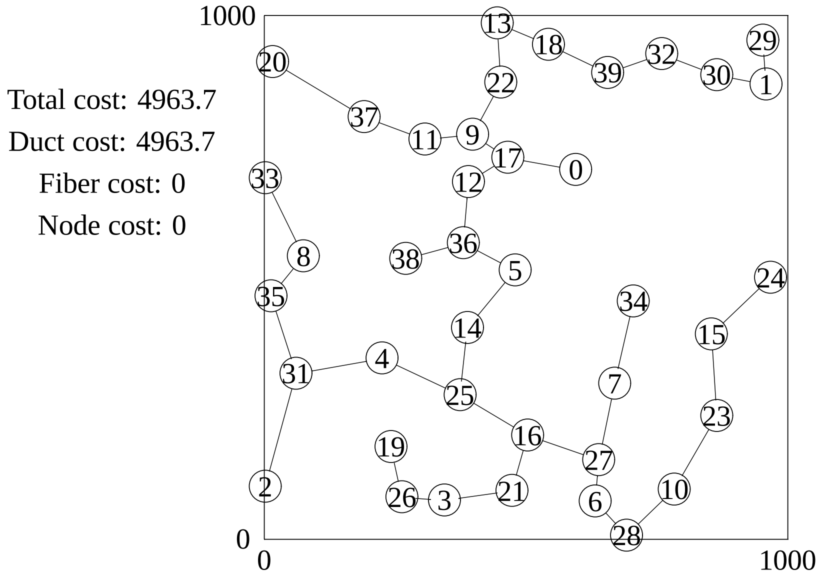

Figure A.15: Design solution for a connected 40 node network.

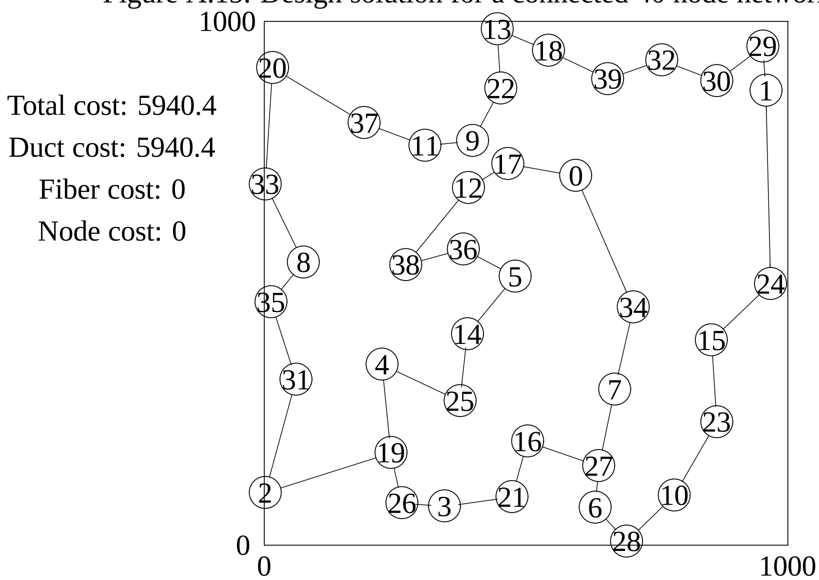

Figure A.16: Design solution for a biconnected 40 node network.

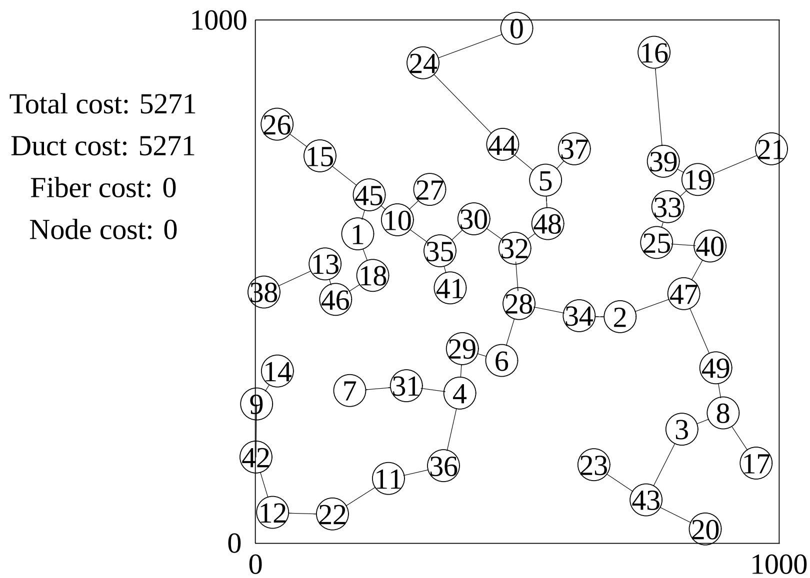

Figure A.17: Design solution for a connected 50 node network.

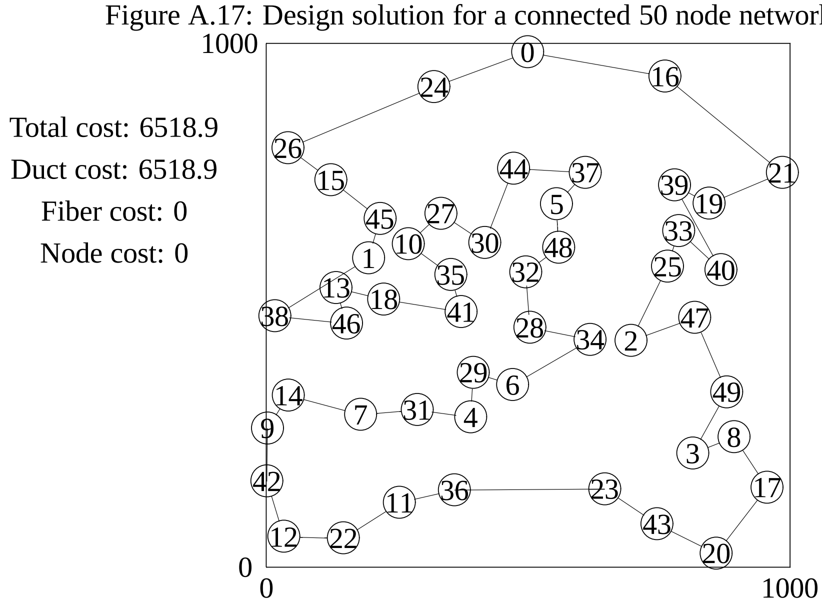

Figure A.18: Design solution for a biconnected 50 node network.

Total cost: 6091.4
Duct cost: 6091.4
Fiber cost: 0
Node cost: 0

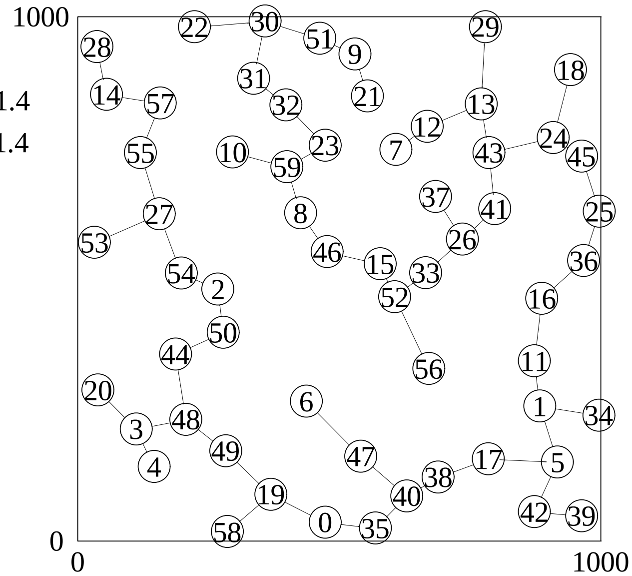

Figure A.19: Design solution for a connected 60 node network.

Total cost: 8316.2
Duct cost: 8316.2
Fiber cost: 0
Node cost: 0

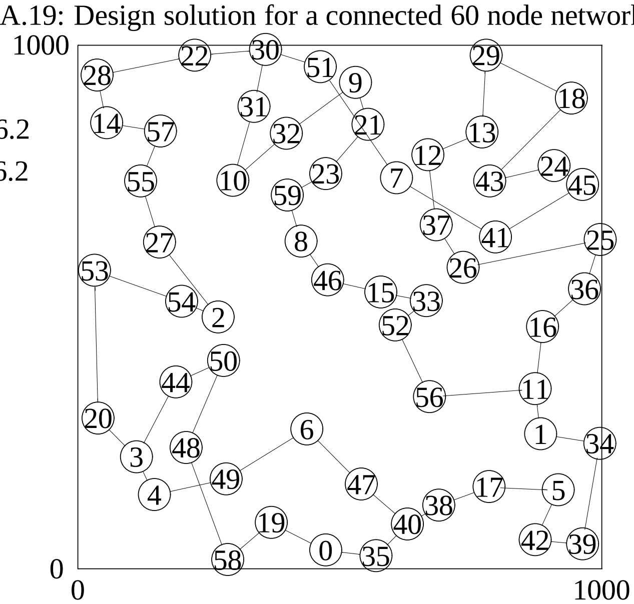

Figure A.20: Design solution for a biconnected 60 node network.

A.2 Full design network - single wavelength

In this section the results from full design network - single wavelength in Section 8.6.2 is displayed. Both duct, fiber, and node costs are include in the network optimization. Figures for nominal design optimization and for limited shared protection optimization are visualized. Network sizes range from 5 to 30 nodes.

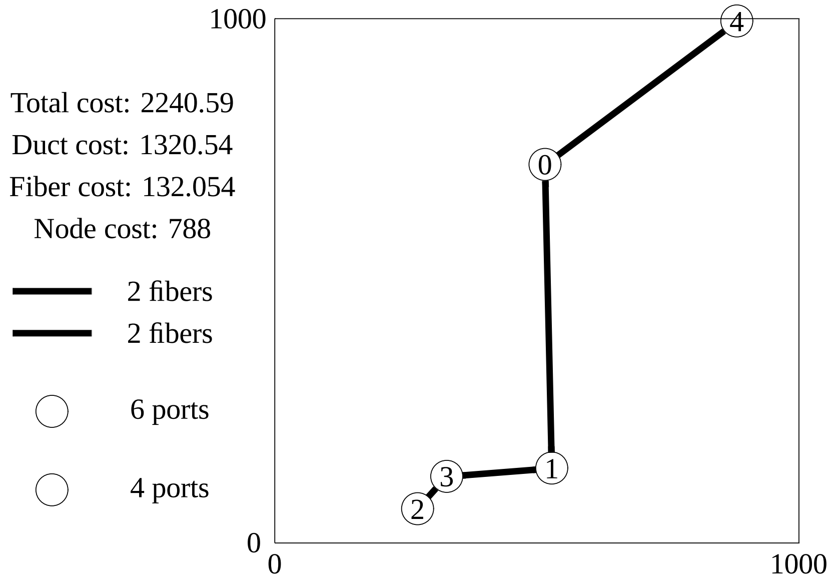

Figure A.21: Nominal design for a 5 node network. $W = 8$, $C^{core} = 100$, $C^{port} = 10$, $C^{switching} = 0.2$, and $f = 0.05$.

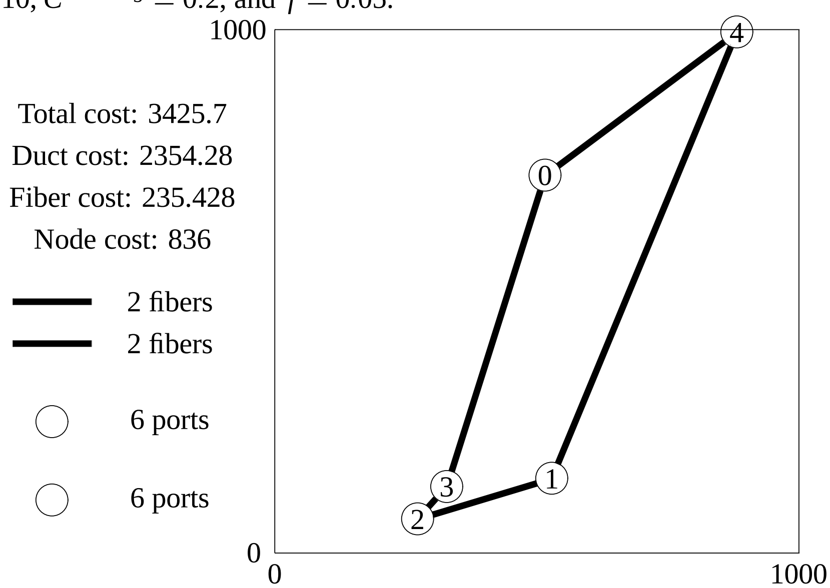

Figure A.22: Shared protection design for a 5 node network. $W = 8$, $C^{core} = 100$, $C^{port} = 10$, $C^{switching} = 0.2$, and $f = 0.05$.

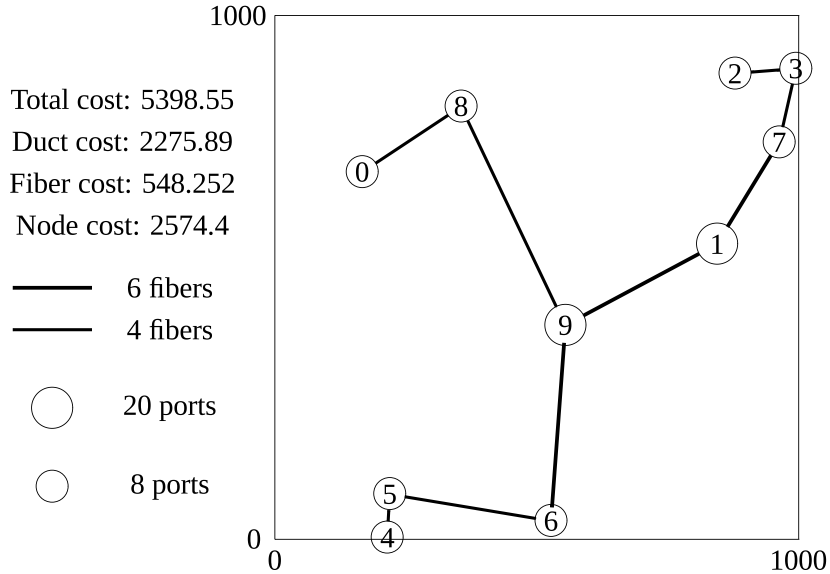

Figure A.23: Nominal design for a 10 node network. $W = 8$, $C^{core} = 100$, $C^{port} = 10$, $C^{switching} = 0.2$, and $f = 0.05$.

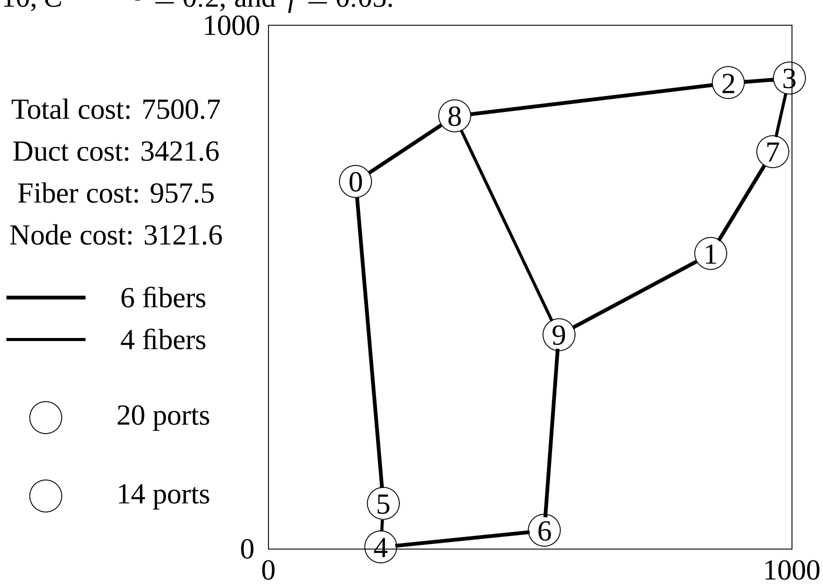

Figure A.24: Shared protection design for a 10 node network. $W = 8$, $C^{core} = 100$, $C^{port} = 10$, $C^{switching} = 0.2$, and $f = 0.05$.

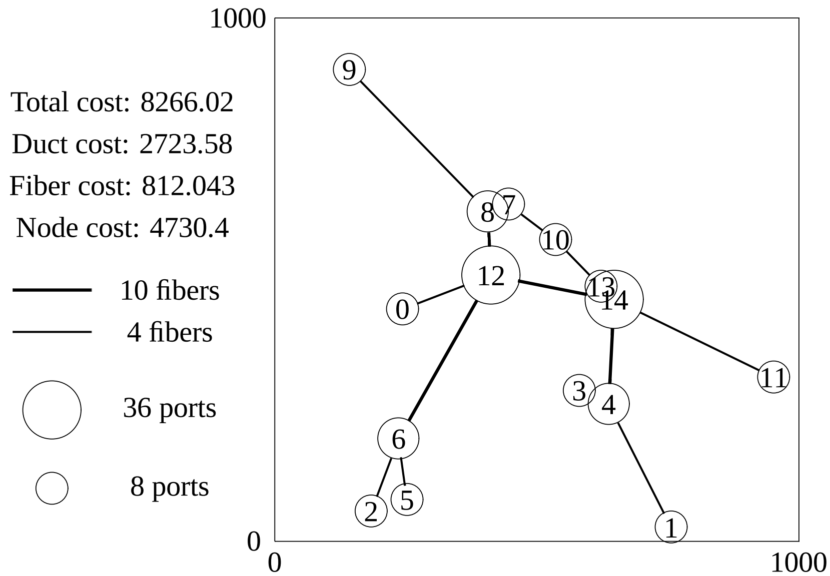

Figure A.25: Nominal design for a 15 node network. $W = 8$, $C^{core} = 100$, $C^{port} = 10$, $C^{switching} = 0.2$, and $f = 0.05$.

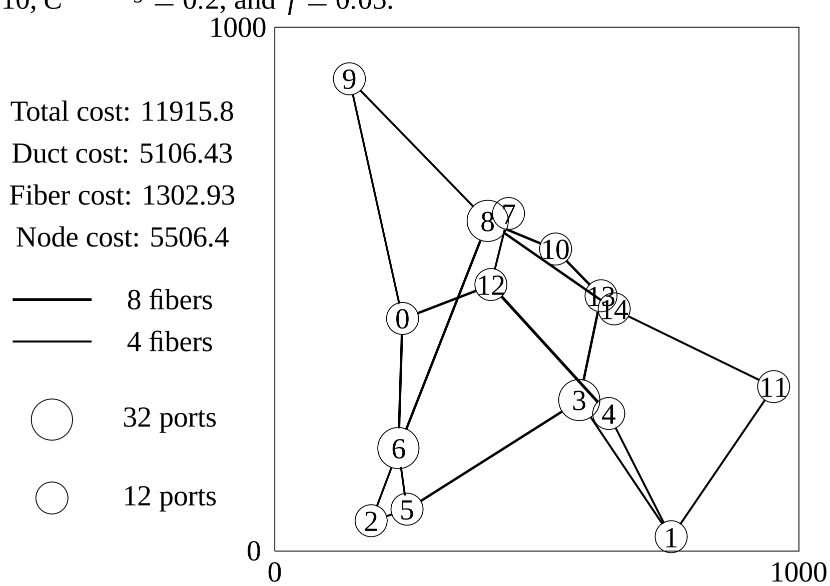

Figure A.26: Nominal design for a 20 node network. $W = 8$, $C^{core} = 100$, $C^{port} = 10$, $C^{switching} = 0.2$, and $f = 0.05$.

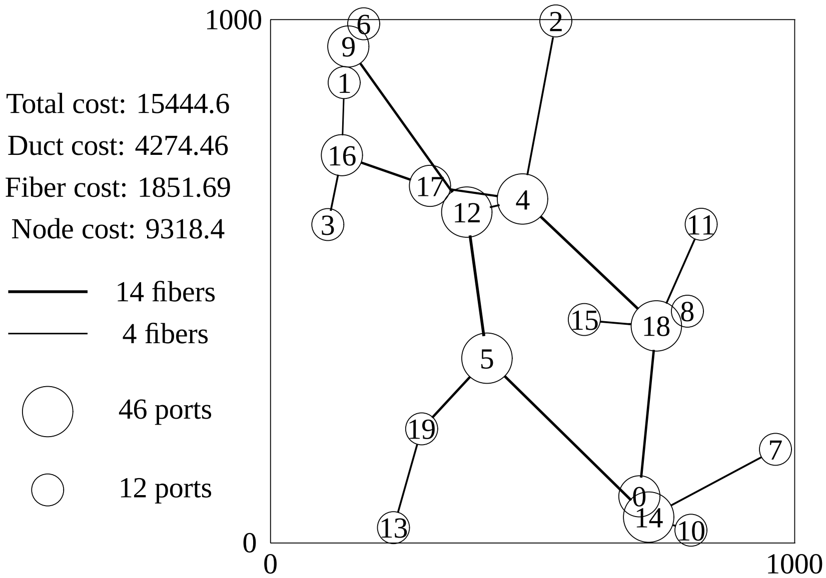

Figure A.27: Nominal design for a 20 node network. $W = 8$, $C^{core} = 100$, $C^{port} = 10$, $C^{switching} = 0.2$, and $f = 0.05$.

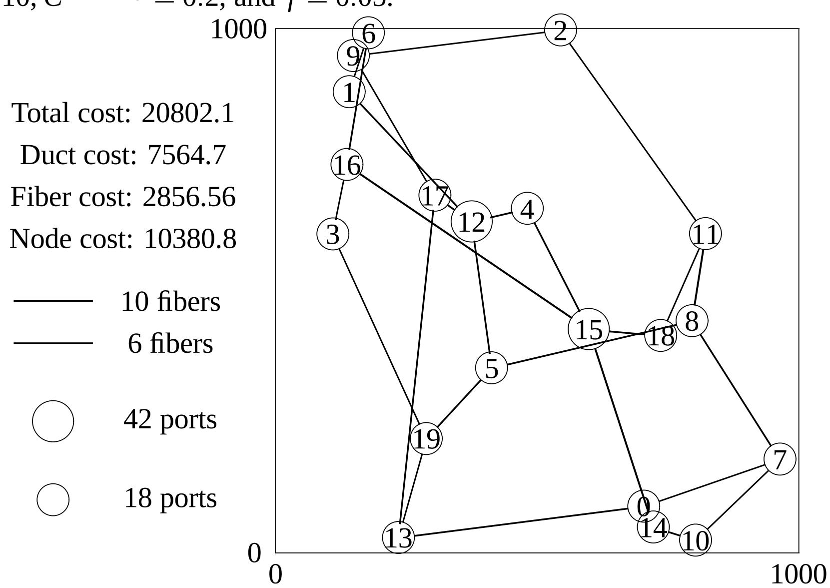

Figure A.28: Shared protection design for a 20 node network. $W = 8$, $C^{core} = 100$, $C^{port} = 10$, $C^{switching} = 0.2$, and $f = 0.05$.

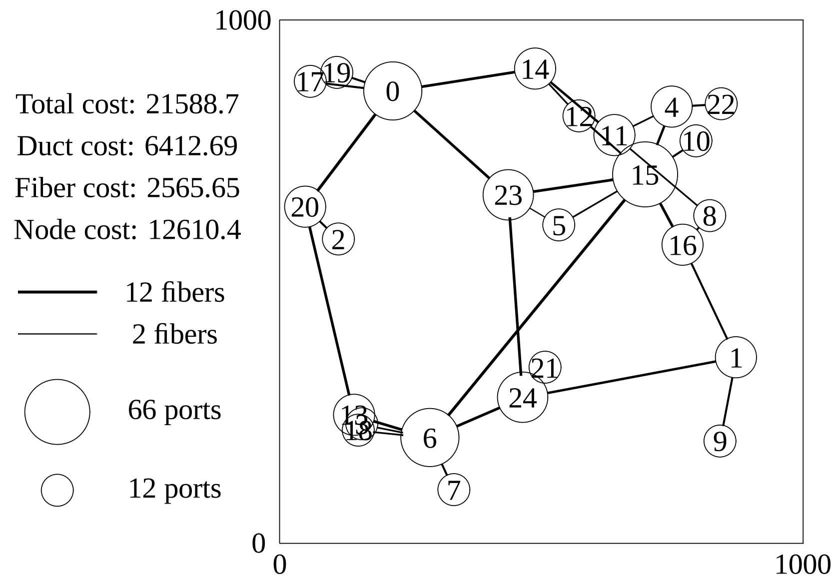

Figure A.29: Nominal design for a 25 node network. $W = 8$, $C^{core} = 100$, $C^{port} = 10$, $C^{switching} = 0.2$, and $f = 0.05$.

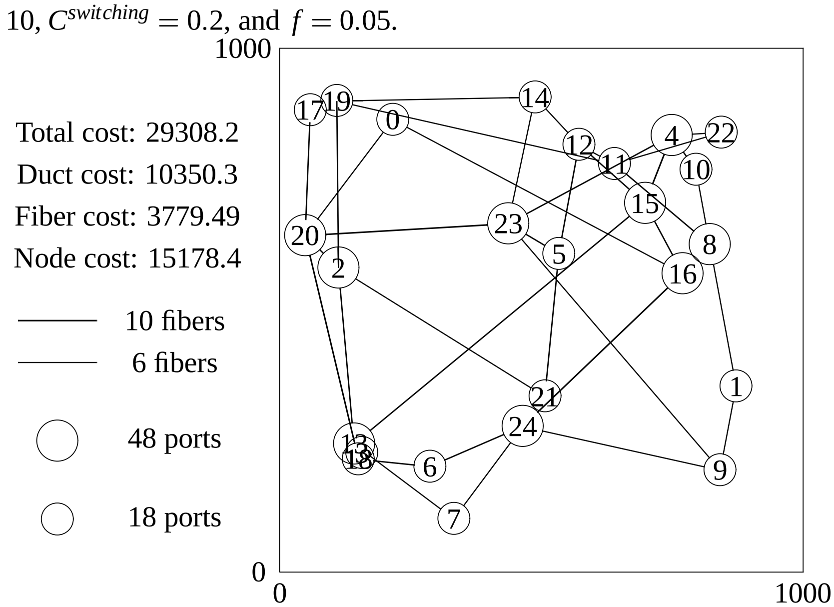

Figure A.30: Shared protection design for a 25 node network. $W = 8$, $C^{core} = 100$, $C^{port} = 10$, $C^{switching} = 0.2$, and $f = 0.05$.

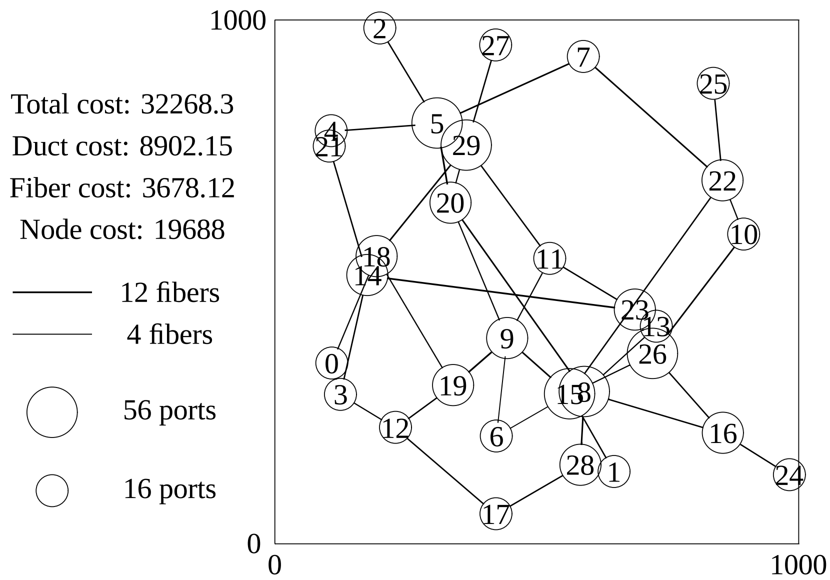

Figure A.31: Nominal design for a 30 node network. $W = 8$, $C^{core} = 100$, $C^{port} = 10$, $C^{switching} = 0.2$, and $f = 0.05$.

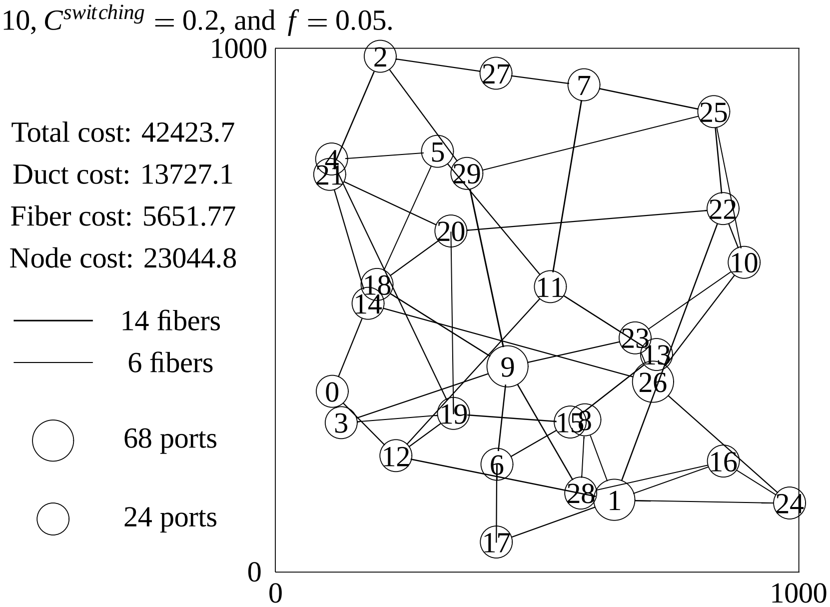

Figure A.32: Shared protection design for a 30 node network. $W = 8$, $C^{core} = 100$, $C^{port} = 10$, $C^{switching} = 0.2$, and $f = 0.05$.

List of Publications

C. Fenger, A.J. Glenstrup, T.J.K. Stidsen, "Greenfield Optimisation of All-Optical Networks for Duct, Fibre and Node Cost", *Technical report*, June 2002.

C. Fenger, A.J. Glenstrup, "Synchronous Optical Hierarchy", submitted to *IEEE/ACM Trans. Networking*, February 2002.

C. Fenger, V.B. Iversen, "Wavelength Conversion by using Multiple Fibres", in Proc. *ECOC 2002*, Copenhagen, Denmark, September 2002.

C. Fenger, R. Tucker, "All-Optical Network Simulations", in Proc. *Networks 2002*, Munich, Germany, June 2002.

C. Fenger, A.J. Glenstrup, "Synchronous Optical Hierarchy", in Proc. *Telecommunication Network and Teletraffic Theory*, pp.255-263, St. Petersburg, Russia, January 2002.

M. Pioro, T.K. Stidsen, A.J. Glenstrup, C. Fenger, H. Christiansen, "Design problems in robust optical networks", in Proc. *Networks 2000*, Toronto, Canada, September 2000.

C. Fenger, "The Self Similarity of Data Traffic", in Proc. *15th Nordic Teletraffic Seminar*, pp.231-242, Lund, Sweden, August 2000.

A.J. Glenstrup, C. Fenger, T.K. Stidsen, "Full Design of Robust Optical Networks", pp. 11-21 in Proc. *15th Nordic Teletraffic Seminar*, Lund, Sweden, August 2000.

C. Fenger, E. Limal, U. Gliese, C.J. Mahon, "Statistical Study of the Correlation Between Topology and Wavelength Usage in Optical Networks With and

Without Conversion", In Lecture Notes in Computer Science, 2000, 1815, pp.168-175, *Networking2000*, Paris, France. May 2000

C. Fenger, E. Limal, U. Gliese, "Statistical Study of the Influence of Topology on Wavelength Usage in WDM Networks", in Proc. *OFC2000, Optical Fiber Conference*, pp.171-173, Baltimore, Maryland, USA, March 2000.

Bibliography

Alok Aggarwal, Amotz Bar-Noy, Don Coppersmith, Rajiv Ramaswami, Baruch Schieber, and Madhu Sudan. Efficient routing in optical networks. *Journal of the ACM*, 46(6):973–1001, November 1996.

AixCom. COMPOSIS®, 2002. URL `http://www.aixcom.com`.

M.F. Arlitt and C.L. Williamson. Internet web servers: Workload characterization and performance implications. *IEEE/ACM TRANSACTIONS ON NETWORKING*, 5(5), October 1997.

D. Awduche and Y. Rekhter. Multiprotocol lambda switching: Combining mpls traffic engineering control with optical crossconnects. *IEEE Comm. Mag.*, March 2001.

P. Bak, M. Paczuski, and M. Shubik. Price variations in a stock market with many agents. *Physica A*, 246:430–53, 1997.

P. Bak, C. Tang, and K. Wiesenfeld. Self-organized criticality. *Phys. Rev. A*, 38: 364–74, 1988.

Stefano Baroni and Polina Bayvel. Wavelength requirements in arbitrarily connected wavelength-routed optical networks. *J. Lightwave Tech.*, 15(2):242–251, 1997.

Stefano Baroni, Polina Bayvel, Richard J. Gibbens, and Steven K. Korotky. Analysis and design of resilient multifiber wavelength-routed optical transport networks. *J. Lightwave Tech.*, 17(5):743–58, May 1999.

R. Bellman. On a routing problem. *Q. Appl. Math*, 16:87–90, 1958.

J. Beran, R. Sherman, M.S. Taqqu, and W. Willinger. Variable-bit-rate video traffic and long-range dependence. *IEEE TRANSACTIONS ON COMMUNICATIONS*, 43(2/3/4), Feb./Mar./Apr. 1995.

A. Bianco, S. Binetti, P.N. Caponio, A. Hill, E. Leonardi, M. Listanti, F. Neri, and R. Sabella. Dimensioning of a single layer optical platform based on the 'switchless' concept for large scale networks. In *Proc. of the IEEE Lasers and Electro-Optics Society Annual Meeting (LEOS'99)*, volume 2, pages 521–522. IEEE, 1999.

A. Birman. Computing approximate blocking probabilities for a class of all-optical networks. *IEEE J. Select. Areas in Commun.*, 14:5, June 1996.

D. Brelaz. New methods to color the vertices of a graph. *Communications of the Association for Computing Machinery*, pages 251–256, 1979.

Anthony Brooke, David Kendrick, and Meeraus Alexander. *GAMS, A Users Guide*. Boyd & Fraser Publishing Company, 1992.

Michel W. Chbat, Emmanuel Grard, Luc Berthelon, Amaury Jourdan, Philippe A. Perrier, Alain Leclert, B. Landousies, A. Ramdane, Noel Parnis, Edwin V. Jones, Emmanuel Limal, Henrik N. Poulsen, R.J.S. Pedersen, N. Flaaronning, Danny Vercauteren, Mario Puelo, Ernesto Ciaramella, Giuseppe Marone, R. Hess, H. Melchior, Wim Van Parys, Piet M. Demeester, P. J. Gødsvang, Torodd Olsen, and Dag R. Hjelme. Toward wide-scale all-optical transparent networking: The ACTS optical pan-european network (OPEN) project. *IEEE J. Selected Areas in Comm.*, 16(7), September 1998.

I. Chlamtac, A. Ganz, and G. Karmi. Lightpath communications: An approach to high bandwidth optical wan's. *IEEE Trans. Commun.*, 40(7), July 1992.

Imrich Chlamtac, Aura Ganz, and Gadi Karmi. Purely optical networks for terabit communication. volume 3, pages 887–96. IEEE Comp. Soc. Press, 1989.

Hsinghua Chou, G. Premkumar, and Chao-Hsien Chu. Genetic algorithms for communications network design - an empirical study of the factors that influence performance. *IEEE Transactions on Evolutionary Computation*, 5(3): 236–49, June 2001.

Tibor Cinkler. ILP formulation of grooming over wavelength routing with protection. In A. Jukan, editor, *Conf. on Optical Network Design and Modelling (ONDM 2001)*, pages 25–47. Kluwer Academic, 2002.

Tibor Cinkler and Péter Laborczi. Joint routing and bandwidth allocation for protected elastic traffic. In *Networks 2002, 10th International Telecommunication Network Strategy and Planning Symposium*, pages 23–30, Munich, Germany, June 2002. VDE Verlag.

Tibor Cinkler, Dániel Marx, Claus Popp Larsen, and Dániel Fogaras. Heuristic algorithms for joint configuration of the optical and electrical layer in multi-hop wavelength routing networks. *INFOCOM 2000*, 2:1000–1009, March 2000.

D.R. Cox. *Statistics: an Appraisal, Long range dependence: A review*, pages 55–74. The Iowa State University Press, Ames IA, 1984.

M.E. Crovella and A. Bestavros. Self similarity in world wide web traffic: Evidence and possible causes. *IEEE/ACM TRANSACTIONS ON NETWORKING*, 5(5), December 1997.

M. Cuppini. A genetic algorithm for channel assignment problems. *European Transactions on Telecommunications and Related Technologies*, 5(2):285–94, 1994.

Sebastian Cwilich, Mei Deng, David F. Lynch, S.J. Phillips, and J.R. Westbrook. Algorithms for restoration planning in a telecommunications network. *LNCS*, 1619:194–209, 1999.

K. DeJong. *An analysis of the behavior of a class of genetic adaptive systems*. PhD thesis, University of Michigan, Ann Arbor, 1975.

B. Dengiz, F. Altiparmak, and A.E. Smith. Efficient optimization of all-terminal reliable networks, using an evolutionary approach. *IEEE Transactions on Reliability*, 46(1):18–26, March 1997a.

B. Dengiz, F. Altiparmak, and A.E. Smith. Local search genetic algorithm for optimal design of reliable networks. *IEEE Transactions on Evolutionary Computation*, 1(3):197–88, September 1997b.

E.W. Dijkstra. A note on two problems in connection with graphs. *Numer. Math.*, 1:269–271, 1959.

Bharat Doshi, Subrahmanyam Dravida, P. Harshavardhana, Oded Hauser, and Yfei Wang. Optical network design and restoration. *Bell Labs Technical Journal*, January–March 1999.

Rudra Dutta and George N. Rouskas. A survey of virtual topology design algorithms for wavelength routed optical networks. Technical Report TR-99-06, Dept. of Comp. Science, North Carolina State University, Raleigh, NC 27695-7534, May 1999.

A.K. Erlang. Løsning af nogle problemer fra sandsynlighedsregningen af betydning for de automatiske telefoncentraler. *Elektroteknikeren*, 13, 1917.

EXPLAIN, 1998–. URL `http://www.explain.dk`.

J. Feder. *Fractals*. Plemum Press, 1988.

C. Fenger, A.J. Glenstrup, Stidsen, and T.J.K. Greenfield optimisation of all-optical networks for duct, fibre and node cost. Technical report, Explain, June 2002.

Christian Fenger and Arne J. Glenstrup. Synchronous optical hierarchy. *IEEE/ACM Trans. Networing*, February 2002a. Submited.

Christian Fenger and Arne John Glenstrup. Synchronous optical hierarchy. In *Int. Seminar on Telecommunication Networks and Teletraffic Theory*, St. Petersburg, January–February 2002b.

Christian Fenger, Emmanuel Limal, and Ulrik Gliese. Statistical study of the influence of topology on wavelength usage in wdm networks. In *OFC2000, Optical Fiber Conference*, pages 171–173, Maryland, Baltimore, USA, March 2000a.

Christian Fenger, Emmanuel Limal, Ulrik Gliese, and Cathal J. Mahon. Statistical study of the correlation between topology and wavelength usage in optical networks with and without conversion. In *Networking 2000*, volume 1815 of *LNCS*, pages 168–175, Paris, France, May 2000b. Springer-Verlag.

Christian Fenger and Rodney Tucker. All-optical network simulations. In *Networks*, June 2002.

Thomas Feo and Mauricio Resende. Greedy randomized adaptive search procedures. *Journal of Global Optimization*, 6:109–133, 1995.

FibreSystemsEurope. Optical switching: unravelling the myths about mems. June 2002.

Matteo Fischetti, Giuseppe Lancia, and Paolo Serafini. Exact algorithms forminimum routing cost trees. *Networks*, 39(3):161–73, March 2002.

R.W. Floyd. Algorithm 97 shortest path. *Communications of the ACM*, 5:345, 1962.

L.R. Ford. Network flow theory. In *Technical Report P-923*, Rand Corp., Santa Monica, CA, USA, 1956.

Piero Gambini, Monique Renaud, Christian Guillemot, Franco Callegati, Ivan Andonovic, Bruno Bostica, Dominique Chiaroni, Giorgio Corazza, Soeren Lykke Danielsen, Philippe Gravey, Peter Bukhave Hansen, Michel Henry, Christopher Janz, Allan Kloch, Roger Krähenbühl, Carla Raffaelli, Michael Schilling, Anne Talneau, and Libero Zucchelli. Transparent optical packet switching: Network architecture and demonstrators in the KEOPS project. *IEEE J. Selected Areas in Comm.*, 16(7), September 1998.

M.R. Garay and D.S. Johnson. *Computers and intractability. A guide to the theory of NP-completeness*. Series of books in the mathematical sciences. Freeman, San Fransisco, Calif., 1979a.

M.R. Garay and D.S. Johnson. *Computers andInteractability: A Guide to the Theory of NP-completenesss*. Freeman, New York, 1979b.

M. Garnot and P.A. Perrier. Planning of WDM networks: Methods, routing node modeling and applications. In *Proc. of the Global Telecomm. Conf. (GLOBECOM'98)*, volume 1, pages 351–355. IEEE, November 1998.

Mathieu Garnot and F. Masetti. Dimensioning and design of the WDM optical layer in transport networks. volume 3230, pages 244–252. Proc. of SPIE, 1997.

Arne John Glenstrup, Christian Fenger, and Thomas Jacob Kjær Stidsen. Full design of robust optical networks. In Johan M. Karlsson, Ulf Körner, and Christian Nyberg, editors, *15th Nordic Teletraffic Seminar (NTS–15)*. Lund Inst. of Technology, Lund U., August 2000.

D.E. Goldberg. *Genetic Algorithms in Search, Optimization, and Machine Learning*. Addison-Wesley, Reading, MA, 1989.

C.M. Grinstead and J.L. Snell. *Introduction to Probability*. online book available at http://www.dartmouth.edu/˜chance/.

Christian Guillemot, Monique Renaud, Piero Gambini, Christopher Janz, Ivan Andonovic, Raimond Bauknecht, Bruno Bostica, Marco Burzio, Franco Callegati, Maurizio Casoni, Dominique Chiaroni, Fabrice Clerot, Soren Lykke Danielsen, Francios Dorgeuille, Arnaud Dupas, A. Franzen, Peter Bukhave Hansen, David K. Hunter, Allan Kloch, R. Krähenbühl, Bruno Lavigne, Alain Le Corre, Carla Raffaelli, Michael Schilling, Jean-Claude Simon, and Libero Zucchelli. Transparent optical packet switching: The european ACTS KEOPS project approach. *J. Lightwave Tech.*, 16(12):2117–2134, 1998.

E.L. Hahne and R.G. Gallager. Round robin scheduling for fair flow control in data communication networks. In *IEEE International Conference on Communications '86. ICC '86*, pages 103–7, 1986.

H. Harai, M. Murata, and H. Miyahara. Performance of alternate routing methods in all-optical switching networks. In *IEEE Infocom*, pages 516–524, 1997.

Andrew G. Hart and Servet Martínez. Sequential iteration of the erlang fixed-point equations. *Information Processing Letters*, 81(6):319–325, 2002.

D.R. Hjelme and S.E. Andersen. Designing physical topologies for wavelength-routed all-optical networks. In G. de Marchis and R. Sabella, editors, *Conf. on Optical Network Design and Modelling (ONDM'98)*, pages 167–174. Kluwer Academic, 1999.

J.H. Holland. *Adaptation in Natural and Artificial Systems*. The University of Michigan Press, Ann Arbor, Michigan, 1975.

Hong Huang and J. Copeland. Hamiltonian cycle protection: A novel approach to mesh WDM optical network protection. In *IEEE Workshop on High Performance Switching and Routing*, pages 31–35. IEEE, 2001.

Nen-Fu Huang, Guan-Hsiung Liaw, and Chuan-Pwu Wang. A novel all-optical transport network with time-shared wavelength channels. *IEEE J. Selected Areas in Comm.*, 18(10):1863–1875, October 2000.

David K. Hunter and Ivan Andonovic. Approaches to optical internet packet switching. *IEEE Comm. Mag.*, 38(9):116–122, September 2000.

David K. Hunter, Meow C. Chia, and Ivan Andonovic. Buffering in optical packet switches. *J. Lightwave Tech.*, 16(12):2081–2094, 1998a.

David K. Hunter, W. David Cornwell, Tim H. Gilfedder, Andre Franzen, and Ivan Andonovic. SLOB: a switch with large optical buffers for packet switching. *J. Lightwave Tech.*, 16(10):1725–1736, 1998b.

David K. Hunter, M.H.M. Nizam, Meow C. Chia, Ivan Andonovic, K.M. Guild, A. Tzanakaki, M.J. O'Mahony, L.D. Bainbridge, M.F.C. Stephens, R.V. Penty, and I.H. White. WASPNET: a wavelength switched packet network. *IEEE Comm. Mag.*, 37(3):120–129, 1999.

Esa Hyytia and Jorma Virtamo. Wavelength assignment and routing in wdm networks. In *Nordic Teletraffic Seminar 14*, August 1998.

ILOG Cooperation. ILOG CPLEX 7.0, users manual, August 2000.

Rong-Hong Jan, Fung-Jen Hwang, and Sheng-Tzong Cheng. Topological optimization of a communication network subject to a reliability constraint. *IEEE T. on Reliability*, 42(1):63–70, March 1993.

J.L. Wang J.L. Jerkins. A measurement analysis of atm cell-level aggregate traffic. In *IEEE GLOBECOM '97*, 1997.

Rajgopal Kannan, Radim Bartos, Kyungsook Y. Lee, and Harry F. Jordan. STWnet: A high bandwidth space-time-wavelength multiplexed optical switching network. In *INFOCOM 1997*, volume 2, pages 777–784. IEEE, 1997.

A. Kapsalis, V.J. Rayward-Smith, and G.D. Smith. Solving the graphical steiner tree problem using genetic algorithms. *Journal of the Operational Research Society*, 44(4):397–406, 1993.

E. Karasan and E. Ayanoglu. Effects of wavelength routing and selection algorithms on wavelength conversion gain in wdm networks. *IEEE/ACM Trans. Networking*, 6(2):186–196, April 1998.

M.G.H. Katevenis. Fast switching and fair control of congested flow in broadband networks. *IEEE Journal on Selected Areas in Communications*, SAC-5 (8):1315–26, 1987.

B.R. Katz. Statistical performance analysis of switched communication networks. In *5th ITC*, New York, USA, 1967.

F.P. Kelly, A.K. Maulloo, and D.K.H. Tan. Rate control for communication networks: shadow prices, proportional fairness and stability. *Journal of the Operational Research Society*, 49(3):237–52, 1998.

Frank P. Kelly. Blocking probabilities in large circuit-switched networks. *Adv. in Appl. Prob.*, 18:473–505, 1986.

Aaron Kershenbaum, Parviz Kermani, and George A. Grover. MENTOR: An algorithm for mesh network topological optimization and routing. *IEEE T. on Comm.*, 39(4):503–513, April 1991.

Milan Kovačević and Anthony Acampora. Benefits of wavelength translation in all-optical networks. *IEEE J. Select. Areas Commun.*, 14(5):868–880, June 1996.

Chun-Ming Lee, Chi-Chun R. Hui, Frank F.-K. Tong, and Peter T.-S. Yum. Network dimensioning in WDM-based all-optical networks. In *Proc. of the Global Telecomm. Conf. (GLOBECOM'98)*, volume 1, pages 328–333. IEEE, 1998a.

K.-C. Lee and V.O.K. Li. A wavelength-convertible optical network. *J. Lightwave Technol.*, 5/6, March/June 1993.

Kyungsik Lee, Kyungchul Park, Sungsoo Park, and Heesang Lee. Economic spare capacity planning for DCS mesh-restorable networks. *European J. Operational Research*, 110(1):63–75, 1998b.

Taehan Lee, Kyungsik Lee, and Sungsoo Park. Optimal routing and wavelength assignment in WDM ring networks. *IEEE J. Selected Areas in Comm.*, 18(10): 2146–2154, October 2000.

W.E. Leland and T.J. Ott. Unix process behavior and load balancing among loosely-coupled computers. In *Teletraffic Analysis and Computer Performance Evaluation. Proceedings of the International Seminar*, pages 191–208, 1986.

W.E Leland, W. Willinger, M.S. Taqqu, and D.V Wilson. On the self similar nature of ethernet traffic (extended version). *IEEE/ACM TRANSACTIONS ON NETWORKING*, 2(1):1–15, 1994.

Lightscape Networks. LightPlan^{TM}, 2002. URL `http://www.lightscapenetworks.com`.

Marco Listanti and Vincenzo Eramo. Architectural and technological issues for future optical internet networks. *IEEE Comm. Mag.*, pages 82–92, September 2000.

B.B. Mandelbrot. Long-run linearity, locally gaussian processes, h-spectra and infinite variances. *Int. Economic Rev.*, 10:82–113, 1969.

S. Maruster, L. Maruster, D. Kalpic, and V.H. Dobric. The stability of steepest descend methods for systems of nonlinear equations. In *ITI'99. Proceedings of the 21st International Conference on Information Technology Interfaces*, volume 2, pages 359–64, 2001.

K.S. Meier-Hellstern, P.E. Wirth, Y.L. Yan, and D.A. Hoeflin. Traffic models for isdn data users: office automation application. In *Teletraffic and Datatraffic in a Period of Change. ITC-13. Proceedings of the Thirteenth International Teletraffic Congress*, pages 167–72, 1991.

Zbigniew Michalewicz. *Genetic Algorithms + Data Structures = Evolution Programs*. Springer, Berlin, 3 edition, 1996.

T.M. Mitchell. *Machine Learning*. Series in CS, McGraw-Hill, 1997.

G. Mohan, C. Siva Ram Murthy, and Arun K. Somani. Efficient algorithms for routing dependable connections in WDM optical networks. *IEEE/ACM Trans. Networking*, 9(5):553–566, October 2001.

A. Mokhtar and M. Aziõglu. Adaptive wavelength routing in all-optical networks. *IEEE/ACM Trans. Networking*, 6(2):197–206, April 1998.

Naohide Nagatsu, Satoru Okamoto, and Ken-ichi Sato. Optical path cross-connect system scale evaluation using path accommodation design for restricted wavelength multiplexing. *IEEE J. Selected Areas in Comm.*, 14(5):893–902, June 1996.

S.C. Narula and C.A. Ho. Degree-constrained minimum spanning tree. *Computers and Operations Research*, 7(4):239–49, 1980.

OPNET Technologies, Inc. OPNET modeler®, 2002. URL `http://www.opnet.com`.

C.C. Palmer and A. Kershenbaum. An approach to a problem in network design using genetic algorithms. *Networks*, 26(3):151–63, 1995.

K. Park, G. Kim, and M. Crovella. On the relationship between file sizes, transport protocols, and self similar network traffic. In *Inter. Conf. on Network Protocols*, October 1998.

E. Parkinson and P.R. Warren. A comparison of graph colouring techniques. *South African Comp. J.*, 14:14–19, 1995.

V. Paxson and S. Floyd. Wide area traffic: The failure of poisson modeling. *IEEE/ACM TRANSACTIONS ON NETWORKING*, 3(3), 1995.

H. Perros. *Computer Simulation Techniques: The definitive introduction!* course pack available at North Carolina State University bookstore, 1999.

Michał Pióro. Solving multicommodity integral flow problems by simulated allocation. 7(1–3):17–28, 1997.

Michał Pióro and P. Gajowniczek. Solving multicommodity integral flow problems by simulated allocation. In *Telecommunication Systems*. Baltzer Science Publishers.

Michał Pióro, Thomas Jacob Kjær Stidsen, Arne John Glenstrup, Christian Fenger, and Henrik Christiansen. Design problems in robust optical networks. In *Networks 2000*, September 2000.

Rajiv Ramaswami and Kumar N. Sivarajan. Routing and wavelength assignment in all-optical networks. *IEEE/ACM Trans. Networking*, 3(5):489–500, 1995.

Rajiv Ramaswami and Kumar N. Sivarajan. *Optical Networks: A Practical Perspective*. Morgan Kaufmann, 1 edition, 1998.

Lawrence G. Roberts. Beyond Moore's law: Internet growth trends. *Computer*, 33(1):117–9, January 2000.

M. Roughan and D. Veitch. A study of the daily variation in the self similarity of real data traffic. In *ITC16*, 1999.

Iraj Saniee. Optimal routing designs in self-healing communication networks. *International T. in Operational Research*, 3(2):187–195, 1996.

M. Schwartz and T.E. Stern. Routing techniques used in computer communication networks. *IEEE Trans. Commun.*, COM-28(4):539–552, 1980.

Giuseppe A. Sena, Dalila Megherbi, and Germinal Isern. Implementation of a parallel genetic algorithm on a cluster of workstation: Traveling salesman problem, a case study. *Future Generation Computer Systems*, 17:477–88, 2001.

Sudipta Sengputa and Ramu Ramamurthy. From network design to dynamic provisioning and restoration in optical cross-connect mesh-networks: An architectural and algorithmic overview. *IEEE Network*, pages 46–54, July–August 2001.

Sajjad H. Shami and Mark C. Sinclair. Co-evolutionary agents for telecommunication network restoration. *Proceedings of Recent Advances in Soft Computing '99*, pages 146–151, 1999.

J.M. Simmons and A.A.M. Saleh. The value of optical bypass in reducing router size in gigabit networks. In *Proc. of the IEEE International Conf. on Comm. (ICC–99)*, volume 1, pages 591–596, June 1999.

Mark C. Sinclair. Optical mesh network topology design using node-pair encoding genetic programming. *Proceedings of Genetic and Evolutionary Computation Conference (GECCO-99)*, pages 1192–7, July 1999.

Thomas Jacob Kjær Stidsen and Arne John Glenstrup. Quantifying optimal mesh and ring design costs. page 14pp, 2002. Submitted.

H. Störmer. Asymptotische näherungen für die erlangsche verlustformel. *A.E.Ü.*, 17(10), 1963.

Suresh Subramaniam and Richard A. Barry. Wavelength assignment in fixed routing WDM networks. In *IEEE Int. Conf. on Comm.*, volume 1, pages 406–410, 1997.

Yong Sun, Jun Gu, and Danny H.K. Tsang. Routing and wavelength assignment in all-optical networks with multihop connections. *International Journal of Electronics and Communications*, 55(1):8, 2001.

T.K. Tan and J.K. Pollard. Determination of minimum number of wavelengths required for all-optical wdm networks using graph coloring. *Electronics Letters*, 31:1895–1897, October 1995.

M.S. Taqqu, W. Willinger, and R. Sherman. Proof of a fundamental result in self similar traffic modeling. *Computer Commun. Rev.*, 27(2):5–23, 1997.

Tellium. StarNet Planner, 2002. URL `http://www.tellium.com`.

K. Thulasiraman and M. Swamy. *Graphs: Theory and Algorithms*, chapter 3. John Wiley & Sons, 1992.

Tushar Tripathi and Kumar N. Sivarajan. Computing approximate blocking probabilities in wavelength routed all-optical networks with limited-range wavelength conversion. *IEEE J. Selected Areas in Comm.*, 18(10):2123–2129, October 2000.

Griselda Navarro Varela and Mark C. Sinclair. Ant colony optimisation for virtual-wavelength-path routing and wavelength allocation. volume 3, pages 1809–1816. IEEE, 1999.

Malathi Veeraraghavan, Ramesh Karri, Tim Moors, Mark Karol, and Reinette Grobler. Architectures and protocols that enable new applications on optical networks. *IEEE Comm. Mag.*, 39(3):118–127, March 2001.

VPIsystems$^{\mathrm{TM}}$. VPItransportMaker, 2002. URL `http://www.vpisystems.com`.

N. Wauters and P. Demeester. Design of the optical path layer in multiwavelength cross-connected networks. *IEEE J. Select. Areas Commun.*, 14(5), June 1996.

Mark Allan Weiss. *Data Structures*. Addison Wesley, 2 edition, 1997.

D.J.A. Welsh and M.B. Powell. An upper bound for the chromatic number of a graph and its application to timetable problems. *The Computer Journal*, 10: 85–86, 1967.

D. Whitley. A genetic algorithm tutorial. *Statistics and Computing*, 4(2):65–85, 1994.

W. Willinger, M.S. Taqqu, R. Sherman, and D.V Wilson. Self similarity through high-variability: Statistical analysis of ethernet lan traffic at the source level. *IEEE/ACM TRANSACTIONS ON NETWORKING*, 5(1):71–86, February 1997.

J. Yates, J. Lacey, D. Everitt, and M. Summerfield. Limited-range wavelength translation in all-optical networks. In *IEEE Infocom*, pages 954–961, 1996.

Hui Zang, Jason P. Jue, and Biswanath Mukherjee. A review of routing and wavelength assignment approaches for wavelength-routed optical WDM networks. *Optical Networks Mag.*, 1(1):47–60, January 2000.

Zhensheng Zhang and Anthony S. Acampora. A heuristic wavelength assignment algorithm for multihop WDM networks with wavelength routing and wavelength re-use. *IEEE/ACM Trans. Networking*, 3(3):281–288, 1995.